BACTERIAL LEACHING FROM DAIRY SHED EFFLUENT APPLIED TO A FINE SANDY LOAM UNDER FLOOD AND SPRAY IRRIGATIONS

A thesis

submitted in partial fulfilment of the

requirements for the Degree of

Doctor of Philosophy

at

Lincoln University

By

Shuang Jiang

Lincoln University

2008

Abstract of a thesis submitted in partial fulfilment of the requirements for the Degree of Doctor of Philosophy

BACTERIAL LEACHING FROM DAIRY SHED EFFLUENT APPLIED TO A FINE SANDY LOAM UNDER FLOOD AND SPRAY IRRIGATIONS

By Shuang Jiang

Land application of wastes has become increasingly popular, to promote nutrient recycling and environmental protection, with soil functioning as a partial barrier between wastes and groundwater. Dairy shed effluent (DSE), may contain a wide variety of pathogenic micro-organisms, including bacteria (e.g. *Salmonella paratyphyi, Escherichia coli. and Campylobacter*), protozoa and viruses. Groundwater pathogen contamination resulting from land-applied DSE is drawing more attention with the intensified development of the dairy farm industry in New Zealand. The purpose of this research was to investigate the fate and transport of bacterial indicator-faecal coliform (FC) from land-applied DSE under different irrigation practices via field lysimeter studies, using two water irrigation methods (flood and sprinkler) with contrasting application rates, through the 2005-2006 irrigation season. It was aimed at better understanding, quantifying and modelling of the processes that govern the removal of microbes in intact soil columns, bridging the gap between previous theoretical research and general farm practices, specifically for Templeton soil. This study involved different approaches (leaching experiments, infiltrometer measurements and a dye infiltration study) to understand the processes of transient water flow and bacterial transport; and to extrapolate the relationships between bacterial transport and soil properties (like soil structure, texture), and soil physical status (soil water potential ψ and volumetric water content θ). Factors controlling FC transport are discussed. A contaminant transport model, HYDRUS-1D, was applied to simulate microbial transport through soil on the basis of measured datasets.

This study was carried out at Lincoln University's Centre for Soil and Environmental Quality (CSEQ) lysimeter site. Six lysimeters were employed in two trials. Each trial involved application of DSE, followed by a water irrigation sequence applied in a flux-controlled method. The soil columns were taken from the site of the new Lincoln

University Dairy Farm, Lincoln, Canterbury. The soil type is Templeton fine sandy loam (Udic-Ustochrept, coarse loamy, mixed, mesic). Vertical profiles (at four depths) of θ and ψ were measured during leaching experiments.

The leaching experiments directly measured concentrations of chemical tracer (Br^- or Cl^-) and FC in drainage. Results showed that bacteria could readily penetrate through 700 mm deep soil columns, when facilitated by water flow. In the first (summer) trial, FC in leachate as high as 1.4×10^6 cfu 100 mL^{-1} (similar to the DSE concentration), was detected in one lysimeter that had a higher clay content in the topsoil, immediately after DSE application, and before any water irrigation. This indicates that DSE flowed through preferential flow paths without significant treatment or reduction in concentrations. The highest post-irrigation concentration was 3.4×10^3 cfu 100 mL^{-1} under flood irrigation. Flood irrigation resulted in more bacteria and Br^- leaching than spray irrigation. In both trials (summer and autumn) results showed significant differences between irrigation treatments in lysimeters sharing similar drainage class (moderate or moderately rapid). Leaching bacterial concentration was positively correlated with both θ and ψ, and sometimes drainage rate. Greater bacterial leaching was found in the one lysimeter with rapid whole-column effective hydraulic conductivity, K_{eff}, for both flood and spray treatments. Occasionally, the effect of K_{eff} on water movement and bacterial transport overrode the effect of irrigation. The 'seasonal condition' of the soil (including variation in initial water content) also influenced bacterial leaching, with less risk of leaching in autumn than in summer.

A tension infiltrometer experiment measured hydraulic conductivity of the lysimeters at zero and 40 mm suction. The results showed in most cases a significant correlation between the proportion of bacteria leached and the flow contribution of the macropores. The higher the K_{sat}, the greater the amount of drainage and bacterial leaching obtained. This research also found that this technique may exclude the activity of some continuous macropores (e.g., cracks) due to the difference of initial wetness which could substantially change the conductivity and result in more serious bacterial leaching in this Templeton soil. A dye infiltration study showed there was great variability in water flow patterns, and most of the flow reaching deeper than 50 cm resulted from macropores, mainly visible cracks.

The transient water flow and transport of tracer (Br^-) and FC were modelled using the HYDRUS-1D software package. The uniform flow van Genuchten model, and the dual-porosity model were used for water flow and the mobile-immobile (MIM) model was used for tracer and FC transport. The hydraulic and solute parameters were optimized during simulation, on the basis of measured datasets from the leaching experiments. There was evidence supporting the presence of macropores, based on the water flow in the post-DSE application stage. The optimised saturated water content (θ_s) decreased during the post-application process, which could be explained in terms of macropore flow enhanced by irrigation. Moreover, bacterial simulation showed discrepancies in all cases of uniform flow simulations at the very initial stage, indicating that non-equilibrium processes were dominant during those short periods, and suggesting that there were strong dynamic processes involving structure change and subsequently flow paths.

It is recommended that management strategies to reduce FC contamination following application of DSE in these soils must aim to decrease preferential flow by adjusting irrigation schemes. Attention needs to be given to a) decreasing irrigation rates at the beginning of each irrigation; b) increasing the number of irrigations, by reducing at the same time the amount of water applied and the irrigation rate at each irrigation; c) applying spray irrigation rather than flood irrigation.

Keywords: bacterial leaching; lysimeter; soil structure; flood irrigation; spray irrigation; macropore flow; drainage rate; pressure head; volumetric water content; tension infiltrometer; dye study; HYDRUS-1D; modelling; parameter optimization; Templeton soil.

Acknowledgments

I would like to express my sincere thanks to my supervisor Dr. Graeme Buchan for his constant encouragement, guidance, patience and friendliness throughout this project. He has walked me through all the stages of the writing of this thesis. Thanks are expressed to my co-supervisors, Dr Mike Noonan who has instructed and helped me a lot in the past three years. I am grateful to my external supervisors Dr. Liping Pang and Murray Close from ESR for their help, advice, encouragement and prompt reading of my writing. I also thank ESR for initiating the project and funding support, and initially Foundation for Research Science and Technology (FRST), currently Tertiary Education Commission (TEC) for financial support from Enterprise Scholarship.

Thanks also go out to Soil & Physical Sciences Group and Microbiological Lab staffs for always being so supportive, with either practical help or good advice whenever it was needed. I am particularly thankful to Neil, Nigel and Trevor, generous giving of their time and their sharing of technical knowledge. Their assistance and co-operation was very much appreciated.

Many thanks go to Prof. Keith Cameron, CSEQ, Lincoln University for his pertinent advice and gracious assistance. The sharing of their lysimeter facility in CSEQ for the duration of my experiment is gratefully acknowledged. I am grateful to Prof. A. McKinnon and Dr. K. Unsworth, Applied Computing Group, Lincoln University, for the help of image analysis. Prof. Jirka Šimůnek provided technical support for HYDRUS-1D modelling. I am very appreciative of his help.

Thanks to Marianne Duncan and Rob Sherlock for their concern about the special computer need for this project. The fast computer made my modeling work easier.

Finally, thanks would go to my beloved family for their loving considerations, tolerance and great confidence in me all through these years. I also owe my sincere gratitude to my friends and my fellows who gave me their help and time in listening to me and helping me work out my problems during the difficult course of the thesis.

Table of Contents

List of Tables

List of Figures

List of Plates

Notations

Abbreviations

AFC	antibiotic-resistant faecal coliform
APHA	American Public Health Association
BTC	breakthrough curve
BMP	best management practice
CDE	convection diffusion equation
cfu	colony forming unit
CSEQ	Centre for Soil and Environmental Quality
d	day
DCD	dicyandiamide
DEC	The Dairying and the Environment Committee
Dexcel	Dairying excellence (DairyNZ)
DSE	dairy shed effluent
ECan	Environment Canterbury
ESR	The Institute of Environmental Science and Research Ltd
ET	actural evapotranspiration
EWRC	Environment Waikato Regional Council
F	flood irrigation
FC	faecal coliform
FRST	Foundation for Research Science and Technology
g	gram
ha	hectare
hr	hour
ISE	ion selective electrode
kg	kilogram
L	litre
LAI	leaf area index
LEACHM	leaching estimation and chemistry model
Lys.	lysimeter
LU	Lincoln University

MACRO	non-steady state model of water flow and solute transport in macroporous soils
MAF	Ministry of Agriculture and Forestry
mg	milligram
µg	microgram
min	minute
mL	millilitre
µm	micrometre
MPN	The Most Probable Number
N	nitrogen
NZ	New Zealand
o.m.	organic matter content
P	precipitation
PET	potential evapotransporation
PSD	particle size distribution
PTFs	pedotransfer functions
PV	pore volume
RMA	Resource Management Act 1991
RMSE	root mean square error
S	spray irrigation
s	second
SMC	soil (sand) moisture characteristic
SWIM	Soil and Water Integrated Model
TDR	time-domain reflectometry
TEC	Tertiary Education Commission
yr	year

List of Symbols

c	solute concentration of the liquid phase (ML^{-3}), or bacterial concentration (cfu 100 mL^{-1})
c.	about
c_o	influent bacterial concentration (cfu 100 mL^{-1})

Cp	volumetric heat capacity ($ML^{-1}T^{-2}K^{-1}$) of the porous medium
C_t *or* C	effluent bacterial concentration (cfu 100 ml^{-1})
Cw	volumetric heat capacity ($ML^{-1}T^{-2}K^{-1}$) of the liquid phase.
D	solute dispersion coefficient ($cm^2\ min^{-1}$),
g	acceleration due to gravity
h	soil water pressure head, or the height of water rise in a capillary tube (mm)
K	hydraulic conductivity (mm hr^{-1} or m d^{-1}) as a function of h or θ ,
K_h	ability of the soil to transmit water (conductivity).
K_r	relative hydraulic conductivity
K_s	saturated hydraulic conductivity (mm hr^{-1} or m d^{-1})
l	the pore connectivity parameter
m	for van Genuchten soil water retention model, m is assumed to be 1 – 1/n. for Freundlich isotherm, m is a constant indicating sorption intensity.
n	empirical coefficient for van Genuchten water retention model
PE	potential evaporation rate (mm d^{-1})
PT	potential transpiration rate (mm d^{-1})
Q	flow rate from the disc infiltrometer (m^3s^{-1})
q	volumetric fluid flux density ($M\ T^{-1}$) given by Darcy's law,
Q_{ss}	steady state flow volume per unit time (v hr^{-1})
R	pore radius (mm or cm)
r_0	disc radius (m)
S	sorptivity (m $s^{-0.5}$)
Se	effective saturation
t	time or detention time (d, hr or min).
V_a	volume of air (cm^3)
V_s	volume of solid (cm^3)
V_w	volume of water (cm^3)
x,z	distance from the soil surface downward (m)
T	temperature (K)

Greek

α	van Genuchten parameter (1/m) in Chapter 6
α	wetting angle of the water and the pore wall (assumed to be nearly zero, therefore cos α=1) in Chapter 5
γ	surface tension of water (N m^{-1})
ε	total porosity (v v^{-1})
ϕ	sinks or sources for solutes (ML^{-3} T^{-1})
λ	first-order die-off rate constant (d^{-1})
θ	volumetric water content (v v^{-1})
θ_{im}	immobile volumetric water content (v v^{-1})
θ_m	mobile volumetric water content (v v^{-1})
θ_r	residual water content (v v^{-1})
θ_s	saturated water content (v v^{-1})
ρ_b	soil or sand bulk density (g cm^{-3}).
ρ_s	particle density (kg m^{-3}).
ρ_w	water density (kg m^{-3}).
σ	surface tension of the air-water interface(kg s^{-2}).
σ	surface tension at the air-water interface
ψ	matric potential (mm head of water)
ψ_m	soil water matric potentials (kPa).
μ	water dynamic viscosity (Pa s).
ω	exchange rate between mobile and immobile regions
ξ	dispersivity (L)

Chapter 1 Introduction

1.1 Background to the study

As public awareness grows regarding environmental problems in the agriculture production sector, governments and authorities face the challenge of designing policies to re-orient agriculture toward safer and more sustainable practices. Environmental laws and regulations increasingly define specific limits and levels of contaminants in soil and groundwater as a function of application regimes and land management procedures.

The dairy farm industry in New Zealand is becoming increasingly important in the national economy, contributing a 20% share of total national export revenue in 2003/04 and 2004/2005 season (Livestock Improvement Ltd. and Dairy InSight NZ 2004-2005; 2005-2006). It is the second largest export industry in NZ. With dairy farming's rapid development, the environmental issue of groundwater protection is drawing more attention (Figure 1.1).

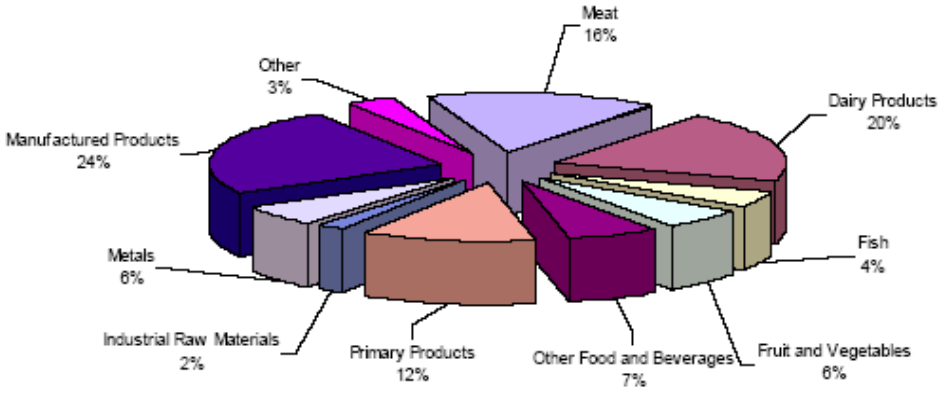

Figure 1.1[*] Composition of NZ's major merchandise export sector, Year to Dec 2005

Soil acts as a "living filter" in the natural process of protecting groundwater in the long term, in terms of its ability to physically, chemically and biologically treat waste, by absorbing and filtering potential water pollutants, pathogenic organisms and retaining nutrients. Land application of dairy shed effluent (DSE) has been practised for many years in dairy farms. It is believed that DSE application improves the soil's long term fertility or

[*] From: *www.marketnewzealand.com*

"soil quality", especially in the upper 10 cm of the profile (Hawke and Summers 2003). When properly designed, land application systems for DSE are efficient for removing contaminants. DSE irrigation can be part of a land treatment system, providing both water and nutrients for pasture, or the renovated water can be safely discharged to ground water or surface water. Without proper design and practices, the soil function of filtration will fail with the intensification of production (Cameron and Trenouth 1999). The microbes including pathogens may go through soil and into groundwater.

In the last 20 years, the average dairy herd size in NZ has more than doubled, to 315 cows in 2004/2005. The total cow population increased to 3.867 million in 2004/2005. Figures from the 2006 Agricultural Production Survey show that the national dairy herd is now 5.2 million, and up 1.6 percent from 2005 (Statistics New Zealand 2007). The industry has also become more widespread as dairy farming has been expanding into new areas. In recent years a growing number of farms have developed to carry 500-1000 cows. There are currently proposals to develop farms stocking up to 5000 cows (Cameron and Trenouth 1999). For the discharge of DSE, about half of the regional councils in New Zealand classify DSE to land as a permitted activity (Dairying and the Environment Committee 1996). However, this practice may exceed the soil's attenuation capacity (e.g., under application to soil waterlogged by rain, high hydraulic loading rates or even normal irrigation). If DSE infiltrates beyond the surface layers of soil there is a risk that groundwater will become contaminated, but if it is subject to runoff, then surface waters are at risk (Aislabie *et al.* 2001; Monaghan and Smith 2004). Moreover, the direct land application without treatment before application provides the least opportunity for the control of any harmful pathogens.

The Canterbury Region of NZ, which is becoming more intensively farmed (South Canterbury has the largest average herd size with 636 cows in 2004/2005, up markedly from the 2000/2001 season's figure of 483 cows). Canterbury had the greatest change in dairy cattle numbers, increasing from 605000 in 2005 to 656000 in 2006. Many of these dairy-farm conversions are occurring on flood-irrigated land. A recent research on well-water monitoring at a south Canterbury site, where border dyke (flood) irrigation was applied, showed that total coliforms were detected on 99% of sampling occasions at levels ranging from <1 to >2,400 MPN[†] 100 mL^{-1}, with an average for all wells of 538 MPN 100

[†] The Most Probable Number

mL^{-1} (Compare the drinking water standard for *E. coli* of <1 MPN 100 mL^{-1}). The overall detection rate for all samples for *E. coli* was 77% (Close *et al.* 2008). The current trend is for greater use of spray irrigation for land disposal of DSE. However, we have little understanding or ability to predict the likely bacteria leaching under these irrigation schemes.

Current regulations for DSE application contain advice and recommendations to enable farmers to minimize the risk of chemical pollution. They focus on N leaching, and, for example, are: 150 kg N ha^{-1} yr^{-1} in Waikato region; and 150-200 kg N ha^{-1} yr^{-1} in Canterbury (ECan and Dexcel Ltd. 2004; EWRC and Dexcel Ltd. 2005). However, the risk of groundwater contamination by microorganisms in DSE, including many potential pathogens also demands attention, especially in Canterbury, which has NZ's largest average herd size (Livestock Improvement Ltd. and Dairy InSight NZ 2004-2005).

Sound water management, (e.g. via regulations, recommendations and disposal guidelines) for reducing the risk of water contamination and achieving sustainable land management practices requires information on appropriate irrigation timing and rate relative to DSE irrigation method and soil properties (Feigin *et al.* 1991). It is essential that we increase our knowledge and understanding of the environmental impacts of intensive dairy farming under both flood- and spray-irrigation schemes. In NZ, no councils operate controls on DSE application rate (in mm hr^{-1}) in relation to the risk of pathogen pollution.

Landcare Research has identified risks associated with the DSE application rate. They indicate that to avoid effluent moving below the topsoil, effluent should be applied at a maximum rate of 10-15 mm hr^{-1} up to a 25 mm of effluent irrigation, or the maximum allowed depth for land application of DSE, which ever is the lower. Higher application rates may result in pathogens and nutrients leaching through to groundwater (McLeod *et al.* 1998). There is no such research reported for Templeton soil, which represents a large proportion of the land used in dairy farms in the Canterbury Plains. Templeton soils cover about 68,000 hectares in Canterbury and are "free draining soils well suited to cropping" (Soil Bureau Bulletin 27, 1968). Also because they have textures ranging from sandy loam to silt loam, they are representative of other common soil types in Canterbury.

1.2 Objectives of the study

Bacterial leaching is a complex and interacting process controlled by soil type, and environmental and management factors. This study aimed to:

- understand the fate and transport of bacterial pathogens from land-applied DSE under different irrigation schemes in a Canterbury soil (Templeton soil) under conditions typical of field practice.
- derive parameters describing transport and transformation that can be used for simulating bacterial transport in the soil type investigated.
- provide information and recommendations for better management practices.

These goals were met through the following objectives:

1. To directly measure the concentrations and amounts of bacteria and chemical tracers leaching from lysimeters under conditions representative of realistic field and farm conditions.
2. To identify and understand the key processes that control the fate and transport of indicator bacteria and chemical tracer irrigated onto soil on the basis of the field lysimeter studies.
3. To develop and assess methods for describing soil structure characteristics important for transport processes, *i.e.* by use of a tension infiltrometer and a dye infiltration study.
4. To apply an existing simulation model (HYDRUS-1D) to describe the fate and transport of bacteria applied to soil, and use experimental data to calibrate the model, in order to derive important transport parameters that can be extrapolated from the lysimeter experiment to field practice.
5. To provide recommendations and suggestions for management practices, in order to promote protection of surface and ground water resources.

1.3 Layout of the thesis

Chapter 2 provides a literature review on the relevant researches relating to microbial (especially bacterial) transport in soils. The chapter presents the current basic knowledge of factors controlling the processes of microbial transport, including soil properties, water input, and the seasonal variation in field conditions. Furthermore, the use of DSE in previous research is reviewed and information on the general properties of DSE is presented. Modelling of microbial transport is described and the solute transport model HYDRUS-1D, employed later in this study, is also explained.

Chapter 3 describes the general material and methods used, starting from the design and set-up of the lysimeter leaching experiments and followed by the lysimeter destructive sampling. The first part of Chapter 3 describes the lysimeters, the pilot trial for determination of the hydraulic characteristic of the lysimeters, the DSE resource, the lysimeter instrumentation, and the experimental design for irrigation schemes and DSE application. The soil properties are presented in the second part.

Chapter 4 presents the experimental results of the first (summer) trial and the second (autumn) trial of the leaching experiment; the measured soil properties; and defines the main factors that affect the bacterial transport.

Chapter 5 looks into the soil structure of the lysimeters as determined by tension infiltrometer and dye studies, and reveals some linkage between the soil structure and bacterial leaching. The impact of structure on bacterial transport is discussed.

Chapter 6 proceeds to modelling, using the HYDRUS-1D software package. The simulation employed the van Genuchten model on the basis of experimental data and other resources. The hydraulic parameters of the lysimeter soils are optimized for pre-DSE-application and post-DSE-application processes, and then the solute transport is simulated by modified parameters optimized by water flow using the mobile-immobile water two regions convection diffusion equation (CDE). The dual-porosity model (in HYDRUS-1D) is employed for two of the lysimeters, which could not be fitted by the single-porosity van Genuchten model. Further, the discussion addresses implications of the results of the modelling to general practices in the field.

Chapter 7 summarises the previous chapters. The main results and conclusions are presented, with suggestions for future research. Some recommendations are provided for management practices aimed at ground water protection.

Chapter 2 Literature Review

2.1 Introduction

Land application of agricultural and industrial wastes has become increasingly popular in the last 20 years, on account of the need for nutrient recycling and environmental protection, with soil functioning as a barrier between wastes and groundwater. Wastes, such as dairy shed effluent (DSE), may contain a wide variety of pathogenic micro organisms, including bacteria (e.g. *Salmonella paratyphyi, Escherichia coli. and Campylobacter*), protozoa and viruses.

According to The Resource Management Act 1991 (RMA), land application of DSE is a permitted activity in New Zealand. However, it posts a potentially threat to humans and other living organisms, due to the potential for surface or groundwater contamination. The proper step, therefore, should be to adjust relevant regulations and recommendations for groundwater protection, based on sufficient information on the possible consequences of land application of DSE.

2.2 Current regulations and practices around New Zealand

Land-based systems are currently actively promoted by regional councils in NZ as the most preferred option for DSE disposal. It is common sense to prevent surface runoff during application. In terms of downward effects (i.e. profile drainage), it is widely accepted that the allowable application amount will vary according to soil water properties, DSE dilution rate, stocking density, and how long DSE is stored for, which affects nutrient mobility. The permitted nitrogen (N) loaded to land is 150-200 kg N $ha^{-1}.yr^{-1}$. The key factors determining regulations have focused on the following.

- **Application rate on the basis of soil type** :

  Freely draining soils with a deep water table are ideal for land application of DSE. The application rate should decrease according to the following order: sand, loamy sand, fine sandy loam, silt and sandy silt loan, clay and clay loam. The maximum recommended application rate is 32 mm hr^{-1} for sand. The suggested ideal application rate for all soil types is 10 mm hr^{-1} or less (Otago Regional Council 2001). The

Dairying and the Environment Committee (DEC) manual (Heatley 1996) specifies DSE land application rates, ranging from 10-32 mm hr^{-1}, depending on soil type. There is a recommended maximum *depth* per application (to avoid leaching through the soil), and a maximum application *rate* in mm hr^{-1} (to avoid surface ponding and runoff).

- **Application depth**

Nearly all regional councils set the application depth of DSE according to the nitrogen loading limit, which ranges from 150-200 kg ha^{-1} per year. A typical maximum application is 25 mm, which is equivalent to 50 kg N ha^{-1} approximately, but varies depending on the stock number and diluting water amount (Taranaki Regional Council. 1995; Auckland Regional Council 1999; ECan 2001; Otago Regional Council 2001; ECan and Dexcel Ltd. 2004; EWRC and Dexcel Ltd. 2005). The calculation is based on certain assumptions about the amount of nitrogen produced per cow, the volume of effluent produced, and the lactation period, all of which can vary greatly. Average values are used to establish upper limits for nitrogen loading.

- **Soil wetness before DSE application**

It is commonly accepted that leaching from DSE application takes place when the soil is at higher degree of saturation (Taranaki Regional Council. 1995; Auckland Regional Council 1999; ECan 2001; Otago Regional Council 2001; ECan and Dexcel Ltd. 2004; EWRC and Dexcel Ltd. 2005). A depth of application less than 50% of the water holding capacity of the soil will help avoid leaching and information of runoff (ECan 2001). However, no recommendation or regulation is given in terms of specific quantities.

There have been reports, both from South and North island locations, that groundwater bacterial indicator or nitrate levels are higher in the most intensively grazed catchments (Taranaki Regional Council 1995; Deely *et al.* 1998; Close *et al.* 2008). Monaghan and Smith (2004) indicate that land application of DSE contributed to the water quality deterioration. The ESR report (Ball 2006) estimates that the number of waterborne infection cases lies between 18,000 and 34,000 a year in New Zealand. Outbreaks of water-borne disease via public water supplies in developed countries continue to be reported, even though there is increased awareness of, and treatment for, pathogen contamination. Precautions for groundwater protection certainly need to

be considered with the increasingly intensified dairy industry in New Zealand, especially in Canterbury.

2.3 Factors affecting bacterial survival and transport

In recent decades there has been extensive research on microbial transport through soil, including experimental research (Smith *et al.* 1985; Fontes *et al.* 1991; McCaulou *et al.* 1994; Tan *et al.* 1994; Weiss *et al.* 1995; Schafer *et al.* 1998; Silliman *et al.* 2001; Quinton *et al.* 2003; Becker *et al.* 2004), theoretical reviews (Keswick *et al.* 1982; Crane and Moore 1986; Harvey 1997; Ginn *et al.* 2002; Jamieson *et al.* 2002; Ferguson *et al.* 2003; Tyrrel and Quinton 2003), and modelling approaches (Corapcioglu and Haridas 1985; Peterson and Ward 1989; Tan *et al.* 1994; Blue *et al.* 1995; Corapcioglu and Choi 1996; Schijven *et al.* 1999).

The survival and transport of bacteria, after field application of DSE depend on the physical and chemical properties of both soil and DSE, the consequences of their interactions (Unc and Goss 2003), climatic conditions, application methods of DSE, as well as the irrigation scheme (Feigin *et al.* 1991; Aislabie *et al.* 2001).

2.3.1 Bacterial survival in soil

Bacteria survival in soil has been well investigated in lab soil column experiments, and and the basic framework of influencing factors has been worked out. These include soil moisture, soil type (including adsorption properties), soil water flux, temperature, pH, effluent or manure application rate, nutrient availability, type of microorganism and competition (Medema *et al.* 1997; Banning *et al.* 2002). The waste (e.g. effluent) application methods, the frequency of application and bacterial biomass (density) are also important. These are further explained as follows:

- *Water content/potential* – Water availability can override the impact of other factors (Gerba and Bitton 1984; Mubiru *et al.* 2000). Cools et al. (2001) found that the best survival of *E. coli* and *Enterococcus* spp. occurred in soils close to field capacity. Mubiru et al. (2000) showed that at the same gravimetric water content, the suction was higher in a silt loam with a clay content of 0.25 g g^{-1} than one with 0.12 g g^{-1}, and the survival of *E. coli* and *E. coli* O157:H7 was also shorter. Microorganisms can survive very dry soil conditions, e.g. Salmonella tolerates

water potentials to –150 bars, while halophilic bacteria can survive down to –350 bars (Harris 1981).

- *Temperature*. Microorganisms can survive longer in cold soils than in warm soils. Bacterial die-off rate approximately doubles with each 10℃ temperature rise in temperature between 5 and 30℃(Reddy *et al.* 1981). In cold soils (< 5℃) bacteria can survive for up to 100 days. Survival of *Enterococcu*s spp. was longer than that of *E. coli* at 5℃, while the opposite was true at 15℃ and 25℃(Cools *et al.* 2001). Survival of non-pathogenic *E. coli* exceeded 60 days at 25℃ and 100 days at 4℃ (Bogosian *et al.* 1996). Previous experiments have shown that low temperatures decrease the mortality of bacteria (McCaulou and Bales 1995). Jiang (2002) showed that the pathogen *E. coli* O157:H7 (the cause of 'hamburger-disease'), survived for 42 to 49 days at 37℃, for 49 to 56 days at 22℃, and for 63 to 70 days at 5℃.

- *pH*. Bacteria are able to survive over a wide range of pH, but growth and activity tend to be less under acidic conditions (Jones 1999; Tawfik *et al.* 2004). *E. coli* bacteria survived for a shorter time in acid soil (pH 3-5) than in alkaline soil (Tawfik *et al.* 2004) .Microbial die-off is minimum in the pH range 6 to 7 (Reddy *et al.* 1981).
- *Organic matter (o.m.) content*. Cools et al. (2001) reported that increased o.m. levels enhanced survival of coliform bacteria, and suggested that this might be related to a variety of factors controlled by o.m., such as water retention, formation and stabilization of soil aggregates, and the formation of microhabitats.
- *Texture*. Bacteria survive longer in fine textured than in coarse-textured soils. However, Cools et al. (2001) reported that while *Enterococcus* spp. survived longer in loamy soils than sandy soils at 25℃, the reverse was true for *E. coli.* It is likely that at least part of the effect of texture is related to the water-holding capacity of these different soils (Mubiru *et al.* 2000).
- *Nutrient availability*. Gagliardi and Karns (2000) reported that *E. coli* O157:H7 was able to replicate in and migrate through cores of various soil types. Numbers of the pathogen in leachate correlated with ammonia and nitrate levels, and the numbers exceeded inoculum levels in all treatments (i.e. soil types, tilled and no till, and rainfall amounts) except in intact clay loam cores.

- *Sunlight* can reduce the survival of bacteria and viruses in soil directly through the sterilising effect of ultraviolet light and as a result of drying (Gerba *et al.* 1975; Gerba and Bitton 1984; Sinton *et al.* 1999; Mubiru *et al.* 2000). However, unless pathogens are located at the immediate soil surface, sunlight will not affect pathogen survival in soils.

The survival time of pathogenic organisms in the soil mainly depends on the type of organism and soil conditions, and can vary from days to months. The absolute maximum recorded survival time of pathogen in soil is one year, and common maximum survival times are about months (Gerba and James E. Smith 2005).

According to Crane and Moore (1986) the die-off of bacteria can be described by an exponential equation:

$$C_t = C_0 \, exp^{-\lambda t} \qquad \textbf{(2.1)}$$

here C_0 is the influent bacterial concentration, expressed by colony-forming units per ml (cfu mL^{-1}), C_t is the effluent bacterial concentration (cfu mL^{-1}), λ is the first-order die-off rate constant (d^{-1}) and t is the time or detention time (d).

This is a basic die-off model of bacteria commonly used in transport models. However, die-off data can often be fitted better using other functions. The die-off rate coefficient is a highly variable parameter, due to the interaction of environmental factors on bacterial die-off.

2.3.2 Bacterial transport in soil

During bacterial transport in the subsurface, many complex and interactive processes are involved (Ginn *et al.* 2002). The attenuation of bacteria in soil is the sum of the following mechanisms: inactivation (including die-off and predation), adsorption, detachment, filtration and sedimentation (Tawfik *et al.* 2004) and air-water interface trapping. The factors influencing bacterial transport include the following:

- Soil physical characteristics: soil particle size distribution (e.g. clay type and content), pore size distribution, organic matter content pH, and bulk density (Gerba and Bitton 1984; Peterson and Ward 1989; van Elsas *et al.* 1991).
- Chemical and microbial factors: ionic strength of soil solution, pH of infiltration water, nature of organic matter in the waste effluent solution (concentration and size), type of microorganism (Fontes *et al.* 1991; Abu-ashour *et al.* 1994).

- Soil environmental factors: temperature, soil water content (degree of saturation) and soil water flux (controlled by weather condition and irrigation) (McLeod *et al.* 1998; Tawfik *et al.* 2004).
- Application conditions: soil drying between applications, bacterial and total biomass loading, and time of application (winter, spring) (van Elsas *et al.* 1991; McLeod *et al.* 1998)

The main factors influencing the fate and transport of bacteria are further explained in *2.3.3* and *2.3.4*.

2.3.3 Effect of soil properties on bacterial transport

Without doubt, different soil properties have different influences on bacterial transport. The physical processes of bacterial transport, such as advection, dispersion, straining and physical filtration (McDowell-Boyer *et al.* 1986; Harvey *et al.* 1989; Harvey and Garabedian 1991) are affected by soil texture (which controls porosity, pore-size distribution and water holding capacity). Bacteria move with the water, the velocity of which is governed by the hydraulic pressure gradient, porosity, pore size distribution, and (in field conditions) by spatial variation in permeability, which is strongly controlled by soil structure. Results from column and field studies suggest that the transport of bacteria through undisturbed soils is primarily controlled by macropore flow phenomena (Smith *et al.* 1985; Jamieson *et al.* 2002)

2.3.3.1 Soil texture

Bacterial transport is influenced by the soil's porosity, pore-size distribution and water holding capacity, and therefore by its texture. Fine texture soils enhance the physical processes in soil, like inactivation straining, filtration and air-water interface trapping (Newby *et al.* 2000; Ginn *et al.* 2002). Therefore, the application depths of DSE should be varied according to the soil type (Auckland Regional Council 1999; Cameron and Trenouth 1999; Otago Regional Council 2001; McIntosh *et al.* 2002). Soil with lower conductivity (soils with more silt or clay) may decrease the leaching on one hand; but increase surface runoff on the other hand (and conversely for coarser textures). Similar studies by Paterson et al (1993) and Gagliardi (2000) suggest that loam and clay soils, which have more water holding capacity than sandy soil, produce less bacteria leaching. However, there may be conflicts between the effects of soil texture and soil structure. More

clay in soil may promote shrinkage and hence create substantial macroporosity, which can fast-track drainage and hence reduce the extent of these processes. The conclusions from other studies show that, under saturated or near-saturated flow, microbial transport will be greater in structured loams or clay soils due to macropore flow (Conboy and Goss 2000; Aislabie *et al.* 2001).

Water repellence has been reported in clay soil in the Netherlands, and in loams in Western Australia (Dekker and Ritsema 1996). When the clay soil is dry, a major proportion of the water from precipitation or irrigation may flow rapidly through shrinkage cracks to the subsoils, by passing the matrix of the clay peds (Dekker and Ritsema 1996).

2.3.3.2 Soil structure

Variation in soil structure, and degree of structure development affects the rate of water flow through soil (McLaren and Cameron. 1996) and micro-biological activity (Bowler 1980). Generally, aggregated soils have a greater saturated hydraulic conductivity than the weakly aggregated soils with only small pores. Stoddard et al (1998) stated that the potential for groundwater contamination depends on soil structure and water flow more than on faecal bacterial survival at the soil surface.

There are different definitions of macropores. Germann and Beven (1981) indicated a matric potential of -1.0 cm as a boundary between macropores and micropores. The equivalent cylindrical pore diameter is *c.* 0.30 cm, calculated on the basis of following equation:

$$\psi = -\frac{2\sigma}{R\rho_w g} \qquad \textbf{(2.2)}$$

here R is pore radius

σ is the surface tension at the air-water interface

ρ_ω is the density of water

g is the acceleration due to gravity, and

ψ is matric potential in units of length, (equivalent to energy per unit weight).

Table 2.1 Some definitions of macropores and macroporosity

Reference	Capillary Potential (kPa)	Hydraulic head (cm)	Equivalent Diameter (μm)
Brewer (1964)			
Coarse	-0.06	0.6	5,000
Medium			2,000-5,000
Fine			1000-5,000
Very fine			75-1,000
Germann and Beven (1981)	>-0.1	>1	>3000
Luxmoore (1981)	>-0.3	>3	>1000
Silva (1999)	>-0.5	>5	>600
Jiang (2004)	>-0.5	>5	>600
McLaren and Cameron (1996)		>102	
Air pores (>300μm)	>-10	>102	>30
Transmission pores (30-300μm)			
Cameron and Buchan (2002)	>-10	>102	>30

Cameron & Buchan (2002) gave the boundary between macropores and micropores as a pore diameter of 30 μm, corresponding to ψ =-10 kPa (equivalent to field capacity in NZ). McLaren and Camerson (1996) stated that macropores include airpores (>300μm) and Trasnmission pores (30-300 μm). Luxmoore (1981) suggests that different pore size of ranges are associated with different types of soil water phenomena.

Much of recent work on macropores has demonstrated that macropore flow takes place in a wide range of soils and pore sizes, and is undoubtedly dependent on the initial moisture conditions in soil and the rate of water supply, as well pore sizes alone. Such flow depends on the nature of the dynamics of the flow process rather than the pore size ranges. Size alone will therefore be, at best, an approximate indication of the likelihood of such flow (Beven 1981).

Only pores which are usually sufficiently greater than the size of a single microbe, with sufficient water content, can possibly form a continuous pathway for the potential movement of the microbes. Considering the fact that water flow is mainly conducted through big pores, exclusion of microbes from pore throats is not usually determined by the ratio of sizes between microbes and pore throats, but the dramatically different water flow rates. Thus, microbes tend to travel much shorter distances in drier soils than under wet conditions, and transport mainly occurs through macropores rather than micropores.

It is well accepted that the movement of microorganisms with water flow through soil can be divided into two fractions: one fraction flows mainly through the soil matrix, which involves physical interaction processes; the other fraction flows through by-pass pathways

(Nielsen *et al.* 1973; Hornberger *et al.* 1990; Kluitenberg and Horton 1990; Bouma 1991; Edwards *et al.* 1993a; Chen *et al.* 1999; Ersahin *et al.* 2002). The latter is defined as macropore flow, which can be very fast in soil. Such rapid movement also relies on the *continuity* of macropores (Smith *et al.* 1985).

While macropores may constitute only a small fraction of total porosity of a soil (e.g. 0.1 to 5.0%), they can greatly influence the transport of water, solute, and pollutants through the soil (Bouma and Dekker 1978; White 1985). Regarding the relation between porosity (or macroporosity) and proportion of macropore flow, Silva *et al* (2000) concluded that pores >600 μm diameter transmitted about 98% of the total nitrogen (N) leached below 700 mm depth in a Templeton soil in NZ. This was based on applying 0.5 kPa suction on a lysimeter.

The existence of preferred flow paths within a medium dramatically changes the transport profiles, confirming the speculation that heterogeneities (macropores, fractures, *etc*) in the subsurface environment may be responsible for much of the long–range transport of microbes (Fontes *et al.* 1991). The infiltrability may be increased by 100% or more (Hillel 1998). Once bacteria have entered macropores with the moving water, adhesion processes do not play an important role (Natsch *et al.* 1996) The water may flow partially independent of the hydraulic conditions in the smaller pores, since this transport through the profile occurs with minimal interaction with the soil matrix. The risk of pathogen leaching is greatest when macropore flow occurs (Cameron *et al.* 1997). Horton (1942) expressed such rapid flows through these macropores as " concealed surface runoff".

Preferential flow through macropores has been observed in both laboratory and field studies (Thomas and Phillips 1979; Beven and Germann 1982; White 1985; Singh and Kanwar 1991; van Elsas *et al.* 1991; Bejat *et al.* 2000; Chu *et al.* 2003). In terms of bacteria transport, many field studies showed a rapid movement and high concentration of bacteria reaching receiving waters. Van Elsas *et al* (1991) found that introduced *Pseudomonas fluorescens* bacteria were transported to lower soil layers to a significantly higher degree in undisturbed soil cores than in repacked cores. The normal explanation is the preferential flow of microorganisms through macropores, including cracks, fractures, wormholes and channels formed by plant roots, or animals in the soil. However, there is difficulty in defining what constitutes macropores and to what extent the macropores dominate the vertical water flow. Most previous research focused on repacked soil or undisturbed soil columns not including the effect of large soil cracks. Field studies are

needed to monitor the effects of large and continuous cracks on water and contaminant transport processes.

The use of dye tracers (1994) allowed a detailed study of the phenomenology of solute transport in field soils, thereby revealing that preferential flow as a consequence of various soil structural features was the rule rather than the exception.
It is important to recognise that soil structure on a visible scale is changeable, especially during wetting and drying cycles (Brewer 1964). These cycles help to break down clods of soil and produce finer aggregates (McLaren and Cameron. 1996). Planes in soil materials originate primarily through shrinking and swelling during wetting and drying. Large planes would originate under very dry conditions (Stirk 1954).

There has been considerable experimental success in batch studies, and in studies involving systems without macropore flow, such as repacked soil columns. In structured soils, however, preferential flow can have a major impact on leaching. As a result, some fundamental problems and questions remain unanswered for specific regions and their soil types.

It is believed that soils under grasslands have a larger proportion of macropores than under arable farming, hence are more susceptible to preferential flow. This is because of greater inputs of structure-building o.m. under grasslands, and the disturbing of soil structure under arable farming. This phenomenon can be seen in other relevant research on transport of chemicals (Heathwaite and Dils 2000; Toor *et al.* 2004a) and bacteria (Joergensen *et al.* 1998).

2.3.4 Effects of season and irrigation regime on bacterial transport

Seasonal variation is controlled by temperature on the one hand, and the water balance (rainfall vs. actual evapotranspiration ET) on the other hand. For bacteria transport from land-applied animal waste over short periods, water inputs and outputs, i.e. weather and irrigation practices are addressed more effectively by changing soil moisture, which also generates changes in soil structure. The dynamic changes of soil structure with regional weather conditions (season) and irrigation schemes certainly influence the transport of water, solute and pollutants. There is only little previous research on the relation between seasonal variation of soil moisture regime and structure, and their impacts on water, solute

and pollutant transport to receiving groundwater. Heathwaite (2000) identified a seasonal variation in P leaching, with more P in leachate in summer which could be related to climate and land management activities.

Summer rainfall in eastern areas of New Zealand is generally much less than the potential evapotranspiration, thus summer leaching is typically minimal or absent in normal conditions. However, bacterial leaching in summer can occur through macropores under irrigation or intensive heavy rainfalls (Figure 2.1).

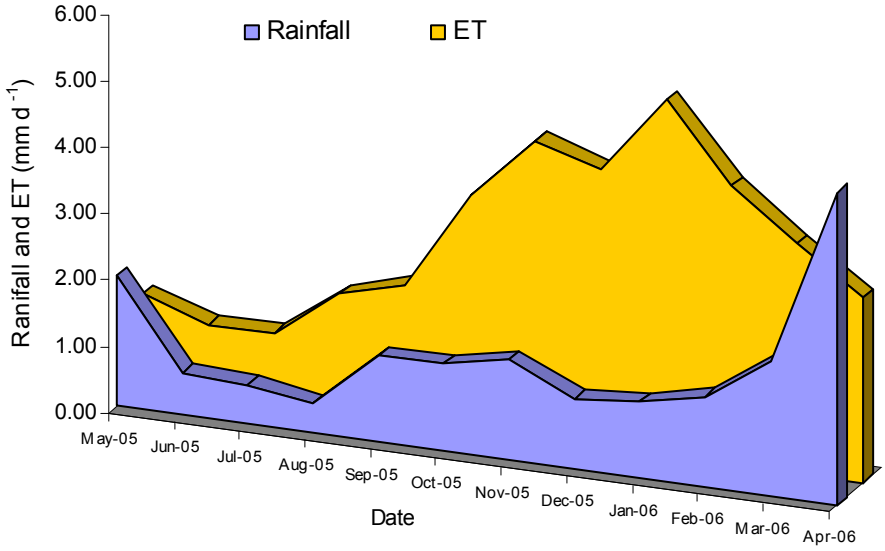

Figure 2.1 Monthly average rainfall and ET in the irrigation season of 2005/2006

An investigation report from Waikato in the North Island found no significant difference in faecal contamination between summer (samples collected between October and March) and winter (collected between April and September) (Collins 2002). There is no similar report on seasonal variation for the South Island or the Canterbury area.

A few studies have focused on the effect of initial soil wetness on preferential flow, though with conflicting results. Soil water content and hydraulic loading rate are important factors in the velocity of downward migration of bacteria and also influence the number of bacteria moved to depth (Hegde and Kanwar 1997; Stevik *et al.* 1999). It is known that high hydraulic loading rate increase the water velocity through larger pores (Bouma *et al.* 1974) and reduces the exchange between mobile and less mobile water. High water flow rates result in more irregular flow patterns as compared with low flow rates, and

consequently the degree of lateral and longitudinal dispersion is higher under high flow rates (Dekker and Ritsema 1996). Hamdi (1994) also found for a conservative tracer that there is higher initial risk of groundwater contamination under ponded irrigation than under sprinkler irrigation, and the variability was much greater for the ponded plots than for the sprinkler plots. This implies that the irrigation scheme is a critical factor for controlling (or preventing) bacteria from travelling to the deeper soil profile and groundwater.

There are two main irrigation regimes for pastoral use in New Zealand: flood irrigation (border dyke) and spray irrigation. Previous solute transport research suggested that flood irrigation results in lower nitrate concentrations in the leachate than spray irrigation, due to the greater dilution of soil solution nitrate by the larger volume of irrigation water applied (Di *et al.* 1998). However, no relevant research has been done for bacterial leaching in Canterbury soils.

Dairy farms need recommendations for better performance to reduce environmental risk. Landcare Research (Hamilton) researchers have investigated bacterial transport within short periods (a few days) with spray irrigation at a constant rate for several New Zealand soil types from both North and South Island. However, further work is needed to find quantitative relationships between irrigation practices, soil properties and microbial leaching under general field practices.

Several publications describe the physical process of bacterial transport as equivalent to simple colloids transport (Bouwer and Rittmann 1992; Albinger *et al.* 1994). However, because bacteria are living organisms, their transport in soil is more complex than is the case for abiotic colloid (Ginn *et al.* 2002).

2.4 Selected biological, chemical and physical characteristics of DSE

DSE primarily consists of faeces, urine and washdown water, but can also contain storm water, spilled milk, soil and feed residue, detergents and other chemicals. Together, these constituents contain nutrients, organic matter, non-harmful or harmful (pathogens) microorganisms, sediments and toxins which are potential contaminants. Pathogenic organisms are found in DSE in various quantities depending on local conditions, e.g. livestock density and season. Vinten *et al* (2002) have reported that dairy farm slurry contains total numbers of *E. coli* from 2.2×10^4 to 5.7×10^5 cfu mL^{-1}. Aislabie et al (2001)

found that the bacterial indicators concentration level is 10^4-10^5 cfu mL^{-1} for faecal coliforms and *E. coli* and 10^2-10^4 cfu mL^{-1} for faecal enterococci. In a pilot experiment conducted by the author for DSE taken from Lincoln University Dairy Farm, in the summer of 2004, the level of total faecal coliforms was found to be of the order 10^4 cfu mL^{-1} (*E. coli* proportion was more than 90%); and faecal enterococci was at 10^{-2} level or less. The pH was 7.6-8.9 (see Table 2.2).

It is important to note that most coliforms are non-pathogenic to humans and animals. However some strains are pathogenic, and thus total faecal coliforms and total *E. coli* are measured as representative indicators of the pathogenic strains.

Cameron (2004) reported that the N-content of DSE from Lincoln University Dairy Farm was 238-350 mg N L^{-1} during the period of 1998-2000. Silva (1999) analysed DSE during May 1996- Feb. 1998 and obtained: pH: 7.1-8.8, total N 120-423 mg N L^{-1}; total C ranged from 750-6500 mg L^{-1} (Table 2.2). Analysis results of DSE obtained by the author in 2005-6 were between 180-530 mg N L^{-1} for N-content, 7.9-8.6 for pH, and 1493-1750 mg L^{-1} for total carbon in 2005/2006. The electrical conductivity was 3.5-3.9 mS cm^{-1}.

Table 2.2 Selected properties of DSE from literature or trial

Date	pH	Total N (mg N L^{-1})	Total C (mg C L^{-1})	Conductivity (mS cm^{-1})	FC (cfu mL^{-1})	Author
1996-1998	7.1-8.8	238-300	750-6500			Silva,1999
1975-2000		180-560				Longhurst,2000
Dec-95	8.6	662	530*			Di, 1998
May-96	8.1	350	650*			"
30-Sep-05	8.5	220	1612	1.56	1.65E+04	Author
8-Mar-06	8.2	280	1014	2.25	3.30E+04	"

* Organic carbon

Longhurst (2000) reviewed the N content of DSE, his results ranged between 180-560 mg N L^{-1}, and increased with years due to the increasing population of cows per ha. The N content of DSE from the same farm varied considerably throughout the lactation. On average, the N-content of DSE rose from the start of lactation to peak during September/ October (in New Zealand) then gradually declined again towards the end of the lactation. No similar research has been done in terms of the seasonal variation of enteric bacteria.

Currently, DSE application loading (depth) depends on its N content and number of application. Across New Zealand about one third of councils specify a nitrogen loading limit 150 kg N ha^{-1} yr^{-1}, and about one third specify 200 kg N ha^{-1} yr^{-1}. One council,

Environment Bay of Plenty (EBOP), uses a nitrogen loading limit of 300 kg N ha^{-1} yr^{-1} (Cameron and Trenouth 1999). In Canterbury, the allowed maximum loading rate is 200 kg N ha^{-1} yr^{-1} (Bidwell and Cameron 2001). The calculation to derive the area required and the depth of applied effluent is based on certain assumptions about the amount of nitrogen produced per cow, the volume of effluent produced, and the lactation period, all of which can vary greatly. It would be useful to know whether there was any correlation between N content and enteric bacteria concentration. Work carried out on pig effluent suggests that there is very little correlation between N content and the number of enteric bacteria (Noonan, 2005 personal communication). Further research about that for DSE needs to be carried out.

2.5 Modelling of microbial transport

A variety of computer models have been used to describe microbial transport processes between the soil surface and groundwater. A large number of conceptual models are now available to make detailed simulations of transient, variably-saturated water flow, heat movement and solute transport in the subsurface (Beven and Germann 1982; Harvey 1991; Harvey and Garabedian 1991; McInerney 1991; Yates and Yates 1991; Bouwer and Rittmann 1992; Blue *et al.* 1995; Corapcioglu and Choi 1996; Deshpande and Shonnard 1999; Schijven and Hassanizadeh 2000; Barkle 2001; Scheibe *et al.* 2001; McGechan and Vinten 2004).

During the past 30 years, the introduction of more powerful computers, advanced numerical methods and improved understanding of subsurface flow and transport processes, now provide opportunities for integrating the various processes involved. There have been recent advances in the availability and usability of reliable numerical models of soil water dynamics, such as HYDRUS (Kool and Genuchten 1991), Leaching Estimation And Chemistry Model (LEACHM) (Hutson and Wagenet 1995), MACRO[‡] and Soil and Water Integrated Model (SWIM) (Ross 1990; Verburg *et al.* 1996). These enable rigorous analysis of water balance scenarios using historical, statistically generated or observed climate data. Much better understood is the quantitative prediction of chemical (e.g. nitrate) transport, but less so for microbes, and this is an area where development is needed (Bond 1998).

[‡] Non-steady state model of water flow and solute transport in macroporous soils

Of all developed soil models, HYDRUS is the most widely used by soil scientists and is also used in this study. The HYDRUS-1D software package is a finite-element numerical model for simulating the one-dimensional movement of water, multiple solutes and heat in variably saturated media. The program numerically solves the Richards equation for variably saturated water flow and advection-dispersion equations for solute transport. The HYDRUS-1D software package has recently been developed to enable simulations in different situations (e.g. a dual-porosity variant of the model) (Šimůnek *et al.* 1998; Šimůnek and Hopmans 2002; Šimůnek *et al.* 2005).

Much more work has been done in batch studies, or with repacked soil columns for solute transport. However there are no risk assessments based on quantified microbial analysis followed by relevant recommendations (Conboy and Goss 2000). There is a need to link the modelling to an analysis of the conditions which increase the risk of microbial transport below the root zone, and hence to develop practical suggestions for water irrigation and waste application practices designed to protect water quality.

2.6 Previous research related to this research topic

As the Regional Council in the leading dairying area in NZ, Environment Waikato brought attention to microbial contamination from pastoral farming in the late 1990's (Ritchie 1999). Landcare Research (Waikato) has identified risks associated with the application rate. Application rates in the Waikato are up to 200 mm hr^{-1}, with 50 mm hr^{-1} being common. It is suggested that to avoid effluent moving below the topsoil, it should be applied at a maximum rate of 10-15 mm hr^{-1} with the maximum depth of 25 mm . Higher application rates may result in pathogens and nutrients leaching through to groundwater and possibly to surface water (McLeod *et al.* 2001; McLeod *et al.* 2003; McLeod *et al.* 2004).

Lysimeters are widely used to study water flow, solute or microorganism transport in the environment(Silva *et al.* 1999; Brown *et al.* 2000; Silva *et al.* 2000; McLeod *et al.* 2003; Abdou and Flury 2004; McLeod *et al.* 2004; Toor *et al.* 2004a; Toor *et al.* 2004b; Toor *et al.* 2005). The major advantage of lysimeters is the ability to control and measure the components of water as well as chemical balance and flux in soil. Due to their large volume, their exposure to climatologic conditions, study on undisturbed soil monoliths in lysimeters are expected to represent field conditions better than laboratory soil columns.

2.7 Summary

The soil can be considered to be a living filter in terms of its ability to physically, chemically and biologically treat dairy shed effluent. That natural water treatment system requires a few conditions to function properly.

Soil properties are the key factors controlling bacterial fate and transport, mainly via the soil hydraulic characteristic. Soil texture determines how much bacteria are filtered in the matrix, while structure determines the proportion of water flow, solute and pollutants going through by-pass flow. The by-pass flow (or preferential flow, macropore flow) poses risks of microbial contamination of groundwater as it can transport most of the water through a low proportion of pore space.

The total amount applied and methods application of both DSE and irrigation water determine, to a degree, the amount of drainage and the pollutants brought down by drainage water. Preferential flow readily happens when the irrigation rate exceeds infiltration rate or the surface water is ponded. A proper irrigation regime could decrease the preferential flow. The soil wetness before DSE application is also an important factor. However, there is conflicting information on its role from previous research.

Some research has identified that preferential flow could be the main factor controlling microbial leaching, but no regulations have taken that into consideration, probably because of a lack of both quantity and certainty of information, especially for specific regions, and for different soil types around New Zealand.

There is a need to bridge scientific research and general practice by using well designed field experiments, e.g. simulating on-farm practices, to understand the real processes of the fate and transport of bacteria. This would lead to information and recommendations to policy makers to adjust current practices in order to minimise microbial contamination resulting from land-applied DSE.

Chapter 3 Materials and Methods: General

3.1 Soil lysimeters

Plate 3.1 Lysimeter location

In order to closely simulate transport under natural conditions, six undisturbed soil lysimeters (500 mm diameter by 700 mm depth) were employed for the field experiments. Those lysimeters were obtained by the Centre for Soil and Environmental Quality (CSEQ), Lincoln University. The lysimeter collecting method was based on the technique of Cameron et al. (1992). They were collected from a pasture site close to Lincoln in 1996, Canterbury (latitude 43°38'south, longitude 172°30'east). The soil type is a Templeton fine sandy loam (Udic Ustochrept, coarse loamy, mixed, mesic) (Silva *et al.* 1999), which is an alluvial soil. Together with the Wakanui soil, it supports extensive areas of the intensive mixed farming on the Canterbury Plain and covers about 75,000 ha of the intermediate terraces of Canterbury lowlands (Cox 1978). The lysimeters were located in the ground alongside an open trench where the leachates were collected (Plate 3.1). The lysimeters had a typical New Zealand pasture mix of ryegrass (*Lolium perenne* L.) and white clover (*Trifolium repens* L.). Pasture was cut periodically to simulate typical grazing practice. The average soil temperatures in the lysimeters ranged from 6-18°C (winter-summer) at 100 mm depth.

The lysimeters were found to be free of faecal coliforms on the basis of an investigation by the author before the two main leaching trials were conducted.

3.2 Die off experiment

The die-off experiment investigated the die-off rate of bacteria at three temperatures in dairy shed effluent (DSE) in aqueous phase. The tested indicator bacteria included: *E. coli*, and faecal coliform (FC). The spiked bacterial tracer was antibiotic-resistant *E. coli* (AFC). The three temperature treatments (6, 12.7 and 18° C) covered the annual range from minimum to maximum temperatures of the lysimeters in the experimental field at the depth of 10cm. All DSE samples were kept in the dark. The concentrations of of *E.coli* and FC were measured once per day. Triplicates were applied in each treatment. See section 3.9 for details of the bacterial enumeration method.

3.3 Measuring the effective hydraulic conductivity of lysimeters under ponded infiltration

To obtain a relative assessment of the bulk flow characteristics of the six lysimeters, which contained intact soils with macropores, a steady-state method was applied to measure saturated flow under ponded infiltration. The steady-state method used the application of a constant rate of water irrigation onto the soil. When the outflow rate had stabilised, the effective conductivity K_{eff} was determined by measuring the constant outflow from the base of each lysimeter under ponded infiltration at the top. A single run was usually completed in a few hours. These K_{eff} values provide a fundamental relative characterisation of the saturated or near-saturated flow properties of the lysimeters (Table 3.1).

Table 3.1 Effective hydraulic conductivity (K_{eff}) of lysimeters A to F

Lys.	K_{eff} (mm hr^{-1})	Drainage class *
A	42	4: Moderate
B	123	5: Moderately rapid
C	250	6: Rapid
D	41	4: Moderate
E	110	5: Moderately rapid
F	33	4: Moderate

* Drainage class assigned by assuming K_{eff} represents an effective whole-lysimeter saturated conductivity, and using the drainage class in Bowler（1980）.

3.4 Dairy shed effluent collection and investigation

Most dairy farms use the method of spray irrigation for DSE application. Carr (2006) reported that 97% of the 541 dairies inspected discharged effluent via spray irrigation in the Canterbury region, for the 2005/2006 season.

The fresh DSE used in this experiment was collected from the nearby Lincoln University Dairy Farm (45% of the soils there are Templeton soils), where DSE is applied by a spray irrigation method. The cows had grazed ryegrass and white clover. The DSE applications at the dairy farm take place between 5-8 am (morning milking) and 3-5:30 pm (afternoon milking) from August to the end of May. During the process of milking, DSE is washed from the milking parlour and flows into a shallow pond then the storage pond (capable of holding 33,000 Litres). When DSE level in the storage pond reaches a certain height, the pump in the pond is started and DSE is transported by 100 mm PVC pipe to the centre of a centre pivot irrigator and distributed through pot spray applicators to pasture. The pump stops working automatically when the DSE level falls below a certain height. A few pulses of DSE are applied during one milking due to the DSE level change.

The actual application rate and depth in a single milking were investigated at this farm during evening milking on 27 Sept. 2005, and morning milking the next day.

Plate 3.2 Investigation of DSE application at LU Dairy Farm

The expected functional area for DSE application is between towers 4 and 5 of the centre pivot irrigator, which have separation distance of 61 metres. Thirty catch-can containers ($17x17x18cm^3$) were placed in a row, two meters apart in the area where the irrigator was heading to, almost parallel with the irrigator arm (Plate 3.2). The application depths were calculated using measured volume collected in each container and exposed area receiving DSE. The covered application area and total volume in a single milking were calculated on the basis of the

moving distance of the irrigator. The application rates were estimated by collected DSE volumes (or depths) divided by the time over one point (refer to section 3.7.1).

The DSE samples required for the lysimeter leaching trials were collected on the day of application at the morning milking and transported to the lysimeter site for both application, and for analysis of key DSE components.

3.5 Instrumentation of the lysimeters

In order to monitor the physical conditions inside the soil columns during water flow, a total of 72 sensors were installed, 12 in each of the six lysimeters. This included 24 tensiometers (with pressure transducers, Figure 3.3), 24 soil water content probes: time-domain reflectometry (TDR) and 24 temperature probes (see Figure 3.1 and Figure 3.4).

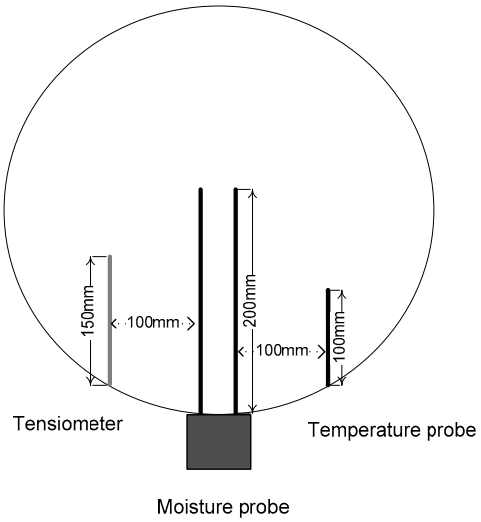

Figure 3.1 Plan view of a lysimeter, showing location of the sensors

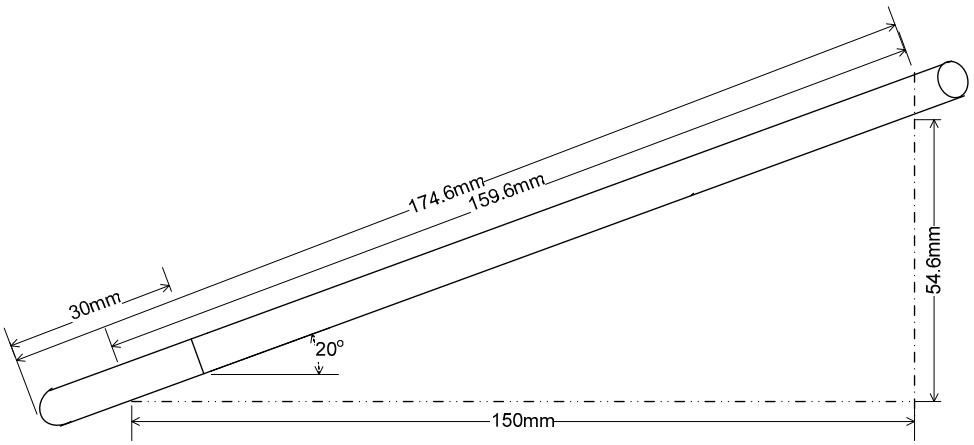

Figure 3.2 Insertion geometry of the tensiometers, at a downward angle of 20°

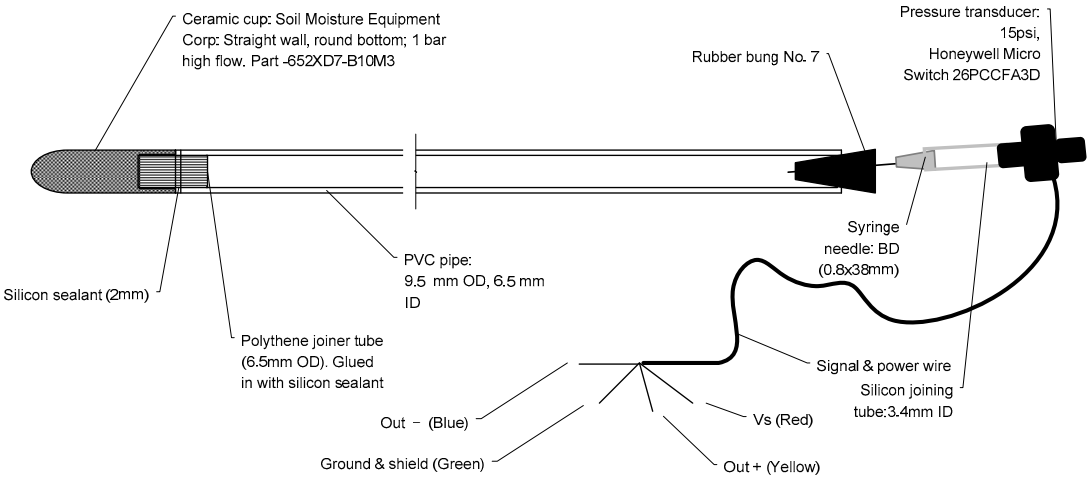

Figure 3.3 Schematic of the tensiometer and pressure transducer (adapted from Jiang 2005)

Each tensiometer consisted of a PVC pipe with a porous ceramic cup, filled with water (Figure 3.2). The top of the tube had a rubber bung used with a portable puncture tensiometer instrument (pressure transducer). This used a hypodermic needle to measure the pressure (suction) inside the tensiometer. As water is pulled out of the soil by plants and evaporation, the suction inside the tube increases; as water is added to the soil, the suction inside the tube pulls moisture from the soil and decreases (Figure 3.3).

Those sensors were calibrated individually in the lab, and then were installed in the lysimeters (Figure 3.4) as follows.

- Tensiometers with water potential transducers at four depths (100, 250, 450 and 600 mm) per column for measurement of soil water potential.
- TDR probes (Campbell Scientific CS 615), each with a pair of 20 cm long stainless steel waveguides, for measurement of soil volumetric water content at four depths (the same depths as for tensiometers).
- Soil temperature sensors (107-L, CSEQ) at the same depths as for tensiometers.

The insertion length of the probes was around 100 or 200 mm in from the lysimeter casing (see Figure 3.1). The temperature probes and water content probes were inserted horizontally and tensiometers were inserted at 20° downward angle through the lysimeter wall (see Figure 3.1 and Figure 3.2).

The datalogger sampling interval was 10 minutes, and the recording interval was 10 minutes for the first 24 hours following each application (DSE and water) and hourly

thereafter. Data from the datalogger were transferred to computer periodically (See Figure 3.4).

3.6 Bacterial indicators and tracers selected

Two indicator bacteria plus one bacterial tracer were used in this experiment: faecal coliform (FC), *Escherichia coli*, andantibiotic-resistant *E. coli* (AFC), which is a naturally-derived antibiotic-resistant *E. coli* (Sinton 1980) and was used as a tracer in trial 2 (the autumn Trial) of this project.

The different categories of coliform can be summarised as follows.

Faecal Coliforms are bacteria that are associated with human or animal waste. They usually live in human or animal intestinal tracts and their presence in drinking water is a strong indication of recent sewage or animal waste contamination. In general, increased levels of faecal coliforms provide a warning of failure in water treatment, a break in the integrity of the distribution system, or possible contamination with pathogens.

E. coli is a specific type of faecal coliform bacteria commonly found in the intestines of animals and humans. The presence of *E. coli* in water is a strong indication of recent sewage or animal waste contamination.

Antibiotic-resistant *E. coli* has considerable potential as a tracer of faecal-polluted water movement. Studies by Sinton (1980) indicate that it appears to meet the safety criteria of non-pathogenicity and inability to transfer its resistance characteristic, or to become established in the human gastro-intestinal tract. It exhibited survival rates in groundwater samples that were similar to that of a non-mutant *E. coli* strain (APHA,1998)

Conservative anions (Br or Cl^-) were added to the DSE, as their transport through soil provides a standard method for characterising dispersive flow through the soil pore space by an unreactive tracer.

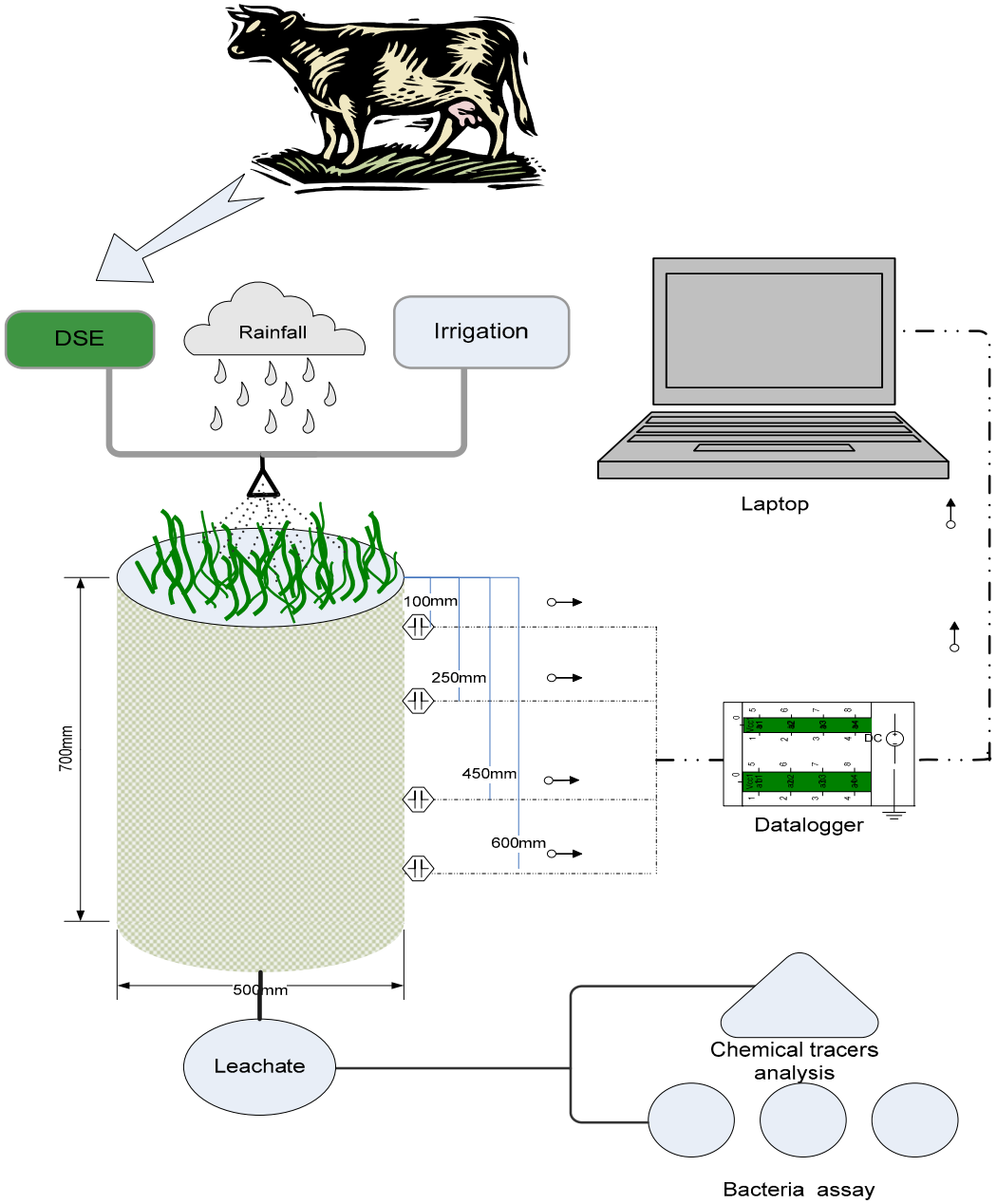

Figure 3.4 Lysimeter set up

3.7 DSE and water irrigation schemes, and seasonal water use

3.7.1 DSE irrigation

Two DSE application trials were undertaken:

Trial 1: summer, 30 Sept 2005 to 31 Jan 2006, nine water irrigation cycles; and

Trial 2: autumn, 6 March – 6 May 2006, four water irrigation cycles.

The depth of DSE application was 25 mm in both trials. This corresponds with the proposed permitted activity rule for maximum application depth, designed to control nitrogen leaching (Bidwell and Cameron 2001)..

The rate of application was based on investigation of LU Dairy Farm general practices. On the basis of investigation (Figure 3.5 & Table 3.2), 25 mm depth DSE was applied in 5 minutes.

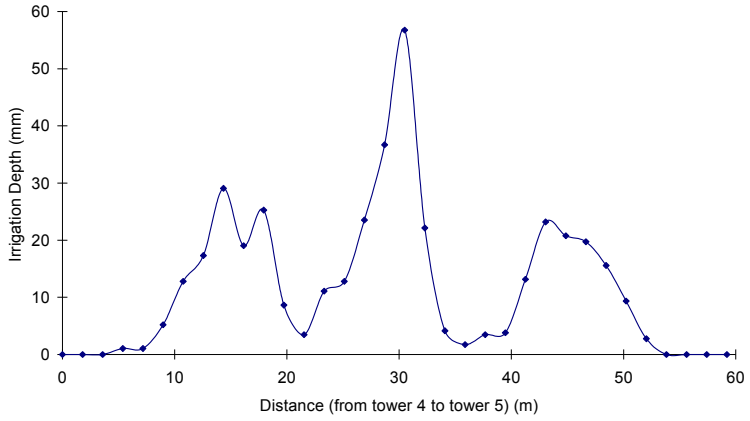

Figure 3.5 Spatial distribution of DSE application along the centre pivot arm at LU Dairy Farm, measured between towers 4 and 5 of the arm [§]

NaBr was spiked into DSE in Trial 1. The concentration of Br^- was 312 ppm, equivalent to an application rate of 100 kg ha^{-1}.

The second DSE application (in Trial 2) was spiked with antibiotic-resistant *E. coli* and NaCl. The concentration of Cl^- was 2000 ppm (Francis *et al.* 1988).

Table 3.2 DSE application at LU Dairy Farm

The total DSE volume per day (L d^{-1})	69890
The volume per cow per day (L cow^{-1} d^{-1})	134.4
Average DSE application depth (mm $application^{-1}$)	12.2
Max DSE application depth (mm $application^{-1}$)	56.8
Min DSE application depth (mm $application^{-1}$)	0
DSE application time over a point	3-5 mins

[§] The DSE is applied using centre pivot irrigator at LU dairy farm. The DSE application nozzles were set up between towers 4 and 5.

3.7.2 Water irrigation

Previous research and investigations have indicated that saturated flow, caused by flood irrigation or heavy precipitation, results in rapid bacterial transport in soils (Powelson and Mills 1998). In order to understand the fate and transport of bacteria in both normal and worst-case situations, two simulated water irrigation treatments were applied. These were one extreme application (on two lysimeters) and one conventional application (on four lysimeters):

- Flood irrigation (extreme): 100 mm on a 14-day cycle. This represents a 'worst case'.
- Spray irrigation (intermediate): 50 mm on a 14-day cycle. This is typical of irrigation regimes used by dairy farmers in the region.

Over the entire experimental period (30 Sep. 2005 to 6 May 2006), two trials were carried out. In Trial 1, one DSE application was followed by nine water irrigation events; in Trial 2, one DSE application was followed by four water irrigation events. All irrigations were applied by an automatic irrigation system designed by CSEQ technical staff, with one circular-pattern sprinkler targeted onto each lysimeter (Plate 3.1) In both trials, the first water irrigation was on the 6th day after DSE application This was based on the assumption that the soil moisture deficit would then be about half of the maximum deficit developed during each irrigation cycle (assuming that the soil was then at c. 50% water holding capacity). DSE application was followed by regular irrigation every two weeks. In Trial 1, applied water depths were 100 mm for flood irrigation fortnightly, and 50mm for spray irrigation fortnightly (see Table 3.3).

However in Trial 2 (autumn), spray irrigation amounts were reduced due to the lower evapotranspiration rates. To enable irrigation scheduling during Trial 2, an irrigation management spreadsheet was developed that carried out a daily water budget based on rainfall, irrigation water applied, and average daily potential evapotranspiration (McIndoe 1998). The use of average Lincoln daily potential evapotranspiration allowed a meaningful forward projection of soil moisture deficits to be made. The intention was to manage the system so that soil moisture deficits of no greater than 40 mm resulted to prevent stress and loss of yield. The calculations were as follows:

$$Average\ potential\ deficit = \frac{\sum_{1}^{14}(PET - RAINFALL)}{14}\ \text{mm d}^{-1}$$

Average potential deficit *14 – irrigation (mm) $\leq$ 40 mm

The averaged value was based on the previous fourteen days.

Flood irrigation was carried out by applying constant water flow into the lysimeter, which was kept ponded until 100 mm depth was completed (after approximately 0.5 hr). Spray irrigation was carried out by simulating dairy farm sprinkler rates, by applying 50 mm in 2 hrs in Trial 1 (which corresponds with the realistic application rate range of 25-40 mm hr^{-1} suggested by McIndoe (1998)), and the altered amounts in Trial 2 (Table 3.4).

The six lysimeters were allocated into two groups: two for the flood irrigation and four for the spray irrigation treatment. The arrangement was determined by the hydraulic conductivity values of each lysimeter obtained from the pilot experiment (K_{eff} , Table 3.1).

In Trial 1, the flood irrigation was applied on two lysimeters with moderately rapid hydraulic conductivity. It is expected to simulate the 'worst case' in dairy farm practices. The spray irrigation was applied on four lysimeters, which included one lysimeter (lysimeter C) with the greatest hydraulic conductivity and three other lysimeters with moderate hydraulic conductivity (Figure 3.6). It was expected to simulate the more general scenario by dairy farm, where spray irrigation is employed currently.

In Trial 2, flood irrigation was shifted to two lysimeters with moderate effective hydraulic conductivity (D and F), and spray irrigation was applied to the remaining four lysimeters (A, B, C and E). This was done in order to see the bacterial leaching in lysimeters with different hydraulic characteristics. Spray irrigation was applied to lysimeter A and C in both trials to observe (or study) the consistency during the whole irrigation season.

Table 3.3 Application schemes of DSE and water in Trial 1 (summer)

Application Date (days after application)		Application of	Label	Amount (mm depth)		Application rate (mm hr^{-1})		Application time (hr)	
				Flood irri.	Spray irri.	Flood irri.	Spray irri.	Flood irri.	Spray irri.
30-Sep-05	(0)	DSE	1st application	25	25	300	300	0.083	0.083
06-Oct-05	(6th)	Water	1-1st application	100	50	200	25	0.5	2
18-Oct-05	(18th)	Water	1-2nd application	100	50	200	25	0.5	2
03-Nov-05	(34th)	Water	1-3rd application	100	50	200	25	0.5	2
16-Nov-05	(47th)	Water	1-4th application	100	50	200	25	0.5	2
29-Nov-05	(60th)	Water	1-5th application	100	50	200	25	0.5	2
13-Dec-05	(74th)	Water	1-6th application	100	50	200	25	0.5	2
27-Dec-05	(88th)	Water	1-7th application	100	50	200	25	0.5	2
13-Jan-06	(105th)	Water	1-8th application	100	50	200	25	0.5	2
26-Jan-06	(118th)	Water	1-9th application	100	50	200	25	0.5	2

Table 3.4 Application schemes of DSE and water in Trial 2 (autumn)

Application Date (days after application)		Application of	Label	Amount (mm depth)		Application rate (mm hr^{-1})		Application time (hr)	
				Flood irri.	Spray irri.	Flood irri.	Spray irri.	Flood irri.	Spray irri.
08-Mar-06	(0)	DSE	2nd application	25	25	300	300	0.083	0.083
13-Mar-06	(5th)	Water	2-1st application	100	30	200	30	0.5	1
29-Mar-06	(16th)	Water	2-2nd application	100	30	200	30	0.5	1
11-Apr-06	(29th)	Water	2-3rd application	100	40	200	30	0.5	1.33
01-May-06	(49th)	Water	2-4th application	100	30	200	30	0.5	1

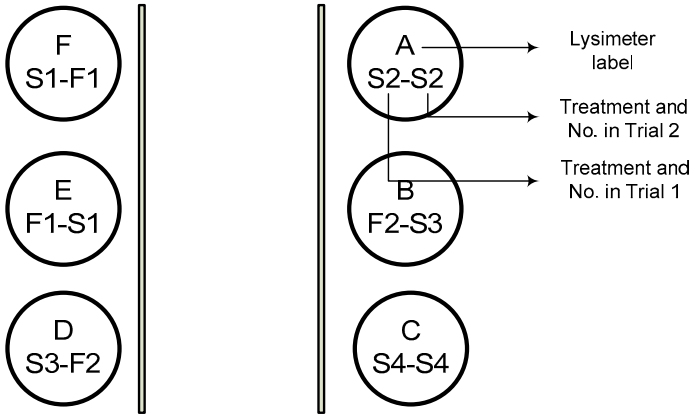

Figure 3.6 Water irrigation treatment overview showing lysimeters A-D and treatments (F=Flood irrigation, S=Spray irrigation)

3.7.3 Seasonal water use (water inputs)

Over the irrigation season (Sept. 2005 - May 2006), 21 (or 19 for flood irrigation) irrigation events took place (DSE irrigations inclusive). Depths applied ranged from 15-50 mm per irrigation for spray, and 15-100 mm per irrigation for flood irrigation. The water inputs (rainfall plus irrigation) were as follows.

Trial 1 (summer): From 30 Sep. 2005 to 31 Jan. 2006, totally 630.2 mm water was applied by spray irrigations (average of 35.6 mm per week), and 1080.2 mm for flood irrigations (average 61.0 mm per week). See Table 3.5.

Between Trial 1 and 2: During 31 Jan. -8 Mar. 2006, all lysimeters were maintained at the appropriate wet condition on the basis of water content readings. The total water input for lysimeters used for spray irrigation in Trial 1, was 131.6 mm (average of 26.3 mm weekly); and for lysimeters used for flood irrigation in Trial 1 it was 101.6 mm (average of 20.3 mm weekly). See Table 3.5.

Trial 2 (autumn)**:** From 8 Mar to 2 May 2006, a total of 346.0 mm water was applied by spray irrigations (average of 43.3 mm per week), and 616.0 mm for flood irrigations (average of 77.0 mm per week). See Table 3.5.

Table 3.5 Water input during irrigation season

		Spray irrigation		Flood irrigation	
Period	Days	Total (irri.+ rainfall) (mm)	Weekly average (mm)	Total (irri.+ rainfall) (mm)	Weekly average (mm)
Trial 1	124	630.2	35.6	1080.2	60.9
Interval between trials	35	131.6	26.3	101.6	20.3
Trial 2	56	346.0	43.3	616.0	77.0

3.8 Collection of leachate

Leachate samples from the lysimeters were collected intensively in the first 12 hrs after each irrigation (either a volume of around 2 L accumulated or every 2 hour, whichever occurred first). After 12 hrs, the leachate samples were taken once a day if they were available. During heavy rain, the leachate was taken as the leachate became available. Leachate was collected by sterilized plastic bag attached to the rubber tube connected to the drainage hole in the lysimeter base plate. The volume of leachate and time of collection were recorded, and subsamples of 100 ml were taken for bacteria assay, and 20 ml for chemical tracer analysis. The samples were put in cool room (4°C) within an hour after sampling. The leachate was collected under sterilized condition. All utensils were sterilized before being used. Enumeration of bacteria was done within 12 hours of collecting the leachate.

3.9 Bacterial assay

The membrane filtration technique was employed for faecal coliform (FC), antibiotic-resistant *E. coli* and *E. coli* measurement (American Public Health Association *et al.* 1998).

For the total FC test, pre-sterilized, gridded, 0.45-μm membrane filters were used for membrane filtration. The filters were inoculated with a sample from an appropriate dilution (one that would yield between 20-200 well-isolated colonies) and placed on Difco mFC agar. After incubation at 44.5$\pm$ 0.2°C for 24 hrs, the blue colonies present in culture media were counted as faecal coliforms.

The *E. coli* test followed the faecal coliform test step. The nutrient agar with MUG (NA-MUG) was used to differentiate the *E. coli*. After additional 4hrs incubation at 35°C, the colonies with sheen at the edge under UV light were counted as *E. coli*.

Antibiotic-resistant *E. coli* was selected by mFC medium with 50 mg-100 mg L^{-1} rifamycin added (Sinton 1980). 99% of faecal coliforms were suppressed, and only *E. coli* PB922 could grow on that medium.

3.10 Inert chemical tracer analysis

Bromide concentration in leachate samples was measured using a Bromide Ion-Selective Electrode (ISE, Orion 250A 96-35 BN, Thermo Scientific, Inc.). Chloride concentration in samples was measured by DX-120 Ion Chromatograph in the analytical lab in Lincoln University.

3.11 Climate data collection

Rainfall was recorded automatically at the experimental site using a tipping bucket gauge connected to a datalogger (Campbell Scientific, USA). Potential evapotranspiration data (mm day^{-1}) were obtained from the Broadfield climate station, located c. 2 km north of the lysimeter site. In this research, actual ET was approximated as the PET value. However the actual evapotranspiration may have varied between lysimeters due to variations in plant cover and health.

3.12 Lysimeter maintenance

During the experiment, the following maintenance actions were carried out:

- Mowing every two weeks or three weeks.
- Keeping PVC tube of tensiometer filled with water, by purging of air. In summer, they needed to be checked every 3 days.
- Application of insecticide when required (to control grass grub damage).
- Weeds were removed manually as required.
- During the interval between the two trials, all lysimeters were maintained with fortnightly spray irrigations of 15 to 30 mm to maintain normal grass growth.

3.13 Measuring hydraulic conductivity with tension infiltrometer

Plate 3.3 Tension infiltrometer apparatus

3.13.1 Tension infiltrometer

The tension infiltrometer consisted of three main components, namely an infiltrometer disc, bubble tower and water reservoir (Plate 3.3 and Figure 3.7). The disc diameter was 480 mm with an effective diameter of 460 mm. The disc base was made of stainless steel mesh with 3 mm diameter holes at 6 mm centres.

The device supplies water under tension or suction to a soil surface. The water tension can be set using the infiltrometer bubble tower. The water is supplied to the soil through the infiltrometer disk covered in a 23 micron gauze membrane.

3.13.2 Field and lab experiments

Measurements were made on the six undisturbed lysimeters (500 mm diam. x 700 mm depth), after completion of the two bacterial leaching experiments (Trials 1 and 2). The soil in the lysimeters was fine sandy loam (refer to section 3.1).

Grass in the lysimeters was carefully trimmed to ground level without disturbing the soil. A polyester cloth (Just Screen, NZ) of 20 μm mesh was laid on the lysimeter surface. Silica sand (Industrial Sands Ltd., NZ) of particle size 75-297 μm was poured on the top of the polyester cloth to a thickness of about 10-15 mm, and was flattened for maximum contact with the infiltrometer disk.

The water reservoir (70 L water tank) was filled with water leaving a small air space volume on the top. The infiltrometer disc was first filled with water to eliminate all air from the disc, and then was put above the contact sand. The bubble tower was calibrated to produce the correct suction in relation to the relative positions of the water-supply tube of the water reservoir and the lysimeter soil surface. All air was removed from the water-supply tube while the infiltrometer was immersed in a water bath. The reservoir was closed air tight and water suction was maintained at 40 mm (assuming that this would disable flow in pores with diameter greater than 750 μ m) (see Figure 3.7 & Plate 3.3). The experiment started with 40 mm suction, and then followed up with 0 mm suction for each lysimeter. Normally flow was maintained until a total of approximately one pore volume[**] (PV) had infiltrated.

As described in Section 3.5, all six lysimeters had been instrumented with tensiometers with water potential transducers, water content sensors (Campbell Scientific CS 615 probes) and temperature sensors (107-L), installed at four depths (100, 250, 450 and 600 mm). A pressure transducer was also connected to the water reservoir to measure changes in its water level. Data from this transducer were recorded every 1 mm increment and every 10 mins, then were stored in a datalogger. The data was used for calculation of infiltration rate (Figure 3.7).

[**] Pore Volume (PV) is defined as the ratio of a porous material's pore-space volume to its total volume, i.e. **pore volume** = total **volume** - material **volume =total porosity x total volume**

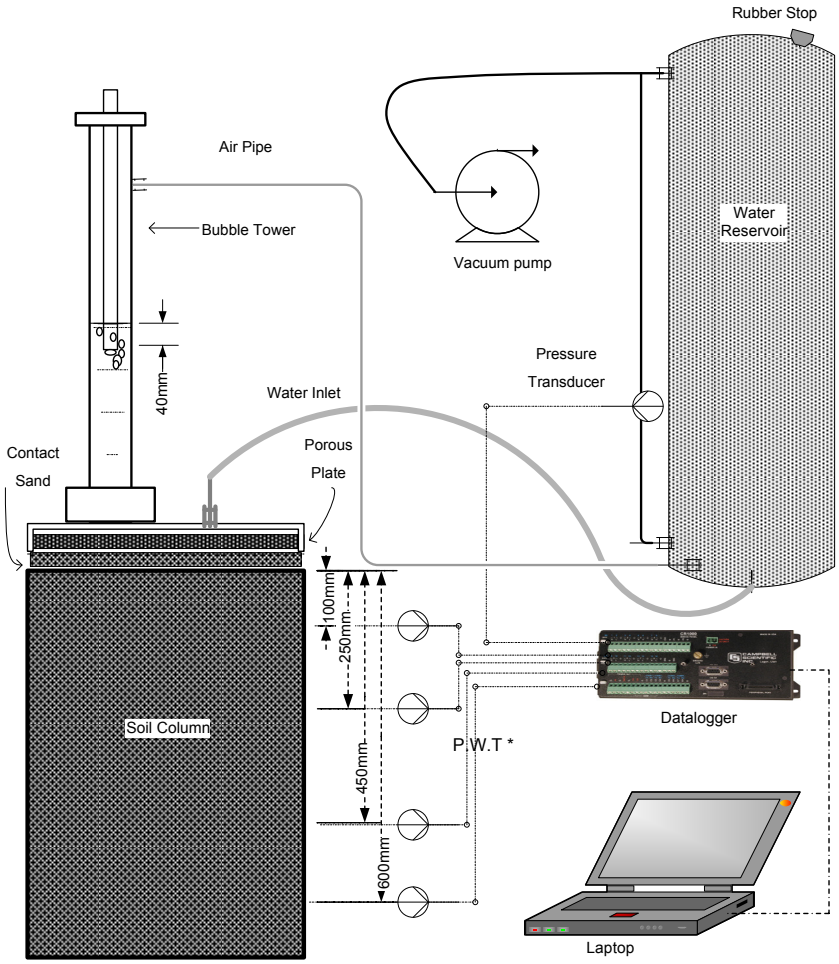

Figure 3.7 Schematic of the tension infiltrometer set-up.

*** P., W., T.= Pressure transducer, Water content and Temperature sensors**

3.14 Dye experiment

Following the tension infiltrometer measurements, a dye infiltration study was undertaken, in order to reveal qualitatively the relative development of macropores and the extent of preferential flow in the six lysimeters. Details of the method used are described in Chapter 5 .

3.15 Lysimeter dissection and sampling

Following all leaching experiments, and the tension infiltrometer and dye infiltration studies, all lysimeters were destructively sampled for final analysis of soil physical and

chemical properties, including bulk density, particle size distribution (PSD), organic carbon content and pH. Visual assessment of soil was also carried out.

Plate 3.4 Lysimeter being lifted out from side of the trench

Each lysimeter was lifted from the trench by a truck (Plate 3.4) and carefully transported to a workshop. The bottom drainage plate was removed and the lysimeter was shifted to a new base plate with a smaller diameter than the lysimeter casing, which was positioned on a specially constructed steel frame for supporting the lysimeter.

Then, soil sampling was done layer by layer. The lysimeter casing was gently lowered according to the sampling depths and the thin layer of petroleum jelly between the casing and soil was removed using a sharp knife. Triplicate samples were taken from each layer for measurement of PSD, organic matter and pH, Separate samples were taken for measurement of water release (refer to section 3.15.3).

3.15.1 Particle size distribution (PSD)

Three 100 g soil samples were taken from each of four depths in each lysimeter, for measuring PSD. For each lysimeter and depth combination, the three samples were mixed together, and a 100g sub-sample was taken. The total of 24 samples was sent to the soil analytical lab at Waikato University for PSD analysis, by a laser scattering method.

3.15.2 Organic matter and pH

Organic matter was measured by ignition at 500°C in a muffle oven, until stirring with a fine wire showed that all the organic matter had disappeared. The calculation is as follows:

% loss on ignition = (oven-dry weight-weight after ignition) ÷oven dry weight) ×100.

pH measurement followed the method in Balkemore (1987). A 15g fresh soil sample was suspended in 25 ml deionised water, which was stirred and left overnight. The suspension pH was read with a pH meter using buffers pH 4 and pH 7.

3.15.3 Pore size distribution

Pore size distribution was measured by methods based on the theory of the retention of water in pores of different size.

3.15.3.1 Sampling

Undisturbed soil core specimens were collected from four vertical sections (0-150 mm, 150-350 mm, 350-550 mm and 550-700 mm) using PVC rings (103.6 mm inner diameter and 50 mm in length) with a reinforced cutting edge. 3 replicates were randomly sampled from each section, giving 12 samples per lysimeter (Figure 3.8) Samples were used for bulk density as well pore size distribution measurement. The ends of each sample were trimmed, enabling determination of sample volume by simple measurement of the cylinder dimensions. Immediately after sampling, samples were wrapped at the lower end with cloth (20 μm) held by a rubber band, then sealed within two layers of plastic bags, then stored in an insulated cooler box.

3.15.3.2 Pore size distribution measurement using tension table

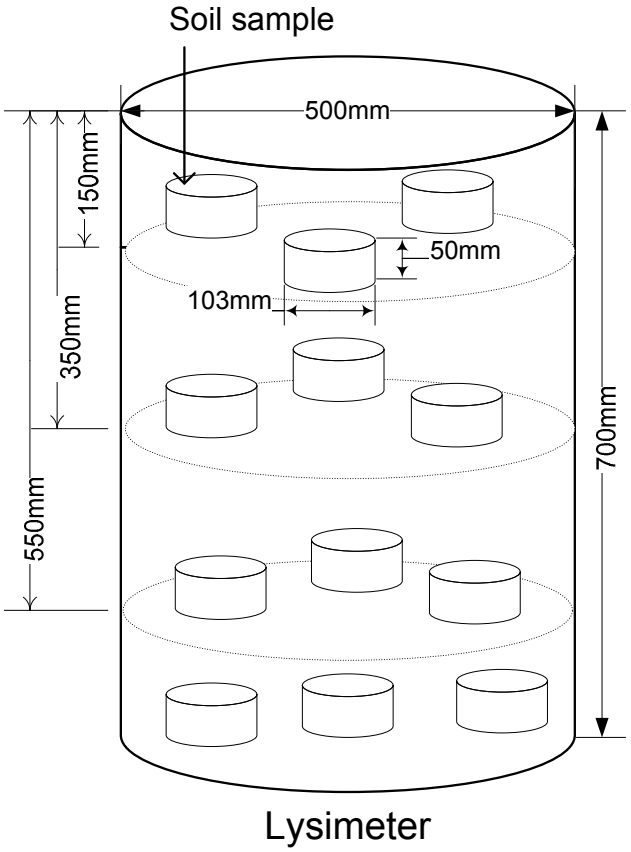

Figure 3.8 Soil samples for pore size distribution

Tension tables were used for measurement of the pore-size distribution and total porosity (Figure 3.9). The apparatus consists of a set of trays (360 mm x 420 mm) filled with saturated fine sand. A known suction is applied to the sand through a hanging water column by an adjustable control level at the side of the tray. Nine soil samples were laid on the surface of the fine sand. A transparent cover was placed on the tank to prevent evaporation. The water potential at any point in the specimen is equal to $-h$, i.e. the distance from that point to the free water surface below. The reference level in each sample was set as the distance from the middle of the core (Figure 3.9).

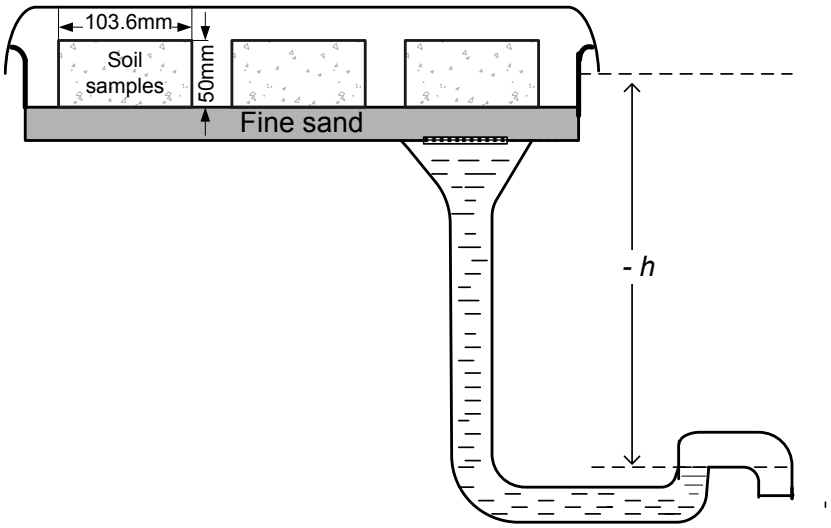

Figure 3.9 Section view of tension table for pore size distribution measurement

The samples were saturated for a few hours before being placed on the tension tables. A film of water was applied to the position on the plate where the specimen was to be placed this improved hydraulic contact. Once in position, the core was embedded by pressing down gently to establish good contact. The suction plate was then set to the desired value for the next measurement step. The suctions (*h*) applied were 40 mm, 100 mm, 200 mm, 500 mm and 1000 mm. Each sample was weighed at 0 mm (saturated), 40 mm, 100 mm, 200 mm, 500 mm and 1000 mm. The volume (derived by weight change) of water removed with each decrease in matric potential was used to determine the soil water characteristic. The equivalent diameter, d, of drained soil pores can be calculated from the following equation (McLaren and Cameron. 1996):

$$d = \frac{0.3}{h} \qquad \textbf{(3.1)}$$

Here, *h* and *d* are both in cm.

Porosity ϕ can be calculated from bulk density ρ_b and the average particle density ρ_s of the soil using the following equation:

$$\phi = 1 - \frac{\rho_b}{\rho_s} \qquad \textbf{(3.2)}$$

Values of particle density were in the range 2.6-2.65 g cm^{-3}.

3.15.4 Soil bulk density

Bulk density was measured from cylindrical core samples taken from the lysimeters. The mass was obtained by oven-drying the specimen to constant weight at 105°C. The procedure was as follows:

- Weigh a dry, oven-proof tin (w1)
- Cores were trimmed and all of the soil was pushed out of the coring ring into the oven-proof container. All soil was carefully cleaned out of the coring ring. The ring was weighed (w2).
- The soil in the container was dried in a well-ventilated oven at 105°C until the weight was constant (usually 24 to 48 hrs)
- The sample was cooled in a desiccator before weighing the container and oven-dry soil (w3)

The soil was then removed, oven-dried and weighed.

The bulk volume V comprises soil solids (s), air-filled pore–space (a) and water (w) at the time of sampling. Dry bulk density is the ratio of oven-dry mass (M_s) to the total volume.

$$\rho_b = \frac{M_s}{V_s + V_w + V_a} \qquad \textbf{(3.3)}$$

3.16 Summary

Six lysimeters were employed in this research. DSE (application depth 25 mm) with bacterial and chemical tracers was applied to the lysimeters twice, in two Trials: Trial 1 in summer and Trial 2 in autumn. Water irrigation was followed up on the 6th day, and then irrigation was applied fortnightly. The irrigation schemes applied were flood irrigation, and spray irrigation according to typical dairy farm practices in the Canterbury region. Leachates were collected for measurement of FC and tracer (Br^- or Cl^-) recovery.

The physical, chemical and biological properties of the lysimeters were investigated, including soil hydraulic and other soil properties. The lysimeters were equipped with probes for soil water content, soil water potential and temperature to enable real-time status monitoring during the leaching experiment. The properties of DSE, and common DSE application practices were also investigated.

This experiment employed natural soil columns, under outdoor climate conditions, using the DSE application method currently used at Lincoln University Dairy Farm and under simulated treatments of flood irrigation and spray irrigation schemes. Even though the above experimental design made the whole process more complicated, it represented a typical farm situation of bacterial transport and should be helpful for understanding the process of bacterial transport at the field scale.

Chapter 4 Transport of Bacteria and a Conservative Tracer through Undisturbed Monolith Lysimeters under Irrigations

Abstract This experiment investigated bacterial transport from land-applied dairy shed effluent, via field lysimeter studies, using two irrigation methods with contrasting application rates, through the 2005-06 irrigation season. Transient water flow and bacterial transport were studied, and the factors controlling faecal coliform transport are discussed.

Two application trials (Trial 1 summer, Trial 2 autumn) were carried out at Lincoln University's Centre for Soil and Environmental Quality (CSEQ) lysimeter site. Six undisturbed soil monolith lysimeters, 500mm diameter x 700mm deep, with a free draining Templeton fine sandy loam (Udic-Ustochrept, coarse loamy, mixed, mesic) were used. DSE was applied with spiked inert tracers: with Br^- as tracer in the summer trial, then Cl^- in the autumn trial. Then both applications were followed up with irrigations. A bacterial tracer (antibiotic-resistant faecal coliform-AFC) was added only in Trial 2 to distinguish applied FC from external or resident FC. Two contrasting water irrigation schemes were applied: flood irrigation (100 mm of water applied fortnightly); and spray irrigation (50 mm fortnightly). Leachates were collected after each water irrigation or heavy rainfall (when applicable) for enumeration of faecal coliforms (FC) and measurement of tracers. All lysimeters were instrumented for monitoring soil volumetric water content (θ), matric potential ψ and temperature at four depths (100, 250, 450 and 600 mm).

The results showed that bacteria could readily penetrate through 700 mm deep soil columns to the bottom, when facilitated by water flow. In the summer trial, FC in leachate as high as 1.4×10^6 cfu 100 mL^{-1}, similar to concentration of DSE, was detected in one lysimeter with higher clay content in topsoil immediately after DSE application, and before any water irrigation. This indicates that applied DSE leached through preferential flow paths without any dilution. The highest post-irrigation concentration was 3.4×10^3 cfu 100 mL^{-1} under flood irrigation. Flood irrigation resulted in more bacteria and Br^- leaching than spray irrigation. Trial 2 (autumn) results also showed significant differences between irrigation treatments in lysimeters sharing similar drainage class (moderate or moderately rapid), flood irrigation again gave more bacteria and tracer (Cl^-) leaching.

Bacterial concentration in the leachate was positively correlated with both θ and ψ, and sometimes drainage rate. Greater bacterial leaching was found in the lysimeter with rapid whole-column effective hydraulic conductivity, K_{eff}, for both flood and spray treatments. Occasionally, the effect of K_{eff} on water movement and bacterial transport overrode the effect of irrigation. The 'seasonal condition' of the soil (including variation in initial water content) also influenced bacterial leaching, with less risk of leaching in autumn than in summer.

These findings contribute to our increased understanding of bacterial transport processes on the field scale.

Keywords Faecal coliform; bacterial transport; chemical tracers; Templeton soil; macropore; soil water content; water potential (suction); drainage rate; irrigation; soil structure; soil texture.

4.1 Introduction

Nowadays, land application of DSE is a common practice around New Zealand, as a means of nutrient recycling and contaminant removal. As the dairy industry trend towards larger milking herd size continues in Canterbury, the potential will increase for both 'point source' and 'non-point source' pollution by land application of wastes. Current regulations for DSE application focus on N leaching, and are: 150 kg N ha^{-1} yr^{-1} in the Waikato region; and 150-200 kg N ha^{-1} yr^{-1} in Canterbury (ECan and Dexcel Ltd. 2004; EWRC and Dexcel Ltd. 2005). However, the risk of groundwater contamination by pathogens also demands attention, especially in Canterbury, which has NZ's largest average herd size (Livestock Improvement Ltd. and Dairy InSight NZ 2004-2005).

Recent reports on groundwater monitoring show that there are N, P and *E. coli* contaminations of groundwater in DSE application areas, both in the South Island and Northland (Monaghan and Smith 2004; Close and Dann 2005). Thus governing authorities face the challenge of designing policies to re-orient agriculture toward safer practices. Information is needed on the effects of DSE land application on microbes in groundwater, under different irrigation and DSE application practices.

Over the last decade, some research progress has been made in NZ, largely on leaching of chemical from land-applied effluent and waste (including nitrogen, phosphorus, pesticides or estrogen) and to less extent of microbes. However the mechanisms of contaminant transport differ between chemicals and microbes. Similar to chemicals, microbes are subject to dilution and adsorption, but unlike chemicals, microbes are subject to die-off/growth, predation, filtration and the pore-size exclusion effect. For nitrogen leaching, as chemical changes are taking place, the form of nitrogen in soil is of great importance. Nitrate is the most susceptible to leaching, followed by ammonium and organic forms of N. An effective mitigation technology to reduce nitrate leaching has been developed by using nitrification inhibitors e.g. dicyandiamide (DCD). It is also found that nitrogen leaching depends on the total N applied, and on the application methods (including timing) (Silva *et al.* 1999; Cameron and Di 2004). Evidence suggests that irrigation schemes influence nitrogen leaching by the way of flood irrigation giving lower concentrations leaching than spray irrigation, while it is generally expected that irrigation would facilitate leaching of microbes. The explanation is probably dilution and enhanced denitrification from flood irrigation (Di *et al.* 1998; Di and Cameron 2005). For phosphorus leaching

from DSE, unlike sewage, it is considered to result in a low risk of leaching, especially inorganic P, due to its strong sorption to soil particles (Toor *et al.* 2004b). However, P leaching is a concern in some sandy soils, and also it has recently been reported that preferential flow brought about great P leaching (Toor *et al.* 2005). There are also concerns about organic contaminations, like pesticides and estrogen, for which biological degradation and sorption are of importance.

It is well accepted that macropore flow can contribute most leaching of chemicals. Only a small fraction of pore volume may conduct more than 90% of water and contaminants. (Silva *et al.* 2000) found that pores > 600 μm, constituting < 20% of total porosity, contributed 98% of total N leached below 700 mm in a Templeton soil. Similar results have been observed in preferential flow research on pesticides or other solutes (Kladivko *et al.* 1991; Trojan and Linden 1992; 1998). This macropore flow impact is expected to be even more significant for microbes because of the size exclusion of microbes (Jiang *et al.* 2005). However, there is some evidence that macropores can also *reduce* the loss of contaminants, such as nitrate, where these macropores are present *within* the ped structure (Goss *et al.* 1993)

Bacterial leaching is a complex process controlled by soil type, environmental and management factors. This study aimed to a) directly measure the concentration and amount of FC leaching from lysimeters after DSE application, under two common irrigation schemes (flood and spray), and hence b) better understand the physical process of bacterial transport in soil by analysis of soil properties .

This can lead to information and recommendations to policy makers to adjust current practices in order to minimise microbial contamination resulting from land applied DSE.

4.2 Materials and methods

The materials and methods for this chapter are given in Chapter 3.

4.3 Results and discussion

4.3.1 The properties of soil

Table 4.1 shows the pH and organic matter content of topsoil (0-100 mm); the values of whole-lysimeter effective hydraulic conductivity (K_{eff}); and depth-averaged soil texture, bulk density, porosity and specific surface area, averaged on the basis of data measured by

layer. Figure 4.1 gives the bulk density and porosity versus soil depth (Table 6.1). It shows porosity varies inversely with bulk density. Soil bulk density and particle density were low in the top soil, and both increased with increasing depth. Soil porosity decreased with increasing depth (Figure 4.1).

Table 4.1 Selected properties for lysimeters A-F. Physical properties are whole-depth (0-70) average, and chemical properties are averages for top 10 cm only

	Soil in					
Property	Lys.A	Lys. B	Lys. C	Lys. D	Lys. E	Lys. F
pH	4.4	5.0	5.8	4.7	4.7	4.1
Organic matter (% w w^{-1})	6.7	6.2	7.2	7.2	6.3	6.1
Clay (% w w^{-1})	13.0	5.9	10.9	10.8	7.6	8.3
Silt (% w w^{-1})	50.6	45.1	49.2	56.3	51.0	52.2
Sand (% w w^{-1})	36.2	49.0	39.8	32.9	41.4	39.5
Specific surface area (m^2g^{-1})	2.75	0.34	1.99	0.55	0.42	0.45
Bulk density (g cm^{-3})	1.29	1.35	1.37	1.37	1.26	1.32
Porosity (% v v^{-1})	0.51	0.49	0.48	0.48	0.52	0.50
Textural class *	Silt loam	Sandy loam	Loam	Silt loam	Silt loam	Silt loam
K_{eff} (mm hr^{-1})**	42	123	250	41	110	33

* McLaren and Cameron (1990)

** Measured by steady state-flow method before the leaching experiment

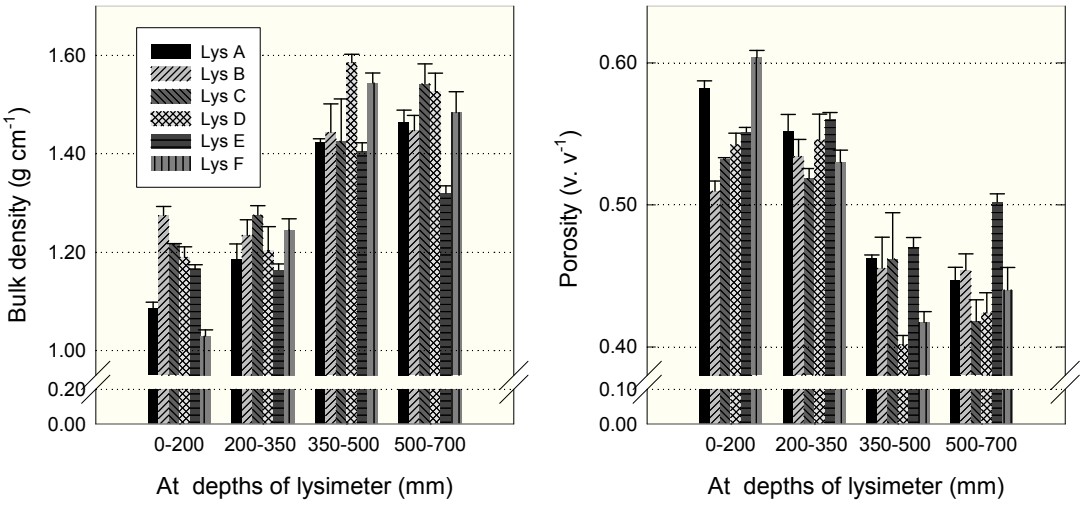

Figure 4.1 Bulk density (left) and porosity (right) in four layers in the six lysimeters (A to F) with standard deviations

Particle size distribution results are given in Table 4.1 and Figure 4.2. Texture varied between lysimeters: Lysimeters A and C had more clay in the topsoil; D had the least sand, especially in the second layer. Soil texture had been classified according to the International Society of Soil Science (McLaren and Cameron. 1996).

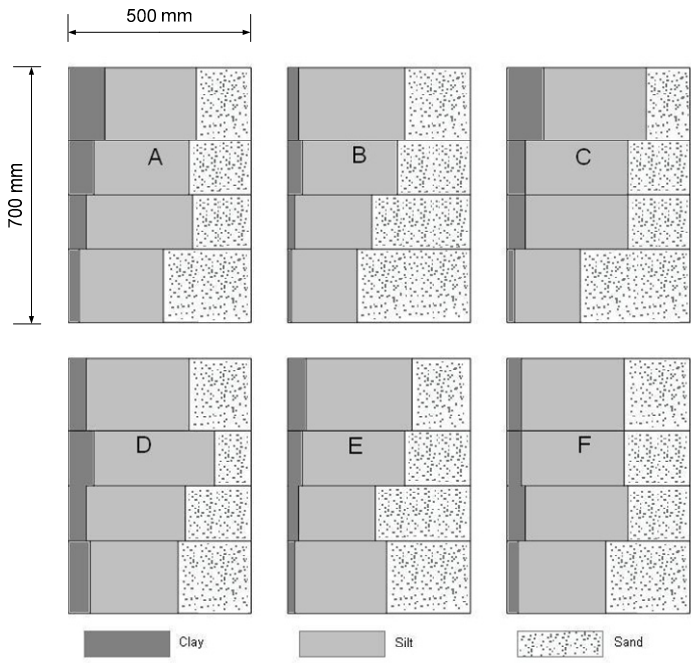

Figure 4.2 Particle size distribution at four depths in lysimeters A-F

4.3.2 The properties of DSE

Table 4.2 Selected biological, chemical and physical characteristics of DSE over 2005/2006

Sampling date	pH	Total N (mg L^{-1})	Total C (mg C L^{-1})	Conductivity (mS cm^{-1})	FC (cfu mL^{-1})	Note
10-Feb-05	8.1	260	1578	3.53	3.05E+04	afternoon mi king
17-Feb-05	8.3	348	1810	3.85	2.90E+04	afternoon mi king
15-Mar-05	7.9	200	1031	1.44	7.00E+03	morning milking
11-Apr-05	8.3	370	2282	1.56	1.00E+04	afternoon mi king
15-Apr-05	8.7	510	2146	3.68	2.20E+04	afternoon mi king
15-Aug-05	8.1	180	621	2.02	1.50E+03	185cows around
31-Aug-05	8.5	200	715	2.67	3.40E+03	400cows around
21-Sep-05	8.2	490	1516	5.42	5.60E+03	520 cows around
26-Sep-05	8.4	530	1939	5.42	1.85E+04	afternoon mi king
27-Sep-05	8.3	260	1605	2.24	1.05E+04	morning milking
30-Sep-05	**8.5**	**220**	**1612**	**1.56**	**1.65E+04**	**morning milking for Trial 1 (summer)**
8-Mar-06	**8.2**	**280**	**1014**	**2.25**	**3.30E+04**	**morning milking for Trial 2 (autumn)**

Note: Milking stoped during 7th June -1st August 2005

The last two DSE samples (shown in bold) in Table 4.2 gave the properties of DSE used in the two trials.

The DSE samples were collected and analysed over the year 2005-2006 for nitrogen, carbon, pH, conductivity and bacterial indicators. The results are given in Table 4.2. pH ranged from 7.9 to 8.9. The level of total FC was reasonably stable and found to be about 10^6 cfu. 100 mL^{-1} (of which the E. coli proportion was more than 90%). The faecal coliform concentration was lower than the value (10^6-10^7 cfu 100 mL^{-1}) reported in the

literature (Aislabie *et al.* 2001; Vinten *et al.* 2002). Total nitrogen and carbon varied, depending on the washing water usage and the population of cows on hold.

4.3.3 Total water balance

4.3.3.1 Weather data for the 2005-2006 irrigation season

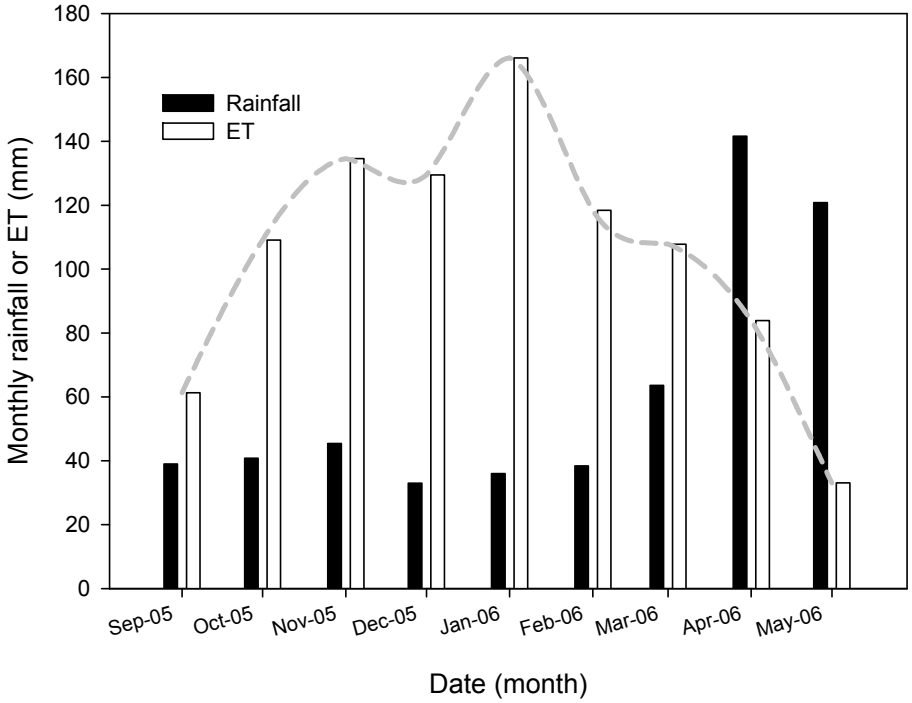

Figure 4.3 Monthly rainfall and PET from Sept. 2005 to May 2006 (irrigation excluded)

The monthly rainfall and potential evapotranspiration (PET) are shown in Figure 4.3. From Sept.2005, monthly rainfall remained below 50 mm until Feb 2006, while PET increased from 60 mm monthly, peaking at 164 mm for Jan. 2006. Trial 1 was carried out during that period. After that, the rainfall increased, while PET decreased, giving higher water deficit in summer than in autumn.

4.3.3.2 Total water inputs, evapotranspiration and drainage

The water budgets are shown in Figure 4.4, Figure 4.5 and Figure 4.6. Figure 4.4 shows daily rainfall, daily ET, DSE and water irrigation amount and dates during the whole leaching experiment. The total water input in Trial 1 (30 Sept 2005-31 Jan 2006) was 1080 mm for flood irrigation, comprised of 155 mm of natural rainfall and 925 mm of flood

irrigation (DSE application inclusive). For spray irrigation, 630 mm was applied, comprised of 155 mm of natural rainfall and 475 mm of spray irrigation (DSE application inclusive). The evapotranspiration was 543 mm during this period. The average drainage was 657 mm (5.3 mm per day) for flood treatment lysimeters, and 124 mm (1.0 mm per day) for spray treatment lysimeters.

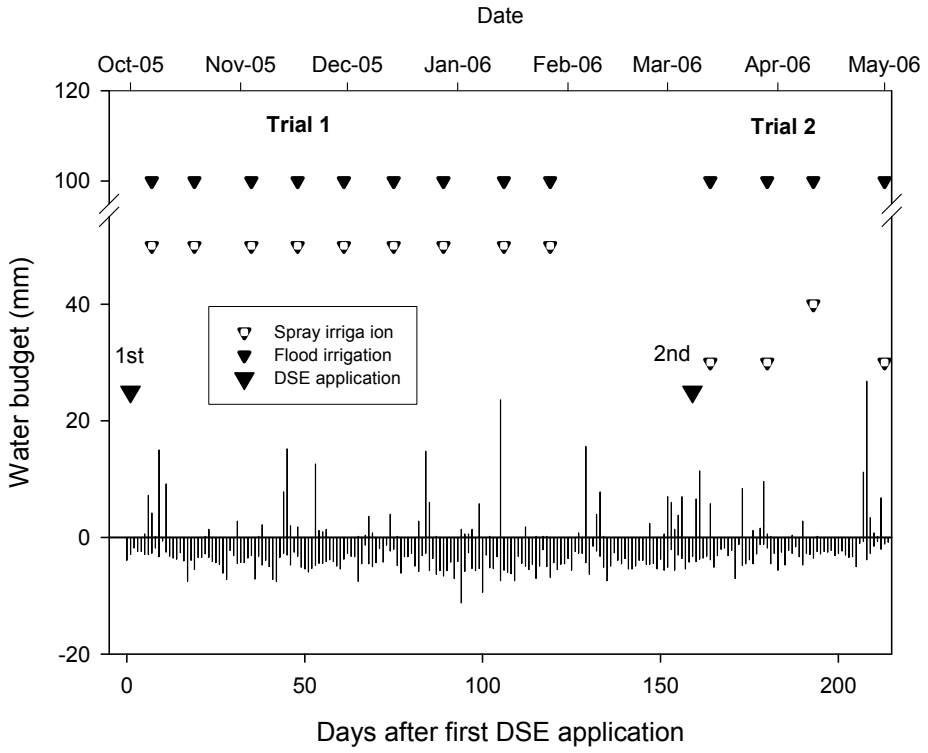

Figure 4.4 Weather data (daily rainfall and PET, DSE application and irrigation dates and amounts.

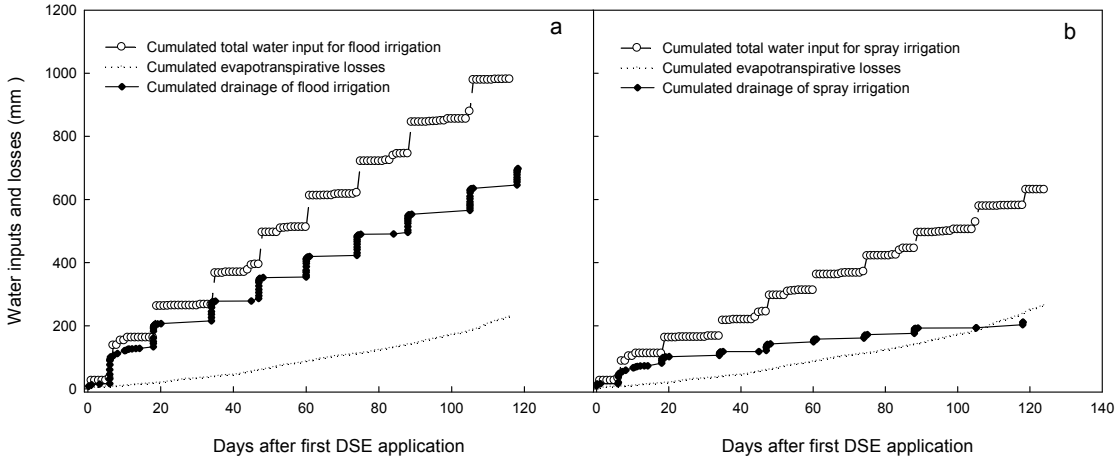

Figure 4.5 Cumulative total water inputs (= natural rainfall and irrigation), PET, and drainage losses from lysimeters during Trial 1 (30 Sept. 05- 31 Jan. 06), and for a) flood, and b) spray treatments.

During Trial 2 (8 Mar 2006- 3 May 2006), total water input was 616 mm for flood irrigation, comprised of 191 mm of natural rainfall and 425 mm of flood irrigation (DSE application inclusive). For spray irrigation, water input was 346 mm (= 191 mm of natural rainfall plus 155 mm of spray irrigation, DSE application inclusive). Evapotranspiration ET was 165 mm during this period. The average drainage was 200 mm for flood treatment lysimeters, and 82 mm for spray treatment lysimeters. The average daily evapotranspiration was 2.93 mm, lower than the 4.38 mm in Trial 1. The average rainfall was 3.41 mm per day, more than the 1.25 mm per day in Trial 1.

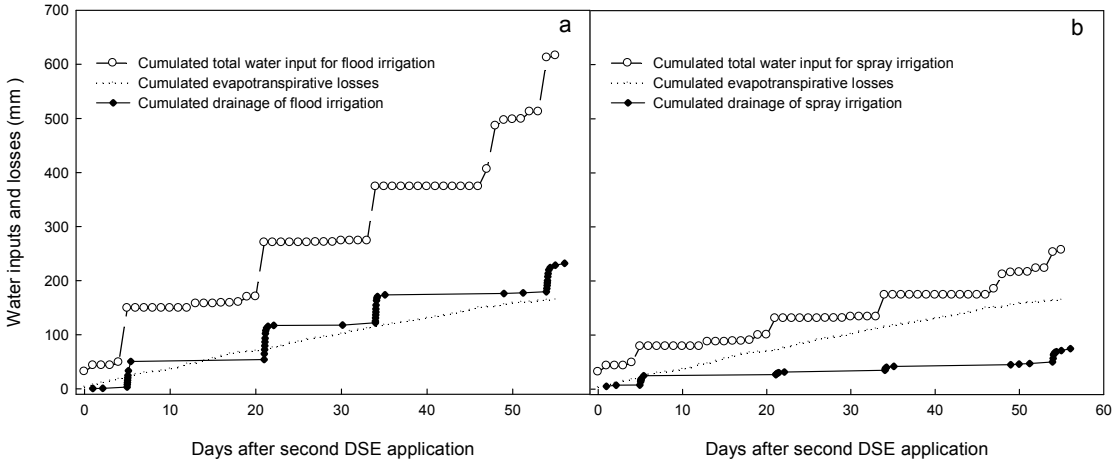

Figure 4.6 Cumulative total water inputs (= natural rainfall and irrigation), PET, and drainage losses from lysimeters during Trial 2 (8 Mar 06- 3 May 06), and for a) flood and b) spray treatment

Daily values of soil water content θ (Figure 4.7) and water potential ψ **(**plot not shown here) show that ψ had greater relative variation than water content, and the variation increased with time. Both water content and water potential data showed that the lysimeters were becoming drier during Trial 1. While during Trial 2 (autumn) θ was higher and kept steady, due to higher rainfall and lower ET. Figure 4.7 shows the daily θ at four depths during the whole irrigation season. The patterns of θ fluctuations in the six lysimeters were different, even within the same flux control treatment (see also section 3.7.2).

4.3.3.3 The status of lysimeters during the experiment period

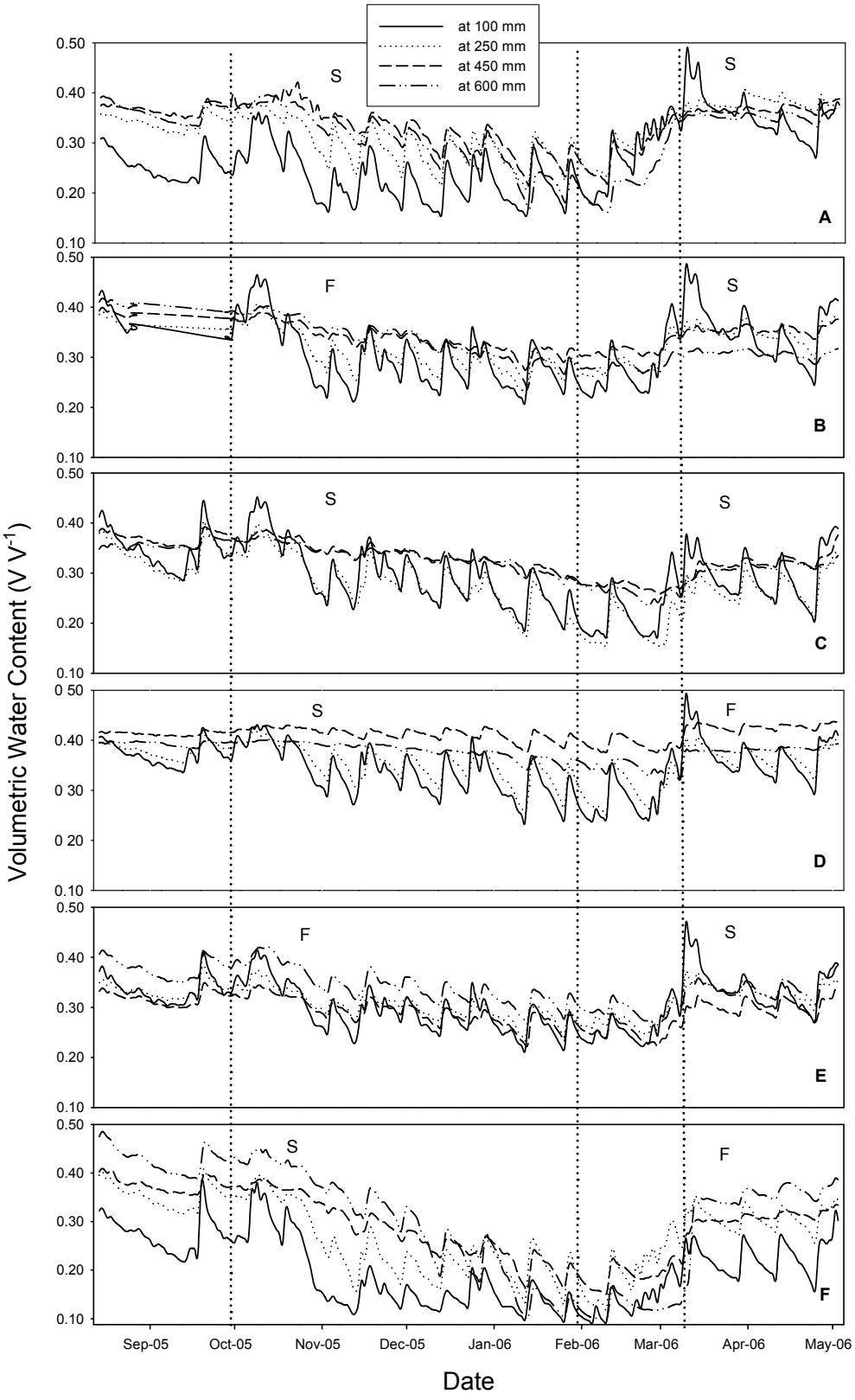

Figure 4.7 Soil volumetric water content at four depths during the whole irrigation season in lysimeters. A-F (divided into four periods by dotted vertical line: pre-application, Trial 1, interval between two trial s and Trial 2. F-flood irrigation, S- spray irrigation).

As mentioned in Chapter 3, in Trial 1 flood irrigation was applied in lysimeters B and E, and spray irrigation was applied in lysimeters A, C, D and F (see Figure 3.6). θ was above field capacity or near saturation prior to Trial 1. The potential deficit was 22 mm, due to 39 mm rainfall and 61 mm evapotranspiration in that period. Over the period of Trial 1, the water content decreased in all lysimeters. For the flood lysimeters, θ remained close to constant during the whole experiment, but with a slight downward trend. In the spray lysimeters, θ presented two situations: for two of them (C and D) θ did not change much during this experiment, but with a slight trend of decrease. For the other two (A and F) θ decreased more markedly, towards the 10% level. These results confirmed progressive seasonal drying of the lysimeters in Trial 1. The shallow layers show 'deep cycle' changes in water content, probably because roots preferred to take up water from shallow soil first. It was found that the water content fluctuation resulting from irrigation or rainfall could be seen in four layers in lysimeters A and F, but could only be seen in the first two layers in lysimeters C and D, not in the third and fourth layers. It is suggested that these lysimeters may have structural differences, or there might have been differences in cover plant composition. Also, there might be interlayer boundaries in or above those two layers where the barrier restricted the water from going deeper. In other words, there may have been water ponded at a certain level, removing the need for plant water uptake from the layer below.

4.3.4 Soil visual description from destructive sampling

The topsoil of the lysimeters was a thin layer (5-10 cm) of dark, loose soil with high organic content and in good structural condition. These layers had a good distribution of friable finer aggregates with no significant clodding. Lysimeter C was slightly different, with few firm topsoil clods. Worm holes and root channels could be seen until 40-45 cm in all lysimeters, but varying between lysimeters. Root penetration reached depths of *c.* 40 cm. Dark soil occupied the upper half column and stopped at around 35-40 cm. Below this, the soil was light brown in colour, constituted by a loam, sandy loam or loamy sand. The texture proportions differed between lysimeters (see also Figure 4.2). Lysimeter D differed in having more clay and silt, and less sand: it alone could be classified as loam in layer 3 and layer 4. Mottles were seen between 35 cm and 40 cm in each lysimeter, suggesting occasional waterlogging there, and thus anaerobic condition. The structure is discussed further below in Chapter 5 .

4.3.5 Characteristics of infiltration rate

Analysis of drainage amounts and rates provided insights about relative flow patterns between lysimeters. Drainage rate in five out of six lysimeters approached a maximum rapidly (between 0.5-2 hrs, after water application stopped), then declined quickly. Dripping continued until next day, from both flood and spray lysimeters in Trial 1. Klandivko (1991) observed a similar phenomenon, called "event-driven" in his pesticide study. However lysimeter D presented a different pattern. Its drainage rate increased gradually, remained steady for a few hours, and approached a maximum after around 6 hrs.

Bacterial leaching was observed in all six lysimeters. The maximum concentration in drainage was 1.4×10^{6} cfu $100mL^{-1}$, on the day of DSE application in lysimeter C without any water irrigation, the highest post-irrigation bacterial leaching was 3.4×10^{3} cfu 100 mL^{-1} in the flood irrigation treatment lysimeter B. The summary of results is shown in Table 4.3.

During **Trial 1** (124 days), lysimeters E and B (both in flood irrigation) gave 672 mm and 644 mm of leachate respectively; lysimeters F, A, D and C (in spray irrigation) gave 27 mm, 103 mm, 161 mm and 203 mm of leachate respectively. These leachate volumes are approximately in the order expected (Table 4.3). Lysimeter F stopped leaching from day 48 (16 Nov. 2005); Lysimeter A stopped leaching from day 49 (17 Nov. 2005). Recovery of FC and bromide is shown in Table 4.3. 0.48%-0.54% FC was recovered in flood treatments; while less than 0.1% FC was recovered in spray treatments, which excluded the bacterial leaching on the DSE application day. 31% and 58% bromide was recovered in the two flood treatments; 6-40% bromide was recovered in three of the spray lysimeters. Thus the irrigation treatment showed obvious effects on bacterial leaching, but no significant difference in bromide recovery. Probably more water application caused more bromide to distribute laterally which then become trapped in the soil matrix. Br^{-} was able to infiltrate through more pores under flood irrigation than under spray irrigation. Thus as deep seepage will occur through preferential flow paths, this will only move a part of the total material whatever the irrigation treatment. However, as bacteria were confined to large pores, more of these pores were accessible under flood irrigation than spray irrigation.

Flood irrigation gave more leachate than spray, enabling more bacterial leaching from lysimeters E (F1) and B (F2). The FC concentration peak was 10^{3} cfu 100 mL^{-1} in flood treatments; and more than 10^{2} cfu 100 mL^{-1} in spray treatments. The dynamics of water

flow contributed to this result. Trapped bacteria might be remobilized by changing water flow, resulting in higher outflow recovery. This differs from results for nitrate leaching research (Di *et al.* 1998), where lower nitrate concentrations were obtained in leachate under flood than under spray irrigation, due to enhanced denitrification at higher moisture content, and/or greater dilution of soil solution nitrate by the greater irrigation volume applied.

4.3.6 Bacterial leaching under different water irrigation schemes

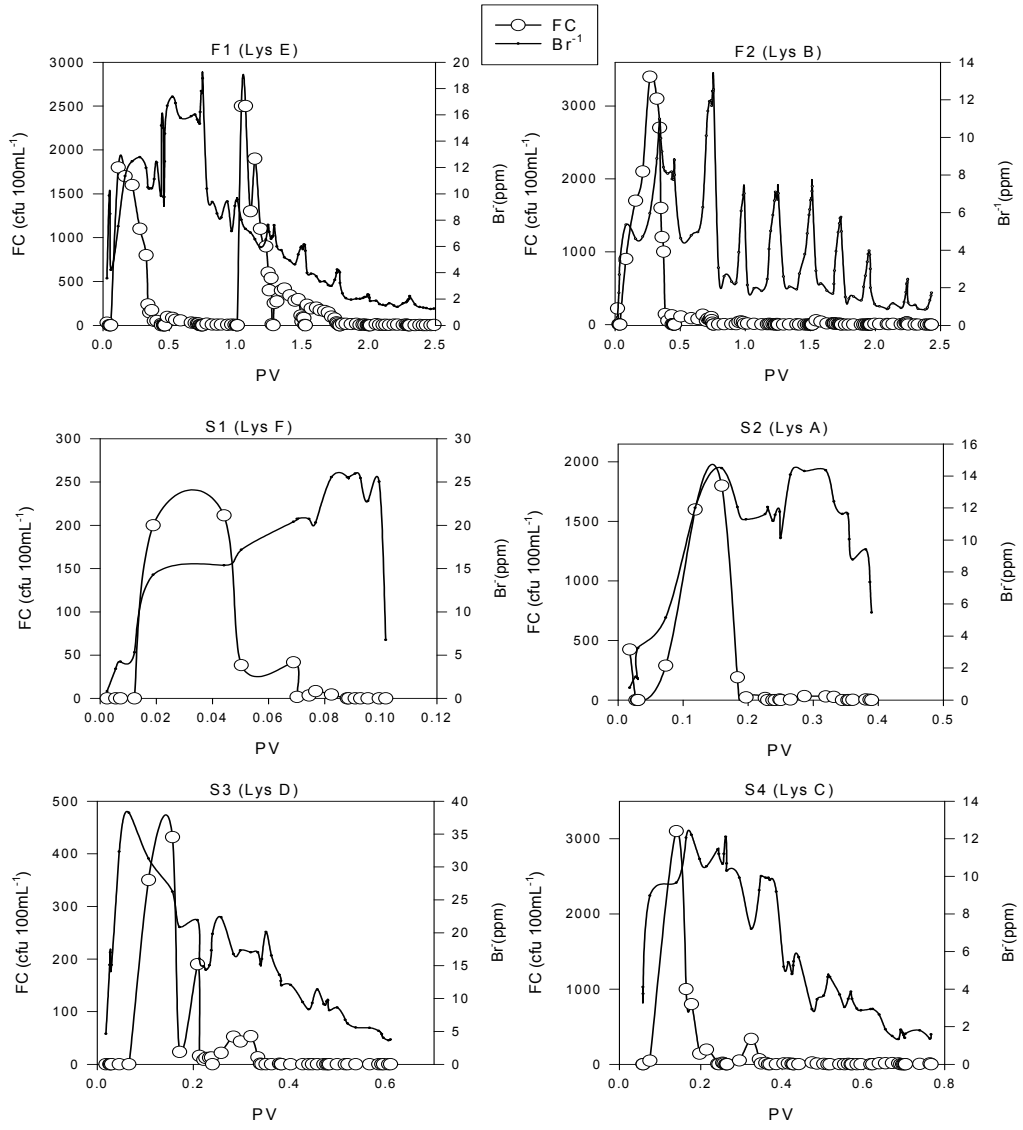

Figure 4.8 Breakthrough curves (BTCs) of FC and Br^- during Trial 1 (DSE application day exclusive)

Table 4.3 Overview of water irrigation effect on bacterial leaching in the two trials (DSE application day exclusive)

	Lys.	*Keff* (mm h^{-1})	Drainage class *	Treatment in Trial 1	Total leachate in Trial 1 (mm)	Bacteria recovery in Trial 1 (%)	Peak concentration of FC in leachate (cfu.100mL^{-1})	Bromide recovery in Trial 1 (%)
Trial 1	A	42	4: Moderate	Spray-2	95	0.10	1.80E+03	14
	B	123	5: Moderately rapid	Flood-2	635	0.48	3.40E+03	31
	C	250	6: Rapid	Spray-4	187	0.016	3.10E+03	40
	D	41	4: Moderate	Spray-3	153	0.029	4.31E+02	33
	E	110	5: Moderately rapid	Flood-1	640	0.54	2.50E+03	58
	F	33	4: Moderate	Spray-1	26	0.0054	2.37E+02	6

	Lys.	*Keff* (mm h^{-1})	Drainage class *	Treatment in Trial 2	Total leachate in Trial 2 (mm)	Bacteria recovery in Trial 2 (%)	Peak concentration of FC in leachate (cfu.100mL^{-1})	Chloride recovery in Trial 2 (%)
Trial 2	A	42	4: Moderate	Spray-2	114	0.001	2.00E+02	30
	B	123	5: Moderately rapid	Spray-3	115	2.7	2.18E+04	49
	C	250	6: Rapid	Spray-4	25	0.23	1.26E+02	31
	D	41	4: Moderate	Flood-2	232	0.007	2.30E+02	78
	E	110	5: Moderately rapid	Spray-1	75	0.001	1.40E+02	19
	F	33	4: Moderate	Flood-1	168	0.61	1.52E+04	53

* Bowler (1980)

The Br^- leaching peak occurred at or before the 3rd water irrigation (3 Nov. 2005) in all six lysimeters, and showed a lognormal-type distribution (Figure 4.8). For flood treatments, the peak Br^- concentration presented at nearly 1 pore volume (PV) of leachate; while for spray, it occurred at c. 0.2 PV. Comparing S1 to S3 with the two flood treatments, the earlier Br^- peak in S1 to S3 (on a pore volume scale) is as expected, and reflects the greater opportunity for trapping of bromide in the spray treatments by its immobilisation in finer pores (Figure 4.8).

Br^- is an inert tracer, while bacteria are subject to die-off, filtration and also bacteria are transported through the soil matrix in different water flow regions (mostly through bigger pores), therefore, they had different BTCs. Thus, recovery of FC was lower than Br^-. (Table 4.3), consistent with FC being a highly "reactive" tracer, while Br^- is largely non-reactive (although it can be trapped in the so-called immobile pore space).The FC peak was earlier than for Br^-. Flood irrigation caused higher flow rates, wetter soils, and thus higher recovery of FC and Br^-. However, there was an exception with lysimeter D (see Figure 4.8), where the peak FC concentration presented later than the peak Br^- concentration, probably due to the structure difference in lysimeter D.

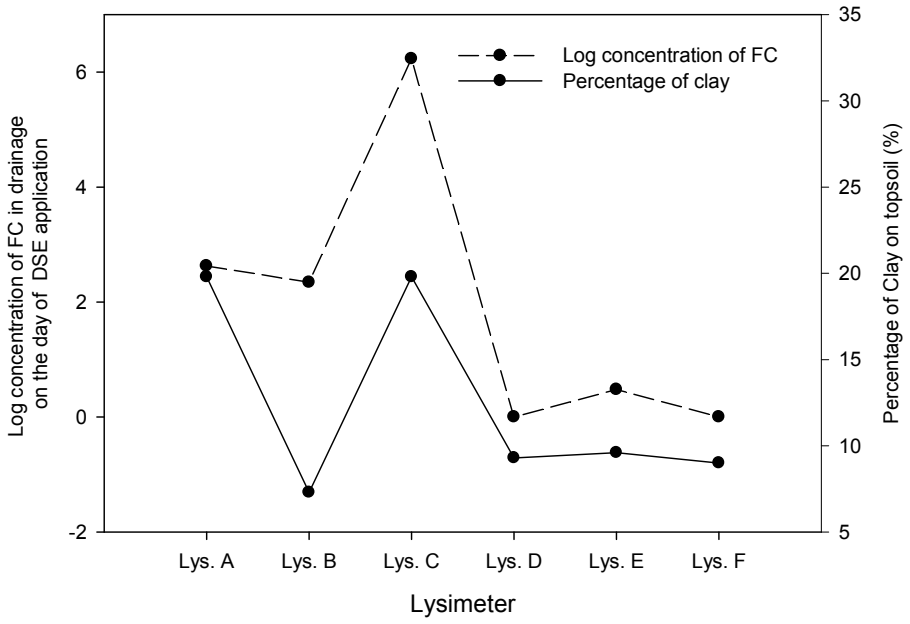

Figure 4.9 The relationship between soil texture (clay content) in topsoil and bacterial concentration in leachate on the day of DSE application

Results from lysimeter C (S4) showed markedly different response compared to other lysimeters receiving spray irrigation (S1, S2 & S3). On the DSE application day, the first sample was collected in S4 immediately after DSE application, with its FC concentration roughly the same as that in DSE (Table 4.4). Both bromide recovery and bacterial leaching in the first two days following DSE irrigation (without any water irrigation) were large: 47% and 36.8% in the first day; 62% and 39.6% in the second day, even though no water irrigation had been applied. The first sample contributed 99.6% of total FC leaching and 79.5% of total bromide leaching. The leaching was obtained just 10 mins after DSE application. It showed lysimeter C was exceptional in its ability to "fast-track" both bromide and bacteria to the lysimeter base, indicating the existence of connected macro-porosity down the whole lysimeter depth. That agrees with Bouma (1991) that the "travel time" for liquid to pass through a soil column by continuous macropores can be a few seconds instead of a day. Paterson (1993) saw a similar phenomenon with the influence of soil type on leaching of *Pseudomonas fluorescens* through intact soil microcosms (35 cm depth). *P. fluorescens* were detected immediately in leachate from the *clay loam* with a steady decline in the concentration with time, while leaching from a *sandy loam* and *loamy sand* only occurred over a few rain events, and total recoveries were lower than from the

clay loam. That shows the effect on leaching pattern due to soil structure, which is caused by the difference of soil texture. Fortunately, such pores are not always continuous in larger natural soil samples, but leaching can still result in serious contamination in shallow groundwater (Howell *et al.* 1995). Figure 4.9 shows the relationship between the clay content in topsoil and bacterial leaching on the day of DSE application. That agrees with the concept that soil with more clay is more likely to develop quasi-planar voids, in which water can rapidly flow through the soil column (Bouma 1991). McLeod *et al.* (1998) found similar results from dye research on two different soils. They found that the poorly-drained clay loam (Te Kowhai) showed more macropores than the well-drained loam (Horotiu). The depth of greatest dye spread (in terms of both horizontal and vertical extent) was generally associated with worm channels in the loam, while for the clay loam dye was also associated with voids between structural units. Their further research (2001) on four types of soil confirmed that a bacterial indicator readily moved through the clayey soils.

Table 4.4 gives the concentrations of nitrogen, FC and Br in the first two samples after DSE application in lysimeter C, which obviously indicated that physical interaction between soil and chemicals or organisms (like adsorption, retention and filtration) were much reduced during transport (Beven and Germann 1981). While macropores may represent a small portion of soil porosity, they can dominate solute transport (Beven and Germann 1982; Bouma 1991; Chen *et al.* 1999; Silva *et al.* 2000; Ersahin *et al.* 2002). Macropore flow probably accounts for the greatest leaching losses when a chemical is applied to the surface of a structured soil (Golabi *et al.* 1995) and a small fraction of macropores appears to dominate deep displacement of water and solutes in soil (Trojan and Linden 1992). That is similar to the conclusion of Silva et al (2000) who found in a nitrogen study that pores >600 μm diameter (under 5 kPa suction on the soil surface) transmitted about 98% of the total nitrogen (N) leached in a Templeton soil.

The existence of preferred flow paths within a medium dramatically changes the transport profiles, confirming the speculation that heterogeneities (macropores, fractures, etc) in the subsurface environment may be responsible for much of the long–range transport of microbes (Fontes *et al.* 1991). Besides, the high application rate for DSE (300 mm hr^{-1}) also contributed to the large macropores flow as it was high enough to cause temporary ponding at the surface.

Table 4.4 Concentration of N and FC in the first two samples of lysimeter C after DSE application

Item	Nitrogen (mg L^{-1})	FC (cfu 100 ML^{-1})	Br (mg L^{-1})
DSE	280	3.30E+06	312
S401	250	1.70E+06	294
S402	245	9.90E+05	223

There is a need to mention the eighth water application in Trial 1. In that application, the water for flood irrigation was given in a different way from the other applications, due to mechanical disorder. The water was given in two pulses. The patterns of bacterial leaching were then different from the other applications. The concentration of leachates fluctuated following water pulses: going down between water pulses and going up again in the second water pulse (Figure not shown here).

In **Trial 2**, four lysimeters were swapped between irrigation treatments. But lysimeters A (S2) and C (S4) received spray irrigation in both trials. In Trial 1, lysimeter C was always the first to give leachate. The situation changed in Trial 2. While the soil was drier before DSE application (θ < 25% in the first layer), lysimeter C gave more leachate. Just before the 1st water application, θ in the first layer was 36%, but no leachate came out in that application. A possible explanation is a change of soil structure. Lower water content (especially below 25% in the first layer) could contribute to crack formation, increasing preferential flow. Brewer (1964) reported that larger shrinkage cracking surfaces were developed only under very dry conditions, and once formed, tended to open in the same place in successive drying cycles, so were relatively permanent.

In Trial 1, after getting leachate, the water flow velocity increased very quickly in flood treatments, and then soon finished leaching. FC leaching in most applications followed the pattern that FC concentration in leachate changed from high to low. Unlike Trial 1, in Trial 2, when the water velocity reached a certain level, it kept constant flow for more than 2 hours. The concentration of FC (or AFC) increased gradually, and then decreased. This suggests that the structure of these lysimeters under flood treatment was different from the structure under flood treatment in Trial 1 (refer to Section 4.3.5).

Table 4.5 Initial water content before water irrigation in lysimeter C in Trial 2

Application	@ 100 mm	@ 250 mm	@ 450 mm	@ 600 mm	Average	Average for first two layers	Drainage (mL)
DSE	0.25	0.21	0.27	0.25	0.25	0.23	1181
1st water	0.36	0.26	0.29	0.29	0.30	0.31	0
2nd water	0.27	0.24	0.32	0.31	0.28	0.25	35
3rd water	0.24	0.24	0.31	0.31	0.28	0.24	1179

On re-wetting, soil swelling can close up cracks, thus no water flow reached the bottom and no drainage was obtained in the 1st water application of Trial 2. In the 4th water application, θ was higher than in other applications at all four measurement depths. With 30mm of water applied, 13.4 mm of leachate (= 45 % of the 30mm) drained from the bottom, presumably because the soil was above field capacity, and excess water drained out.

Table 4.3 compares bacterial leaching in Trials 1 and 2. In Trial 1, soil water content θ decreased with time, due to summer build-up of water deficit. Especially for spray treatment, θ could decrease to below 15% in the first two layers (Figure 4.7). In Trial 2, θ kept stable and was mostly above 25%. The weather data gave average daily evapotranspiration (E) and rainfall (P) values as follows: E = 4.38mm day^{-1}, P = 1.25 mm day^{-1} during Trial 1; and E = 2.93 mm d^{-1}, P = 3.41 mm d^{-1} during Trial 2. Thus in Trial 1 (summer), the drier conditions contributed to the formation of cracks, promoting preferential flow and greater bacterial leaching.

4.3.7 Correlation between drainage rate and FC concentration

Only for lysimeter E in Trial 1, the drainage rate and FC concentration show a significant correlation in all water applications. Figure 4.10 shows that the relation between drainage rate X and FC leaching is a linear correlation expressed by:

$$Y = aX + b \qquad \textbf{(4.1)}$$

here Y is FC concentration. The slope "a" does not seem to correlate with the soil water content or water potential (see Figure 4.10). It might relate with the background FC concentration in the soil column. There was no similar typical pattern observed in any other lysimeters.

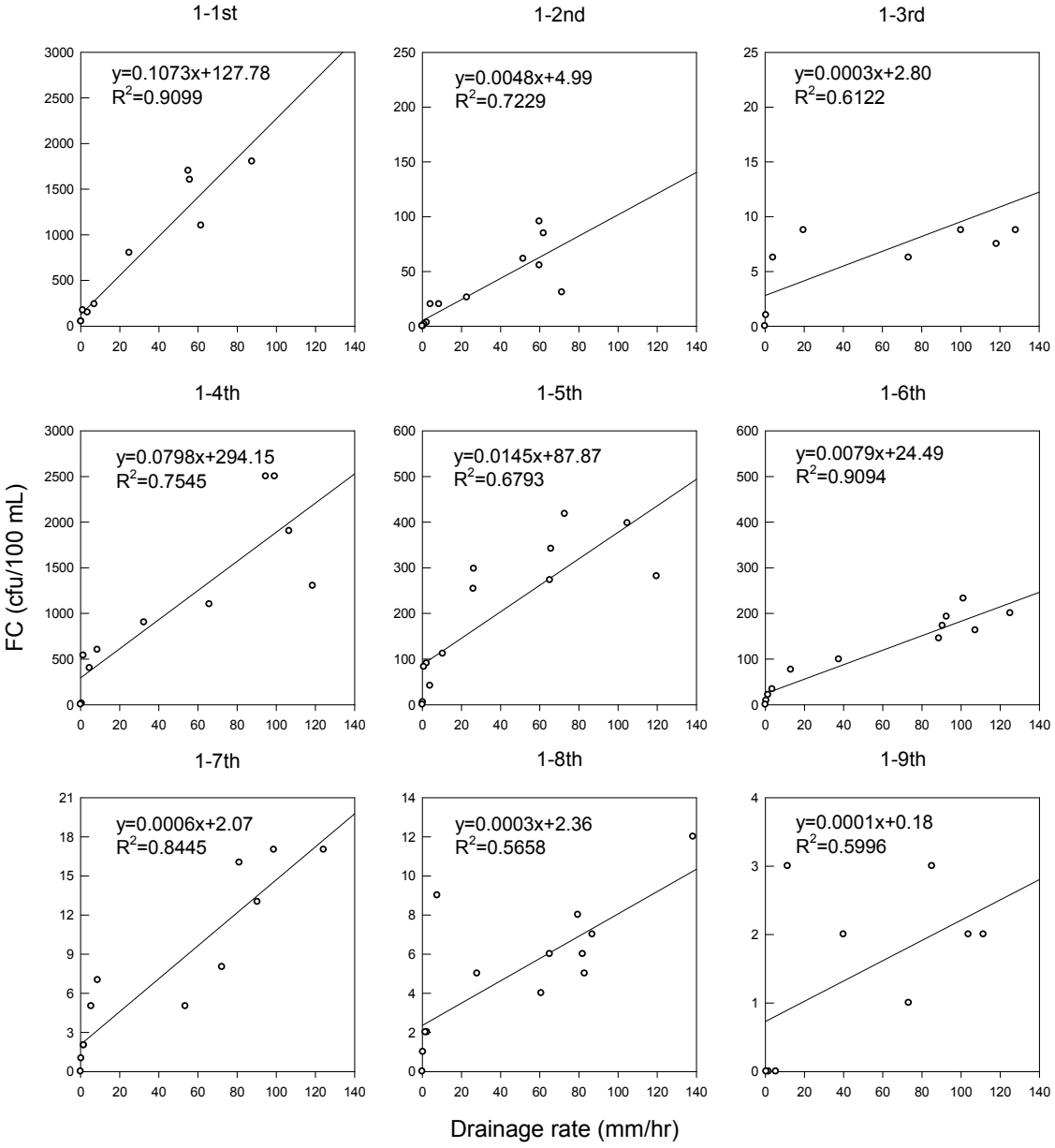

Figure 4.10 Correlation between drainage rate and leachate FC concentration in lysimeter E (F1) in Trial 1, for the nine water irrigations

Figure 4.11 shows the relationship between drainage rate and FC concentration for the 6th water application in F1, as an example of the relationship between drainage and FC leaching. The square of correlation coefficient (RSQ) is 0.90($P<0.005$).

The soil texture in lysimeter E (Figure 4.2, F1) is quite uniform through the four depths and more permeable compared with lysimeter A, C, D and F. Lysimeter B is closer to E in texture, which did not present the same pattern.

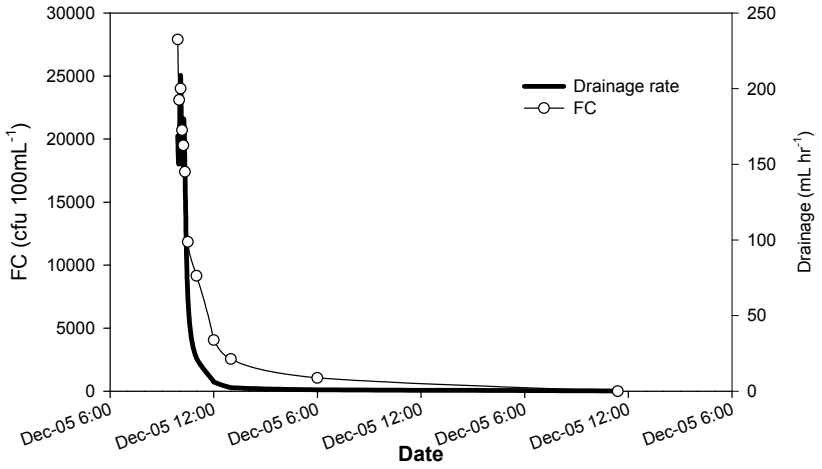

Figure 4.11 The drainage rate and the concentration of FC for F1 following the sixth water application

4.3.8 The relationship between soil water content, water potential and FC concentration of leachate

Figure 4.12 were plotted on the basis of 10-minute real-time monitoring data of soil water content and water potential. Both water content and water potential at the first two layers had larger fluctuations than at the third and fourth layers.

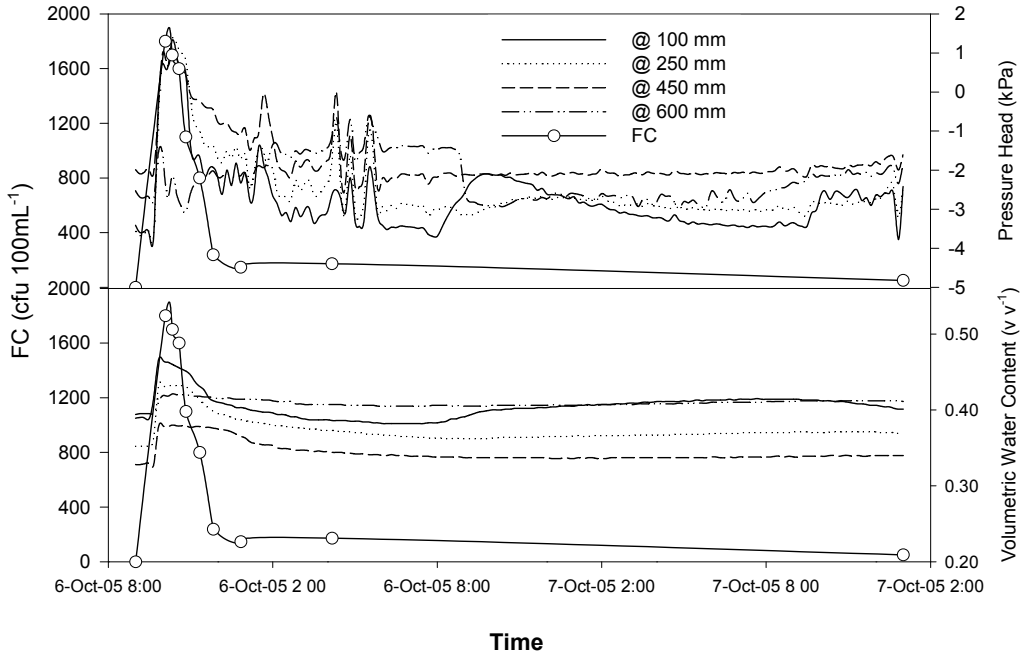

Figure 4.12 Example of correlation between bacterial leaching and pressure head or water content (recorded every 10 mins) on one of irrigation days (lysimeter E)

Usually, bacterial leaching increased with increasing water pressure and water content in every single application. Occasionally, the bacterial leaching did not follow the soil water content changes. There was higher bacterial leaching when water content did not obviously change in one single application. Probably that leaching went via by-pass flow, so did not affect the zone of TDR measurement. Generally speaking, water content is less sensitive to changed soil wetness than water potential. Thus, it should be easier to correlate bacterial leaching with suction, not water content. However, the limited measurement volume of tensiometers may fail to catch the soil volume carrying water flow. From that viewpoint, water content could be a better indicator.

In most leaching events, peak FC concentrations occurred at the start of each new flow event. Concentrations dropped rapidly as the flow continued. But the Br^- leaching did not have the same pattern. Kladivko *et al* (1991) found in their research that pesticide leaching presented the same way as FC leaching in this research. One possible explanation according to Kladivko *et al* (1991) for the observed behaviour is non-equilibrium sorption/desorption in the preferential flow paths. At the start of a flow event, bacteria in the existing soil solution are flushed rapidly through large pores and into drainage water. Desorption is not rapid enough to maintain an equilibrium solution concentration in new water flow, so continued water flow through those pores contains much lower concentrations. When drainage ceases, the equilibrium within the large pores is re-established, and a new flow event again contains a high initial concentration of bacteria. Another explanation (Hallberg *et al.* 1986) is that the initial part of the flow event is dominated by drainage from large pores, in which water and chemicals have a short residence time. As the drainage slows down, much of the water being delivered to the drainage is from smaller pores, where the chemical is retarded in the soil profile for longer times, and therefore concentrations are much lower. The leaching patterns differ between bacteria (or pesticide) and Br^-. That is because bacteria or pesticides are “reactive”, i.e. they react physically with soil particle surfaces via adsorption and desorption, while Br^- is an “inert” tracer.

4.3.9 Effects of residual bacterial concentration in soil columns

The residual bacterial concentration decreased gradually after DSE application. Generally the bacterial leaching decreases with time if there is no additional bacterial input, partly because FC will exponentially die off with time in soil (Crane and Moore 1986) .

$$C_t = C_0 \, exp^{-\lambda t} \qquad \textbf{(4.2)}$$

Here C_0 is the initial bacterial concentration, expressed by colony-forming units per mL (cfu mL^{-1}), C_t is the bacterial concentration (cfu mL^{-1}) at time t (d), λ is the first-order die-off rate constant (d^{-1}).

In most situations, the concentration of FC in leachate indicated an exponential decline. However, in Trial 1 there were two non-typical events, in which leachate FC concentration increased abruptly: the 4th application to F1 (see Figure 4.8); and the 6th application to F2 (The latter is invisible with the current scale in Figure 4.8, see Appendix I). The wetness conditions before these applications were similar to previous applications (The starting average water potentials before these two applications were -1.83 kPa and -2.48 kPa. The starting water potential was even lower than that in the 5th application).The average soil temperature during the 4th to 6th water application period was *c.*18°C. The applied FC may have been stored in the end of preferential flow paths, and later was leached out because of soil structure change. There was a possibility of bacteria growing in summer time. It is also suggested there was a change in the background FC concentration at that time. Roslev *et al.* (2004) reported that faecal pollution indicators may persist longer under anaerobic conditions, and higher temperature enhances their survival rate in anaerobic conditions.

Gagliardi and Karns (2000) reported that *E. coli* O157:H7 was able to replicate in and migrate through cores of various soil types in field conditions in Maryland, USA. Numbers of the pathogen in leachate correlated with ammonia and nitrate levels, and the numbers exceeded inoculum levels in all treatments (i.e. soil types, tilled and no till, and rainfall amounts) except in intact clay loam cores.

AFC, as a bacterial tracer, was added into DSE in Trial 2. The leaching pattern of AFC was closely similar to FC. That indicates that the abnormal rise of FC in leachate was the consequence of the structure change, or bacteria growth in soil, other than external contamination. The abnormal rising in leachate also has been seen in P leaching research (Toor 2002).

This study showed that there was a clear difference of bacteria concentration in leachate under irrigation compared with natural rainfall. When leachate resulted from rainfall, no FC was found in samples.

4.4 Conclusions

Three main factors affected bacterial transport: lysimeter 'hydraulic conductivity' (K_{eff}, a whole-soil column property); irrigation treatment; and seasonal variation. The six lysimeters could be divided into two categories based on their conductivity K_{eff}, and the performance of bacterial transport:

Category I - with moderate or moderately rapid K_{eff};

Category II- with rapid K_{eff} and obviously with big macropores (Bowler 1980). Results are summarised as follows.

- In Category I lysimeters with moderately rapid K_{eff}, flood irrigation resulted in bacterial leaching at concentrations around 10^3 cfu 100 mL^{-1}.
- In Category I lysimeters, spray irrigation resulted in bacterial leaching at concentrations c. 10^2 -10^3 cfu 100 mL^{-1}.
- For Category II lysimeters with rapid K_{eff}, there were no obvious effects of the irrigation schemes. High risk of bacteria contamination occurred in both flood and spray treatments, especially in summer season.
- In the summer, irrigation posed more threats for shallow groundwater contamination by bacteria than in autumn due to the drier condition of soil columns, especially those with more clay content in topsoil, when shrinkage cracks could form, promoting preferential flow and facilitating bacterial leaching.

Current practices for land-applied DSE may cause shallow groundwater contamination by microbes where strongly structured, fine-textured soils directly connect with shallow ground-water, especially in dry conditions. In this research, while only one soil type was used, the variation in soil properties shows the effect of soil texture and structure on preferential flow, which is the main cause of bacterial leaching. Practical measures are required to protect groundwater from pathogen contamination, including: 1) To apply spray irrigation instead of flood irrigation; 2) To monitor soil water content and schedule irrigation to avoid soil getting extremely dry, especially in summer; 3) For this type of soil, to decrease the DSE application depth by increasing irrigator groundspeed, or improve irrigator design to increase application uniformity.

In this study, our principal purpose was to evaluate the effect of irrigation scheme on the fate and transport of bacteria in soils with similar properties. We observed that the extent of effect of irrigation is significant in some cases but minimal in others. The differences in properties of the soils used influenced these results. It is too variable between lysimeters to detect a dependence on conditions and the variability presumably reflects the continuity of flow paths through macropores if any. The dynamics of structure changes are influenced by initial water content, wetting and drying cycles, root growth biotic activity etc.

Further advances can be expected from future research that exploits these and other new experimental techniques to relate macropore structure to observations of contaminant transport and, ultimately, to model parameters.

Our results suggest that bacterial leaching was not interrelated with total porosity. Pore sizes, pore space heterogeneity and continuity are clearly more important for leaching. In this longer-term field trial, multi-factorial interactions complicated the research, so that observations revealed trends rather than results with strong statistical significance.

Chapter 5 Macropore Transport of Bacteria as Influenced by Soil Structure Differences:

A: Tension infiltrometer study

Abstract: Macropore flow is typically a prominent process in grassland soil profiles, and can generate leaching and lead to groundwater contamination. To protect water resources against contamination from land-applied dairy shed effluent, it is important to better understand the transient flow processes, which are controlled by the conductivity characteristics of the soil. In this part of the research, disc tension infiltrometers were used to investigate the hydraulic characteristics of the six lysimeters used for the bacterial transport (faecal coliform) trials, after completion of those trials. Zero suction was first applied in order to measure the saturated conductivity K_{sat}; and then 40 mm suction was applied in order to measure one value of unsaturated conductivity $K\text{-}_{40}$. The contribution of macropores with diameters > 0.75 mm to conductivity (macropore flow) in each lysimeter was thus determined from the difference of the two infiltration rates. The results showed in most cases a significant correlation between the proportion of bacteria leached and the flow contribution of these macropores. The greater the K_{sat}, the greater the amount of drainage and bacterial leaching obtained. This research also found that this technique may exclude the activity of some continuous macropores (e.g., cracks) due to the difference of initial wetness which could substantially change the conductivity and result in more serious bacterial leaching in this Canterbury fine sandy loam soil.

5.1 Introduction

Field research reported in the literature has revealed situations where rates of movement of contaminants in soil were much faster than could be explained by basic transport and adsorption mechanisms for the soil material. These situations have been well documented and are often attributed to the occurrence of macropores (Beven and Germann 1982; White 1985; Singh and Kanwar 1991; Chen *et al.* 1999; Ersahin *et al.* 2002). Early laboratory investigations dealing with chemical transport indicated that contaminatant or tracer movement through soil columns was well described by classical convection-dispersion equations (Jiang *et al.* 2005). However, field experiments demonstrated that even

chemicals with a high affinity for the soil matrix can bypass expeditiously vast portions of the soil matrix to groundwater (Gish *et al.* 1991; Kladivko *et al.* 1991; Flury 1996)
Knowledge of the infiltration process as it is affected by the soil's properties and transient conditions, and by the mode of water supply, is therefore a precondition for understanding the biophysical environment and for efficient soil and water management (Hillel 1998). Field bacterial transport research needs supplementary information on certain soil hydraulic properties to better understand the phenomena of bacterial leaching. Many of the traditional methods of assessing transport phenomena and porosity rely on small cores of disturbed samples and characterize pores within the capillary size-range. To an extent, soil hydraulic properties can be estimated from soil composition properties, including particle size distribution, bulk density and porosity (Smettem and Bristow 1999; Smettem *et al.* 1999; Schaap *et al.* 2001). However, there is a drawback in determining such pedotransfer relationships. Soil disturbance is unavoidable during the measurement of hydraulic properties. As a result, the many attempts to relate measured saturated hydraulic conductivity K_{sat} to measured soil properties have met with limited success.

It is important to remember that drainage of pore sequences also depends on pore continuity. A large pore cannot drain unless it is part of a pore sequence into which air has entered under the applied tension. Thus, in addition to macropore volume, the drained porosities reflect, to some degree, the continuity of macropores (Kluitenberg and Horton 1990). As described by Smettem and Collis-George (1985), because a single, continuous 0.3 mm diameter macropore can conduct more water than the rest of a 100 mm diameter sample, pore continuity, in addition to total porosity, must be recognized. In contrast with the above pedotransfer techniques, the tension infiltrometer can represent the realized situation closely.

By applying a range of (different) matric suctions to soil, research investigations have distinguished the contributions of various sized macropores, to transport of both chemical contaminants (or an inert tracer) and bacterial tracers (or indicator). Ersahin (2002) investigated transport of nonreactive Br^- under matric heads of 0 to -10 cm using undisturbed soil columns (grassland soil). He found that the difference, among each of the values on pore water velocity, fraction of mobile water content and lateral mass exchange rate for the different horizons, decreased sharply with decreasing matric head until about -3 cm, and remained fairly unchanged with further decreases in the matric head. This suggested that most of the variability in macropore transport of bromide for these horizons

was caused by pores with diameter greater than about 1 mm. A pressure head of – 5 cm was used by Silva (2000) and Jiang (2005) to identify nitrogen and bacteria (*Bacillus subtilis*) leaching caused by macropore diameters greater than 0.6 mm. The results of Silva (2000) showed those macropores were responsible for more than 98% of nitrogen leaching. So, technically, matric heads of -5 cm (disabling pores >600 μm diameter) or - 4 cm (disabling pores> 750 μm in diameter) have been used as the boundary of macropores and micropores for purposes of studying leaching or matrix flow in New Zealand and Australian soils (Watt and Burgham 1992; Smettem and Bristow 1999; Silva *et al.* 2000; Jiang 2005).

The use of disc tension infiltrometers has been extended to include subsurface soil. The disc infiltrometer has become an established device for *in situ* measurement of soil hydraulic properties (Clothier and White 1981; White and Sully 1987; Ankeny *et al.* 1991; Reynolds and Elrick 1991; Xue *et al.* 2004). This research employed tension infiltrometers made by CSEQ staff, in order to assess the contribution of certain macropores to water flow, for those lysimeters which had been used for the previous bacterial transport trials.

5.2 Material and methods

5.2.1 Theoretical background

Conductivity at a pressure potential of -40 mm water was measured using the method of Clothier and White (1981). Watt (1992) applied a suction of -40 mm water to define unsaturated hydraulic conductivity (K_{-40}) of 8 NZ soils, and Smettem and Bristow (1999) defined this pressure head as the value for measurement of matrix saturated conductivity. They pointed out that disc permeameter measurements at a supply pressure of -40 mm strongly reflect the textural character of these soils (Smettem and Bristow 1999) This determination eliminates the contribution of continuous pores greater than 750 μm diameter (see later calculation). Removal of the effect of these macropores should reduce the range of field heterogeneity.

The following equation relates the height of capillary rise (h) to pore radius:

$$r = \frac{2\gamma \cos\alpha}{\rho g h} \qquad \textbf{(5.1)}$$

Here γ is the surface tension of water (N m^{-1}), α is the wetting angle of the water and the pore wall (assumed to be nearly zero, therefore $\cos\alpha \cong 1$), ρ is the density of water (kg m^{-}

^{3}), g is acceleration due to gravity (m s^{-2}). It can be simplified as (McLaren and Cameron. 1996):

$$d(cm) = 0.3 / h(cm) \qquad \textbf{(5.2)}$$

Here d is the diameter of the largest water-filled pores. The sequence of our measurements of K was 40mm water suction followed by zero water suction.

This study assumes that the equivalent pores smaller than the d value estimated by Eq. 5.1 or 5.2 are full of water and are responsible for 100% of the water flux for a given water pressure head. Also, it is assumed that pores with equivalent diameter d larger than the value calculated from Eq. 5.1 or 5.2 are air-filled and do not contribute any of the water flux; at least those assumptions are applied to the surface soil.

During the infiltration process, there is a short equilibration time. The flow rate per unit area from a disc maintained at a constant potential can be written as follows for one-dimensional flow:

$$\frac{Q}{\pi r_0^2} \approx 0.5 S t^{-1/2} \qquad \textbf{(5.3)}$$

Here Q is the flow rate from the disc infiltrometer ($m^3 s^{-1}$), r_0 is the disc radius (m), S is the sorptivity (m $s^{-0.5}$), and t is time (s). The sorptivity is dependent upon the initial water content, supply water content and the diffusivity function. Integration of (5.3) with respect to t results in the cumulative infiltration per unit area (m):

$$I = S t^{1/2} \qquad \textbf{(5.4)}$$

For short time, S is simply the slope of I versus $t^{0.5}$. For large times a steady state is reached, approximated by an empirical infiltration relationship of Hussen (1993):

$$I = S t^{1/2} + \frac{Q_{ss}}{\pi r_0^2}\left\{ t + \left(\frac{a}{c}\right)\left[1 - \exp(-ct)\right]\right\} \qquad \textbf{(5.5)}$$

Here a and c are empirical constants, Q_{ss} is the steady state flow volume per unit time. McLaren and Cameron (1996) describe of the infiltration rate of a soil using the equation:

$$I = S t^{1/2} + K_h t \qquad \textbf{(5.6)}$$

Here K_h is the ability of the soil to transmit water (conductivity). Equation (5.6) characterizes the infiltration process under the infiltrometer due to capillary forces and

gravity. Their effect on the infiltration process changes with time. For short times, gravity can be ignored, while for long infiltration time capillarity can be ignored:

$$i = K_h \quad \textbf{(5.7)}$$

$$\text{and } I = K_h t \quad \textbf{(5.8)}$$

K_h is simply the slope of infiltration I versus time t.

5.2.2 Tension infiltrometer

(refer to section 3.13.1)

5.3 Results and discussion

Usually, after the infiltrometer was set up and water started running through it into the soil, it took 1-2 hrs before reaching a stable infiltration rate. The length of that time period depended on the antecedent wetness and the pore connectivity of the soil column. Drier soil took longer time to attain steady state. The infiltration rate kept relatively constant, although there was slowing down and some jumping, until it finished. The infiltration lasted a few days or until the water tank was emptied. Measurement at 40 mm suction was longer than at zero suction. Figure 5.1 shows an example of infiltration at both suctions. Figure 5.1b shows that the infiltration rate at the initial stage for 40 mm suction was much more than that for zero suction. It should be the other way round. The difference for those two measurements was initial wetness: the 40 mm suction infiltration started at a dryer condition, while the zero mm suction process followed the 40 mm suction and so started at a wetter condition. When infiltration takes place into an initially dry soil, the suction gradients at first can be much stronger than the gravitational gradient, and the initial infiltration rate into a horizontal column approximates the infiltration into a vertical column; when infiltration takes place into an initially wet soil, the suction gradients are weak from the start and become negligible much sooner (Hillel 1998). Figure 5.2 shows the pressure head data at four depths during the beginning of infiltration at zero suction. In the early stage of infiltration, sorptivity *(S)* is the dominant term as defined in Equations (5.3) and (5.6). S is related to the soil texture, structure and antecedent wetness. Thus the early infiltration rate is more rapid. As shown in Figure 5.2, the initial pressure head increased during the sorptivity process and thus the early infiltration rate declined until

steady flow was attained. The pressure heads at 250 and 450 mm depth were higher than at 100 and 600 mm. This suggested that the hampering layer was probably between 250 mm and 450 mm depth in this lysimeter. That is consistent with the results from particle size analysis (refer to section 4.3.1) and visual morphology observation: at around 300 mm depth, there was the highest clay and silt content for the second layer in lysimeter D. The soil was loosely aggregated and higher density with brown mottles, and no visible macropores were found in this layer. The results further revealed that the macropore flow generated in the topsoil may be hampered in the underlying soil, suggesting that the position and depth of a barrier layer needs to be considered in leaching studies and modelling macropore transport of contaminants (Ersahin *et al.* 2002). The same mechanism also applied to the water-facilitated bacterial transport in this lysimeter. This layer was critical for bacterial transport. The results from leaching experiments showed that this lysimeter was the least permeable for bacterial transport.

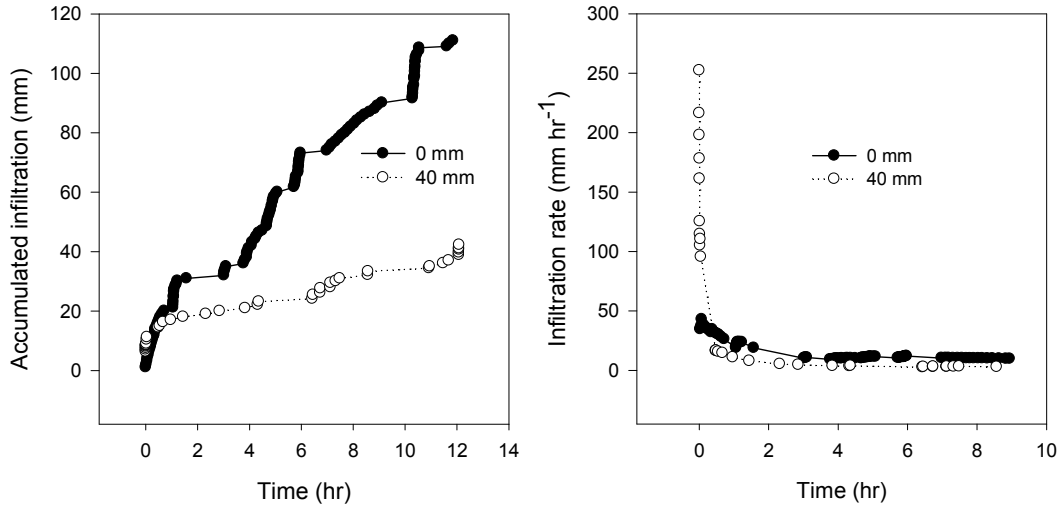

Figure 5.1 a) Accumulated infiltration vs time for lysimeter D; b) Infiltration rate vs time in the first few hours for lysimeter D

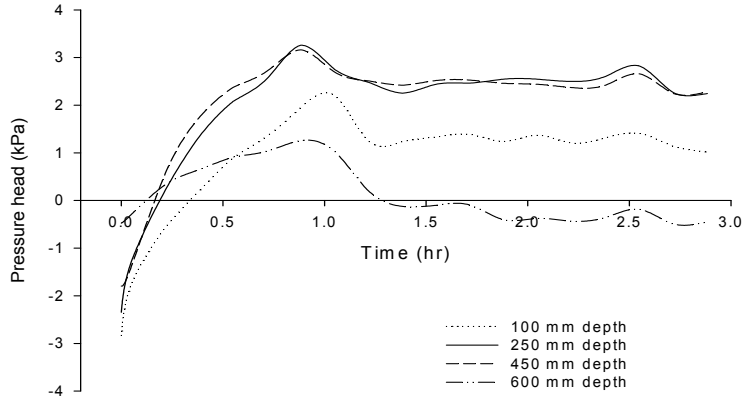

Figure 5.2 Presssure head in soil vs time in the first few hours of infiltration into lysimeter D at zero suction

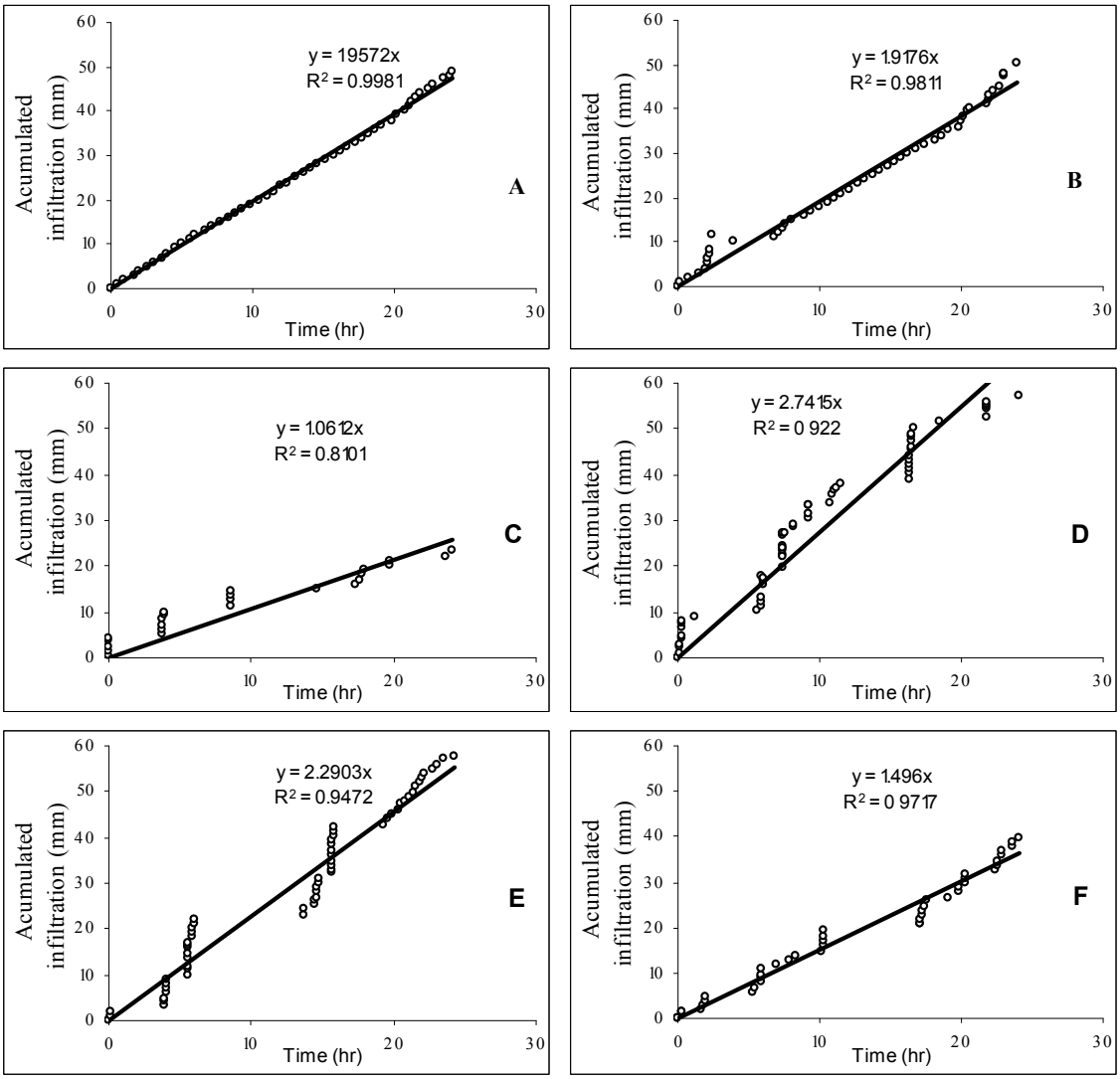

Figure 5.3 Steady infiltration at 40 mm suction in the six lysimeters using tension infiltrometer

Figure 5.3 and Figure 5.4 show the later stages of infiltration of the six lysimeters, when the infiltration rate kept constant at 40 mm suction and zero suction. The conductivity or steady-state infiltration rates at any suction are the slope of the cumulative infiltration (see Equation (5.8)) (Smettem and Collis-George 1985). In Figure 5.3, for lysimeters C to F, the pattern of water infiltration is different from lysimeters A and B. For C to F, the water appeared to enter the soil in 'steps' may have been due to either pulsed entry of the water into soil, or wind speed change causing pressure changes in the reservoir. However, the stepped nature of the curve does not affect the slopes, i.e. infiltration rates.

The unsaturated conductivity K_{40mm} in the six lysimeters (matric flow) ranged from 1.06 to 2.74 mm hr^{-1}, reflecting differences in their structure and texture. There is little relationship between K_{40mm} and the bacterial or Br^- transport (see Table 5.1). This suggested that the matric flow did not facilitate bacterial or Br^- transport. The bacteria or Br^- were absorbed or retained in soil during passage through the soil matrix. That agrees with results from numerous other contaminant distribution researches, which show that soil acts as a bio-filter in most situations. E.g. Shiptitalo and Edwards (1996) observed that most applied chemicals were retained predominantly within the upper portions (0-5 cm) of the soil. Gerba *et al* (1975) reported that more than 90 % of bacteria applied to soil remain within the first few centimetres.

The K_{sat} at zero suction for the six lysimeters ranged from 4.02 to 27.4 mm hr^{-1}. According to Hillel (1998), the infiltration rate for different soil types (from clayey to sandy) ranges from 1-20 mm hr^{-1}, though these values exclude cracked or well-aggregated soils. Obviously, in lysimeters B and E there was more macropore flow. This is consistent with the K_{eff} measured with ponded water (refer to section 3.2). Silva (2000) and Clothier and White (1981) both got the result that the infiltration rate at 0 kPa was higher by about an order of magnitude and more variable than at 0.5 kPa, in that situation the pores larger than 600 μm in diameter was disabled.

The results showed that lysimeter C has finer texture according to the matric flow characteristic. (See. K_{40mm} values in Table 5.1). That agrees with the texture analysis result, that lysimeter C had the largest clay content in the first layer of the six lysimeters (refer to Table 6.1). It might be well structured with aggregates in the subsoil.

Table 5.1 Comparison of the fate of bacteria and Br^-, and hydraulic conductivity values (at 0 suction and 40 mm suction).

Lys.	Drainage (as fraction of irrgation input, mm mm^{-1})	Recovery of Br^-(%)	Recovery of FC (%)	K_{eff} (mm hr^{-1})	Drainage Class*	K_{-40} (mm hr^{-1})	K_{sat} (mm hr^{-1})
A	0.23	14	0.1	42	Moderate	1.96	4.02
B	0.72	31	0.48	123	Moderately rapid	1.92	27.4
C	0.44	78	49	250	Rapid	1.06	8.11
D	0.35	34	0.029	41	Moderate	2.74	7.58
E	0.75	59	0.54	110	Moderately rapid	2.29	13.4
F	0.06	6	0.0054	33	Moderate	1.5	9.24

*(Bowler 1980)

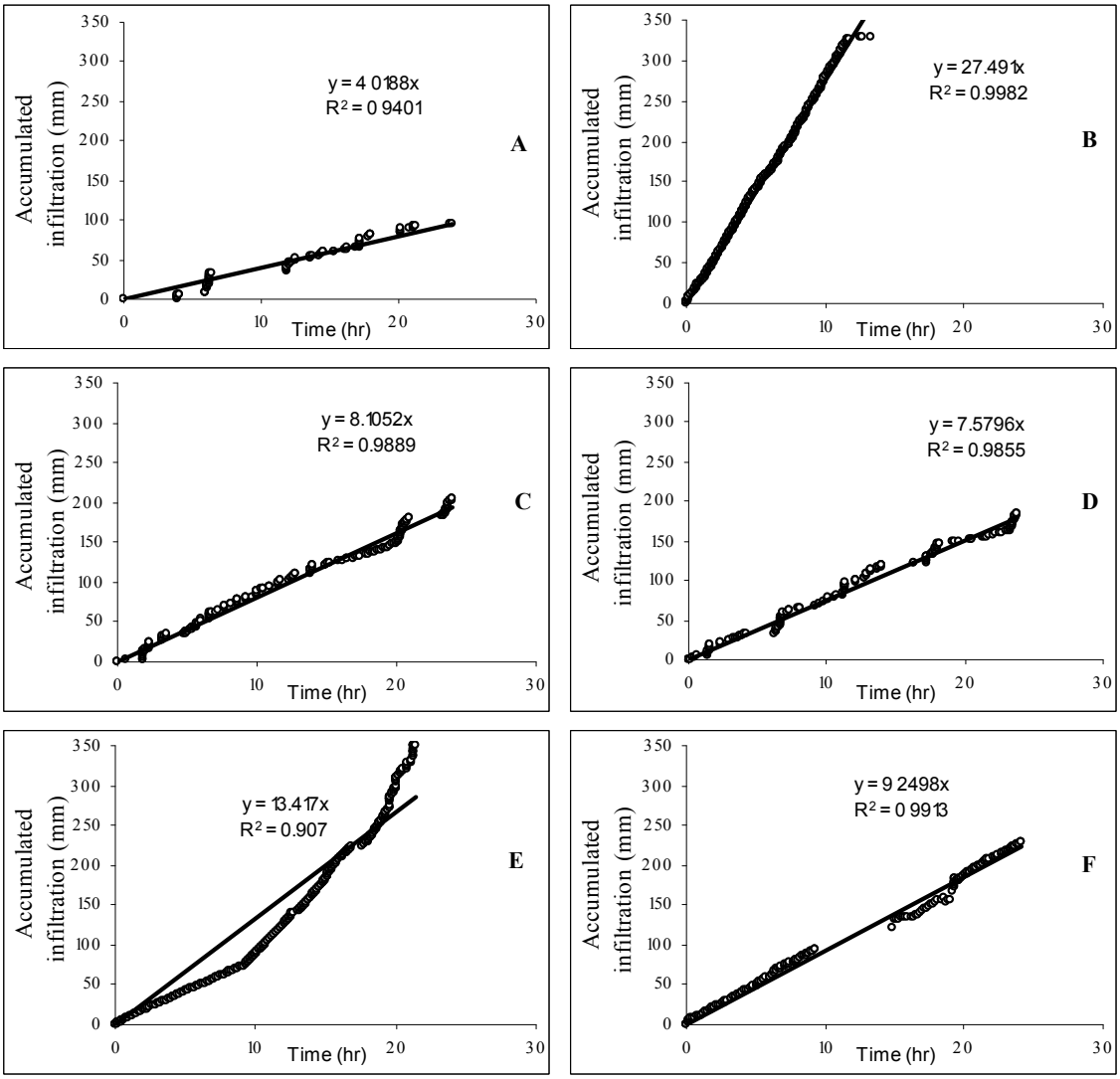

Figure 5.4 Steady infiltration at 0 mm suction in lysimeters using tension infiltrometer

In most cases, the saturated conductivity is related to the bacterial leaching. There is an exception in lysimeter C. Combining the data from the previous measurement by steady-

flow method in saturated lysimeters, and the observations made from the earlier bacterial leaching experiments, it is suggested that there were continuous channels (or cracks) in certain lysimeters in some situations (e.g. when soil water content fell below 25% in the dry season), especially in lysimeter C, which was in the rapid drainage class (Table 5.1). However, lysimeter C had much lower K_{sat} than lysimeters B and E, which belonged to the moderately rapid class (Table 5.1). The experimental observations also support this viewpoint (refer to Chapter 4). Compared with $K_{sat,}$ K_{eff} may be more related to the leaching results of FC and Br^- in flood irrigation. The measurement under a ponded condition is similar to flood irrigation (e.g. border strip irrigation) in practice (Figure 5.5). The value of K_{sat} is much less than $K_{eff.}$ The difference resulted from the impact of macropores with different initial water content. K_{sat} was obtained when the soil was fully wetted up after a few days measurement of K_{-40mm}, while K_{eff} was determined under a few hours surface-ponded conditions. Increased water content disabled or decreased the size of some macropores due to soil swelling. Nevertheless, in most cases, K_{sat} was related to $K_{eff.}$

According to Bouma (1991), there are five types of macropores: (1) simple packing voids that are voids due to random packing of single grains; (2) compound packing voids that are voids that result from the packing of compound individuals, such as peds, which do not accommodate each other; (3) vughs are voids that are significantly larger than simple packing voids, and they appear as discrete entities at the magnification at which they are recognized; (4) channels that are voids that are significantly larger than simple packing voids and generally have cylindrical elongated shape; and (5) planes that are voids that are planar according to the ratios of their principle axes. It requires only a few pores to conduct much water if they are continuous (Bouma 1991), thus this may largely control the conductivity.

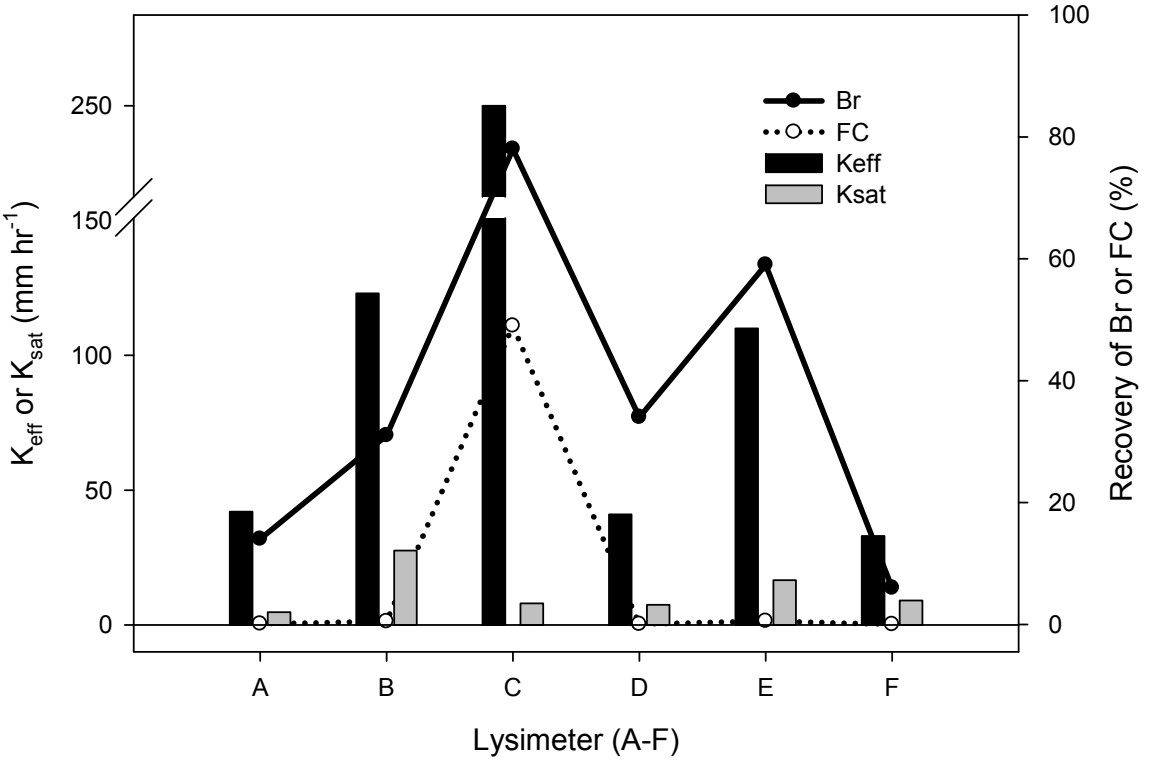

Figure 5.5 Comparison of hydraulic conductivity measured by steady-flow and infiltrometer methods; Illustration of relationship between hydraulic conductivity, and recovery of bacteria and FC

Soil shrinking and swelling could result in continuous formation and destruction of macropores in undisturbed columns. Kutilek (1996) suggested that when cracking clay soils are wetted, the majority of cracks are reduced in size and transformed into mesopores of dimensions approaching those of the interpedal pores. Shipitalo & Edwards (1996) found similar results when pesticides were applied to dry and wet soils. Kätterer's (2001) investigation of the effect of initial water content showed that solutes can be displaced much faster when applied at the surface of initially dry soil, than when applied to wet soil; or when the solutes were resident in the soil matrix. The simulation results suggested that solute transport under initially dry conditions was governed by preferential flow of infiltration water through macropores, by-passing the matrix due to shrinkage cracks and water repellence of matrix pore surfaces. Also, as mentioned by Hillel (1998), the depth of crack penetration can vary from several centimetres to perhaps a metre, depending on the soil properties and the climate. During the infiltrometer measurements, the saturated conductivity was measured just after the unsaturated measurement, when the soil had already received water running for at least a week. Thus the soil was wholly wet up. The original soil cracks might close up or become smaller. So the zero suction infiltration

might not include the continuous channels, which were dominant during bacterial transport. In that case, the water flow speed decreased greatly (see Figure 5.5).

The advantage of the tension infiltrometer method is that it enables us to quantify the conductive character of the whole lysimeter. However, as the lysimeter was pre-wetted during the process of setting up, it was not possible to represent the behaviour of cracks starting from a dry condition. Another possible explanation is that the tension infiltrometer technique disabled surface initiation. When macropore flow was initiated at the soil surface, most of the macropores received very little water while a few macropores received a large proportion of the total inflow. In contrast, when macropore flow was initiated from a saturated or nearly saturated soil layer, macropore flow rate variation was much lower (Weiler and Naef 2003). Therefore, the main macropore flow may be disabled during this measurement.

Shiptitalo and Edwards (1996) concluded that although the larger macropores dominated the flow at all moisture levels, the matrix became increasingly involved in the wetter blocks, or, involvement of the matrix in the flow processes increased with increasing soil moisture content.

Bouma (1982) has defined the problem in his study of measuring the hydraulic conductivity of soil horizons with continuous macropores. K_{sat} changes continuously in clay soil as a result of swelling and shrinkage. And K_{sat} is a function of sample size due to the effect of macropore continuity shrinkage (Bouma 1982). The soil used in this research is not clay soil, but this phenomenon happened in the lysimeter with highest clay content in the topsoil. There has been no such result reported in this type of soil before. It may need further experiments to verify this.

5.4 Conclusions and further recommendations

Bacterial transport is controlled by a soil's conductive characteristics, which are strongly determined by soil structure, not only by the structure of the surface layer, but also the subsoil structure. Soil wetness also influences the structure, and further controls K_{sat}.

Undeniably, unlike texture, soil structure is a dynamic system. The relative proportions of macro-pore and less permeable matrix pore systems changes with environmental conditions, e.g. the initiation of macropore flow during infiltration is controlled by initial matrix water content, water application rate and amount, matrix hydraulic conductivity, and soil surface contributing area (Bouma and Wosten 1979). There are high degrees of

temporal and spatial variations in soil structure, even within soils with identical textures (Trojan and Linden 1992). When investigating structural control of contaminant leaching, a main concern when designing methods or instruments should be keeping the conditions consistent.

Only a few studies have monitored the effects of large and continuous cracks on water and solute transport processes (Paterson *et al.* 1993; Toor *et al.* 2004a), or detected bacteria immediately in leachate from an intact soil on a clay loam. More attention is needed to the seasonal dynamics of structure changes in the same soil samples.

Regarding development of best management practices (BMPs), one problem which needs to be solved by improved soil and water management, is to decrease the number of "planar voids", and hence K_{sat}.

There is a need for another method to visualize the large channels, e.g. by a dye infiltration experiment. Use of the dye method in this project is described below.

Abstract: The spatial variability of preferential pathways for water and contaminant transport in soils, as visualized through dye infiltration experiments, was studied by applying an image analysis technique – the Robolab software package (2.5.4 c) - to determine two-dimensional dye distributions. After dye infiltration into the lysimeters, which had been previously used for bacterial transport and infiltration rate studies, dye staining cross sections were photographed, and the images of dye distribution were analysed. Our results suggest that, following flooding of the lysimeters with dye solution, there was considerable variation between lysimeters in the pattern of water flow, as indicated by the distribution of dye in vertical and horizontal directions, and most of the flow reaching deeper than 50 cm resulted from macropores, mainly visible cracks. This process could threaten groundwater quality by contaminant leaching.

5.5 Introduction

Characterization of water and contaminant transport in the variable matrix of a soil system, by detecting the spatial pattern of preferential flow pathways, is difficult. However, the dye staining method can visualize the complicated pattern of water movement with a very high spatial resolution. Thus it could help interpret the vertical contaminant experiment results in a better way. Research in preferential flow relies heavily on the use of dye tracers (Flury and Wai 2003). Brilliant Blue FCF ($C_{37}H_{34}N_2$ $Na_2O_9S_3$) is a valuable dye tracer for visualizing water flow patterns due to its non- toxic nature, moderate mobility, and absorbability (hence visibility) (Flury and Flühler 1995; Mon *et al.* 2006). It has been widely used in hydrological research in soils (Steenhuis *et al.* 1990; Flury and Flühler 1994; Flury *et al.* 1994; Lin and McInnes 1995; Flury and Wai 2003; Kim *et al.* 2004; Nobles *et al.* 2004).

Recent further investigation by German-Heins and Flury (2000) indicated that in aqueous solution, the absorption spectrum of Brilliant Blue FCF is not sensitive to pH nor ionic strength. Though increasing ionic strength led to increased sorption of Brilliant Blue FCF in soil (so that the simultaneous use of other ionic tracers will decrease Brilliant Blue FCF mobility), it may still be considered to be one of the best compromises available to date as a dye tracer for hydrological studies.

Compared with tension infiltrometer and chemical tracer methods, dye tracer is more visible and can be applied with any controlled initial wetness, but it is less quantitative. Dye tracer data can provide detailed visual information on the three-dimensional flow in soil (Yasuda *et al.* 2001)The use of dye tracers is not only common for experiments in the unsaturated zone, but also for the saturated zone to reveal water flow patterns (Flury and Wai 2003).

Here, we report observations of the flow patterns of water obtained with the use of dyes in the six lysimeters previously used in the bacterial leaching study. Previous studies on those lysimeters demonstrated an accelerated movement of water and bacteria in lysimeters with moderately rapid drainage class, thus suggesting the involvement of extensive preferential flow. This study attempted (1) to overcome some of the limitations of previous approaches; (2) to identify some complex soil features; and (3) to provide direct evidence for the presence of preferential flow channels in soil and to give some information on the nature and the extent of the flow channels involved.

5.6 Materials and methods

5.6.1 Soil lysimeter information

(Refer to Section 3.1)

5.6.2 Properties of dye tracer; and previous relevant research

Brilliant Blue FCF was obtained in food grade quality from Five Star Paints Ltd, NZ. This dye is a member of the class of triarylmethane dyes (Figure 5.6). The experimental conditions and the types of dye used differ from study to study. The recommendation for toxic safety according to Flury and Fluhler (1994) is that the total amount of this dye should be selected such that the final concentration in water is below 1 mg L^{-1}. According to Flury (1995), the concentration of Brilliant Blue FCF application ranges from 5-10 g L^{-1}. He applied 40 mm in 8 hrs over a soil area of 1.4 x 1.4 m. The soil type was loamy-sand. The maximum visible dye depth was below 30 cm. He applied 40 mm in 1 minute to 14 soils by both sprinkling and flood application (1994). The penetration depth ranged from 30-120 cm. Kim (2004) applied 150 L at a concentration of 5g L^{-1} to a soil with an area of 1 x 1m, and for certain structured soil, the Brilliant Blue FCF reached 70 cm. Nobels *et al.*(2004) applied 53 L (approximately 2 pore volumes) Brilliant Blue FCF solution at a concentration of 30 g L^{-1}. This was applied manually into a soil column with 35 cm

diameter and 150 cm depth, and with volumetric moisture content of 25%. The dye reached 100 cm depth.

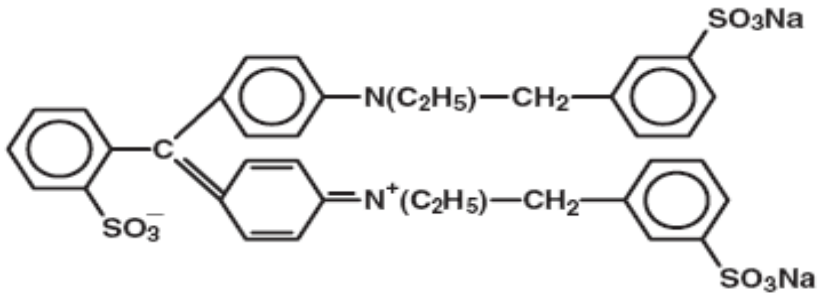

Brilliant Blue FCF (C.I. Food Blue 2, C.I. 42090)

Figure 5.6 Molecular structure of Brilliant Blue FCF

5.6.3 Dye application and images taken

This dye study was carried out after the tension infiltrometer measurements were finished. Before application, the soil columns were covered for a few weeks (but opened occasionally on sunny days) to prevent rain entry, and to leave them at field capacity or even dryer. The top rim of the lysimeters was fitted with an extension ring to prevent over-flow of the applied dye solution. The rings had a depth of 150 mm and diameter slightly smaller than the lysimeter steel wall. They were connected to lysimeters by a rubber loop and were sealed up using silicone (Figure 5.7). 50 mm depth of dye solution at the concentration of 10 g L^{-1} (10 L in total) was poured into each lysimeter, and the lysimeters were shifted to a shed for section cutting and for taking images after at least 24 hrs (Figure 5.7).

The lysimeters were excavated from the middle to form a horizontal section (half circle cross section) every 15-20 cm. Following this, we also created one whole vertical cross section for taking images, and also extracted samples at four depths for soil properties (particle size distribution, pore size distribution, and bulk density). The images were taken by a digital camera (Nikon Coolpix 8800) under daylight conditions. For each image an additional 'scaling' photo was taken with a reference ruler or square frame (5 cm x 5 cm).

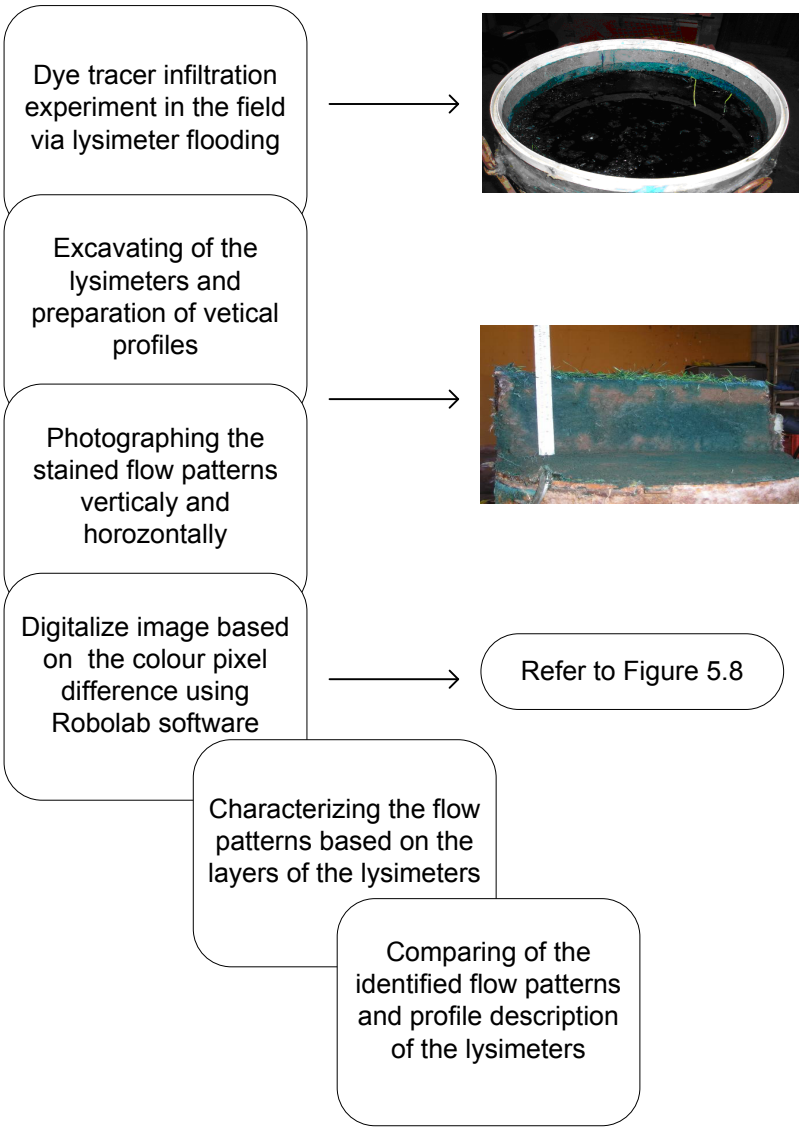

Figure 5.7 Flow chart of dye analysis in this study

5.6.4 Image analysis

Binary analysis of images was carried out: the images were analysed using Robolab software (developed at TUFT University, College of Engineering, Medford, MA USA) with program modified by Professor A. McKinnon and Dr. K. Unsworth, Applied Computing Group, Lincoln University. This software is capable of digitizing images and distinguishing stained and unstained areas by setting up thresholds of pixel, colour density and saturation value. The image analysis investigations were carried out as indicated in the sequence illustrated below in Figure 5.8: (1) The image was selected; (2) the area to be analysed was decided with known width and depth; then (3) the appropriate thresholds for pixel, colour density and saturation were adjusted and selected. The image turned out to be a black and white version, showing dye distribution with white colour (3). (4) shows the

dye coverage (%) with depth. The scale of *x* and *y* were adjusted according to the known length and depth of the soil profile. The dye coverage plot shows the percentage stained versus depth.

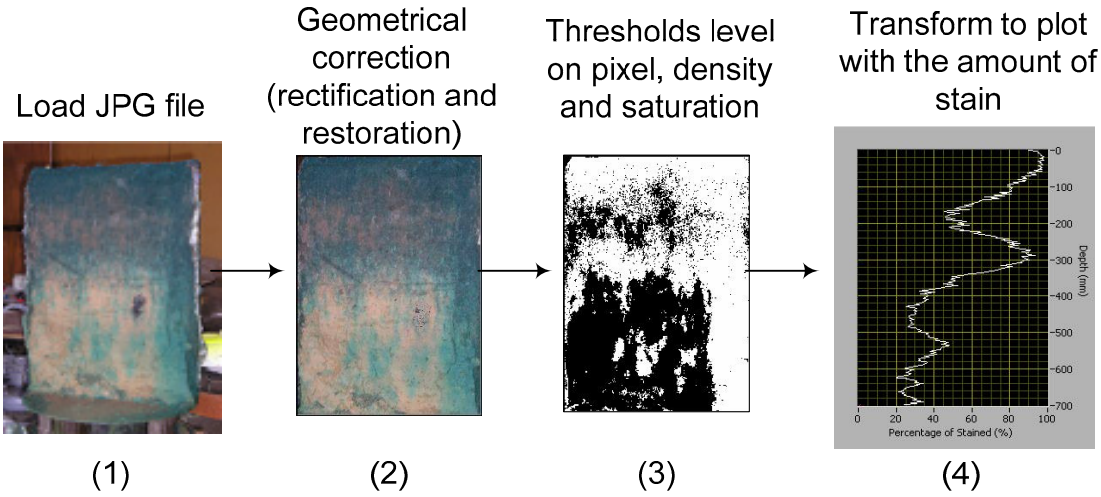

Figure 5.8 Method and procedures of image analysis

5.7 Results and discussion

5.7.1 General description

Dye reached the bottom of all lysimeters with this 50 mm flood application of dye solution. However, the staining pattern and area were different depending on the structure and texture. All lysimeters produced leachate except lysimeter D (in which the dye solution spilled over from a hole in the lysimeter casing at 250 mm depth, where a sensor had been plugged in previously during transfer from field to shed). Very often the topsoil dye patterns appeared to be generated by water flowing around wormholes, cracks, roots or loose soil, unless the soil was loose and high in organic matter. The water flow followed the large pores which connected to deeper parts of the profile. Larger stained areas were found at the ends of a few of the channels, indicating the appearance of internal trapping zones or pockets. Data for the horizontal dye coverage also strongly supports the flow pattern observed in the horizontal image.

***Top soil*:**

There were mainly two types for the staining pattern of topsoils. In lysimeters C, B and A, most of the dye was transported through worm holes through the topsoil. By contrast the topsoil staining areas in lysimeters D, E and F were more than 80%. Figure 5.9 shows examples of horizontal views of lysimeters D (left) and A (right).

In lysimeter D, the patterns showed a frequent appearance of horizontal transport over several centimetres right at the topsoil-subsoil interface, indicating a higher hydraulic conductivity in the horizontal direction than in the vertical direction. The horizontal transport observed in this zone may serve to distribute the water to underlying vertically oriented earthworm channels. While in lysimeter A there was a belt, roughly 5 cm thick, with fine texture right below the interface, where there were relatively few stained areas appearing on horizontal cross sections (Figure 5.9, right). The stained areas were centred on wormholes, as we have seen visually.

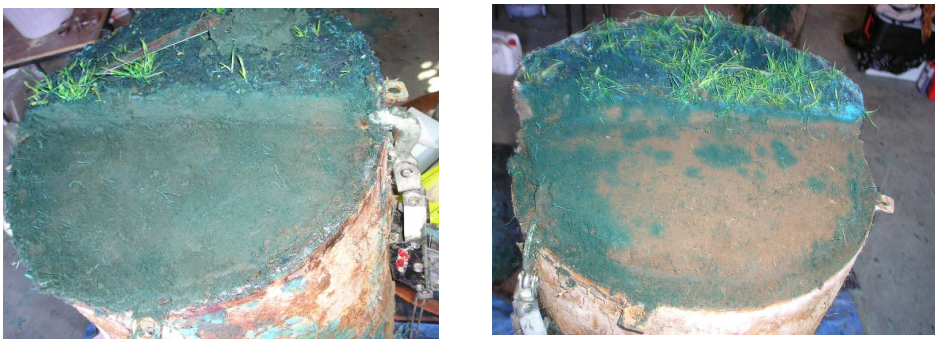

Figure 5.9 Staining patterns (horizontal cross section at 5 cm depth) viewed on the topsoil of lysimeter D (left) and lysimeter A (right)

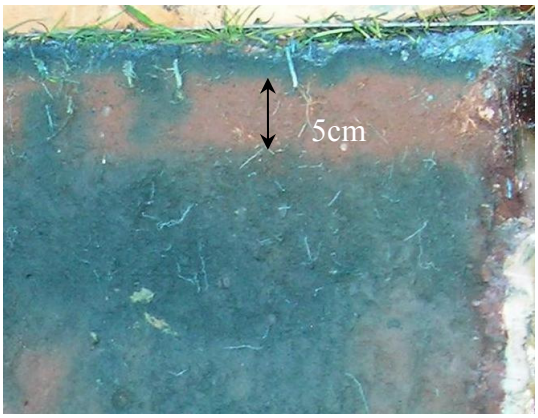

Figure 5.10 Staining pattern (vertical cross section view) in the topsoil of lysimeter A

Soil between 30 - 50 cm

The dye was distributed where the wormholes or cracks presented in this layer, however no visible macropores were seen in lysimeter D at these depths. There were cracks made visible by dye in Lysimeters A, B and E at depths around 40 to 50 cm. There were also wormholes without dye coming through. That suggested discontinuity of pores.

Soil below 50 cm

In all lysimeters the soil below 50 cm (55 cm in lysimeter D) was sandy soil, and the dye (if it reached there) was spread over the adjacent area.

5.7.2 Flow pattern and bacterial leaching

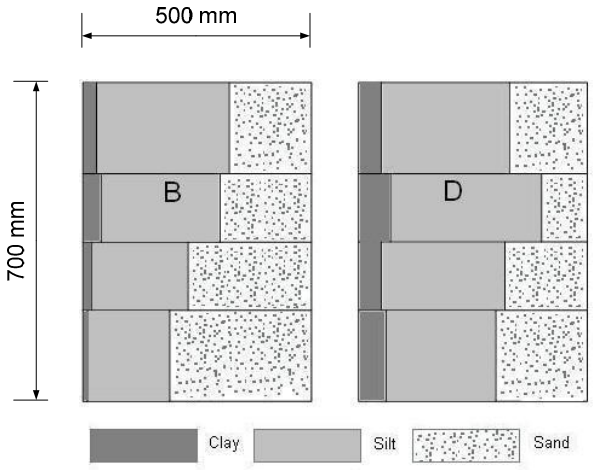

Figure 5.11 Particle size distributions in the four layers

Two typical flow patterns were observed, and are illustrated here for lysimeters B and D. This somewhat arbitrarily chosen example will be used mainly to illustrate the effects of the structure on flow pattern and bacterial leaching. Table 5.3 summarises the measured bacterial and chemical tracer leaching on the day of DSE application in Trial 1, during the earlier bacterial transport study; and also the hydraulic characteristics obtained from infiltrometer measurements. Figure 5.11 and Table 5.2 give the soil texture information for those two lysimeters.

Table 5.2. Physical properties of two of the lysimeters (B and D) used in this study

	Depth (mm)	Clay (%)	Silt (%)	Sand (%)	Specific surface area (m^2 g^{-1})	Textural Class*	BD (g cm^{-3})	Porosity (%)
	0-200	7.34	55.69	36.97	0.41	Silt loam	1.27	0.51
	200-350	7.93	51.67	40.41	0.43	Silt loam	1.23	0.53
	350-500	5.55	40.29	54.16	0.32	Sandy loam	1.44	0.46
Lys B	500-700	3.37	33.12	63.52	0.22	Sandy loam	1.45	0.45
	0-200	9.32	57.47	33.22	0.50	Silt loam	1.19	0.54
	200-350	14.10	66.41	19.58	0.69	Silt loam	1.20	0.55
	350-500	9.92	54.69	35.40	0.52	Silt loam	1.59	0.40
Lys D	500-700	10.48	48.88	40.64	0.52	Loam	1.53	0.42

* McLaren (1996)

Table 5.3 Selected characteristics of lysimeters B and D including hydraulic conductivity, and results of bacterial and chemical tracer leaching from Trial 1

Lys.	K_{eff} (mm hr^{-1}) Drainage Class*	Drainage (mL)**	FC Concentration (cfu 100mL^{-1})**	Br^- Concentration (ppm)**	K_{-40} (mm hr^{-1})	K_{sat} (mm hr^{-1})
B	123 Moderately rapid	960	2.20E+02	0.43	1.89	27.6
D	41 Moderate	970	0	4.63	2.42	7.41

* Bowler 1980

** Data for the day of DSE application

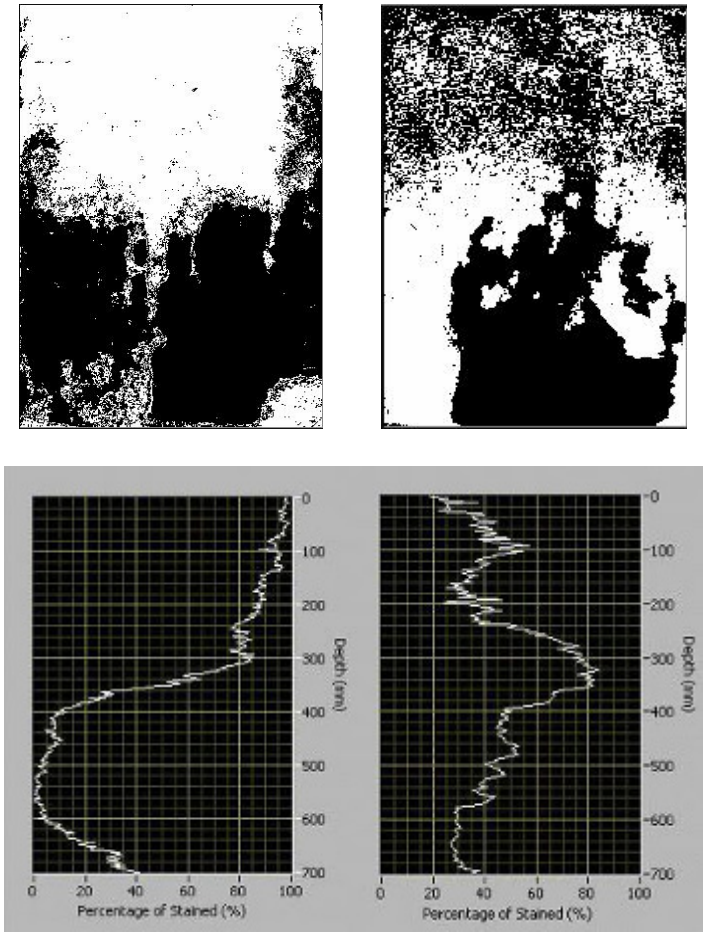

Figure 5.12 Vertical dye coverage in lysimeters D (left) and B (right)

The image analysis results of the two lysimeters are shown in Figure 5.12. In lysimeter D the dye tracer penetrated quite uniformly down to a depth of 30 cm, where the dye coverage was greater than 80%, due to matrix flow. A barrier layer may have restricted most of the water in this upper layer. Light staining was observed in the centre of the profile below 30 cm depth, where a sharp decrease of dye coverage was seen. This type of 'fingering' flow has been observed to develop at the boundary of a finer-textured upper layer and coarser-textured sublayer (Hillel 1998; Kim *et al.* 2004). This is consistent with the results of texture measurements (Figure 5.11), which show finer textured layers on the top (higher clay and silt content) and coarser ones at the bottom where the sand content is

much higher. The second layer (refer to previous chapter) was also the barrier layer for water and contaminant transport. After the wetting front arrived at the interface of these two layers, the downward movement of the wetting front stops due to the higher suction of the finer textured soil (Baker and Hillel 1990). The fingering reached 50 cm, and below that, the soil was more sandy, the dye was spread out and more coverage could be seen. Lysimeter D contained no representative cracks or a developed root system which could have influenced the dye infiltration.

In lysimeter B, the water flow went partly through the topsoil. The dye coverage was around 30-50 % above 20 cm depth and maximum coverage was around 30 cm depth. A big crack was seen around 35-40 cm depth. Water flow just went through that crack and also stained laterally around it. The other part of that layer was left unstained. Flury et al. (1994) also found that macropore flow along cracks led to the deepest dye tracer penetration in well-structured and fine-textured soils.

According to the bacterial transport and infiltrometer measurements, there was more leaching and faster flow rate in lysimeter B than in lysimeter D. Macropores were expected in lysimeter B. This experiment confirmed that point of view. Table 5.3 gives the bacterial leaching on the day of DSE application in Trial 1. While lysimeters B and D got similar amounts of leachate on the day of DSE application, lysimeter B produced leachate faster than D, and the FC concentrations in leachate of those two lysimeters were significantly different, i.e. 2.2 x 10^2 cfu 100 mL^{-1} in B's leachate, and leachate absent in D. That suggests that leaching by macropores results in greater risk of groundwater contamination.

Soil structure is an important factor controlling contaminant leaching. Soils may have similar texture, but different structure, and water will flow faster through easy pathways. Therefore, the average texture may not always represent the conductive properties of soil. For macropore flow, the water flow typically goes through without much lateral distribution. Thus the lateral dye coverage measured in this research is not an accurate quantitative measure of contaminant leaching, for which chemical tracers probably represent a better way. However a dye study can improve the usefulness of soil–morphological information for simulation purposes (Bouma *et al.* 1982).

5.8 Conclusions and suggestions for future work

Binary imagery of dye patterns detects the dye's presence or absence. This type of analysis has revealed the nonuniformity of water infiltration and water flow in the soil profile. This

dye study clearly showed the water flow pattern in lysimeters. The patterns can be divided into two categories: 1) matrix flow dominant, and 2) macropore flow dominant. For lysimeters with macropore flow dominant, macropore flow mostly occurred along cracks and only stained the adjacent area of the cracks, with least interaction with soil. Hence this type of leaching is a great concern for ground water contamination. Cracks were predominantly responsible for deeper contaminant transport.

Lysimeter C was the one of the lysimeters in which we expected to see an obvious macropore staining pattern. Unfortunately, it was accidentally caught by rain after dye was applied, so the staining pattern was not detected clearly.

In this research, we were unable to investigate the interactive effect of management parameters such as irrigation method, and soil surface structure on the relative contribution of macropores to water flow, due to a limited number of lysimeters and their variability. That can be a suggested topic for further research.

Chapter 6 Modelling Water Flow and Bacterial Transport in Undisturbed Monolith Lysimeters Using HYDRUS-1D

Abstract: Knowledge of the fate and transport of bacteria in soils is crucial for assessing the leaching risk of pathogens from land-applied effluent to groundwater. However, there is a lack of information on quantitative field experimental data derived from structured soils and modelling of bacterial movement through these soils. As described in previous chapters, leaching experiments were conducted in six undisturbed soil lysimeters containing a Templeton fine sandy loam, to which were applied dairy shed effluent (DSE) spiked with bromide (Br^-) followed by 9 events of fortnightly water irrigations (flood or spray). This chapter describes simulations of water flow and transport of Br^- and faecal coliforms (FC) using the HYDRUS-1D model.

In order to assess the impact of DSE and water irrigation on soil hydraulic properties, transient water flow was simulated separately for pre- and post-DSE application periods, respectively. The measured daily rainfall (and irrigation for post-DSE period) and potential evapotranspiration from nearby Broadfield station were used as a time-variable boundary. The hydraulic parameters for the two periods were optimised to match the measured water contents. The initial inputs of the hydraulic parameters were estimated from either fitting the measured water retention curves with RETC or using the neural network prediction in HYDRUS-1D from the measured soil texture (percentage of sand, silt and clay) and bulk density. Measured effective saturated hydraulic conductivities, K_{eff}, were also used as input for the model. Model results show that soil lysimeters demonstrated large variations in their hydraulic characteristics. Simulations of water flow for the post-DSE period yielded commonly decreased saturated water contents (θ_s) in comparison with the pre-DSE period, suggesting the presence of macropore flow, which could be enhanced by irrigation.

The optimised hydraulic parameters of the post-DSE period were kept constant when Br^- and bacteria data were simulated. A two-region mobile-immobile water transport model (MIM) was applied to Br^- and bacterial data. Dispersivity ξ, immobile water content θ_{im}, mass exchange rate α, and first-order removal rate (for bacteria) were optimized to match the measured Br^- and bacterial concentrations in the lysimeter leachate. A single value was assigned for each of these parameters. For the four lysimeters that had low K_{eff} values,

simulated bacterial concentrations matched very well with measured concentrations using the single porosity hydraulic model in HYDRUS-1D. However for the other two lysimeters that had high K_{eff} values, the good agreement between model-simulated and observed concentrations could only be achieved by using a dual porosity hydraulic model. Bacterial concentrations were under-predicted at the very initial stage in all simulations, indicating that non-equilibrium processes were dominant during those short periods, and suggesting that there were strong dynamic processes involving change in structure change and subsequently flow path. The observed earlier breakthrough of bacteria than Br^- is in consistent with the size exclusion theory.

Keywords: Bacterial transport; undisturbed soil; HYDRUS-1D; MIM model; dual-porosity model; parameter optimization; simulation

6.1 Introduction

Numerical models have been developed in recent years, enabling researchers to simulate complex situations of water flow and contaminant transport especially processes in heterogeneous undisturbed soil columns with variable saturation. There is a need to acquire numerical connection between general field practices, and numerical models for bacterial transport, by defining hydraulic and solute transport parameters on the basis of available measured datasets. Modelling can be a powerful tool to build understanding of a system, and to reduce the complex process to a set of mathematical equations with parameters characterizing the system. Also, modelling enables extension of difficult-to-obtain results to a wider range of conditions or situations and provides tools that can inform practical actions as well as contribute to policy and theory in informatics. That will benefit soil and water management in the dairy industry.

It is vital to describe bacterial transport in porous media more quantitatively and relate it to known soil properties and processes. Much work has been done in modelling bacterial transport in sand column, or repacked columns (Harvey and Garabedian 1991; Tan *et al.* 1994; Blue *et al.* 1995; Deshpande and Shonnard 1999; Shein *et al.* 2002; Jiang *et al.* 2007), but less has been done for undisturbed soil (McGechan and Vinten 2003; Pang *et al.* 2008).

Gerke and van Genuchten (1993)have given a comprehensive review of various theoretical and experimental attempts to deal with water and solute movement in saturated and unsaturated structured soil during steady and transient water flow conditions. Further

progress has recently been made in simulating preferential flow (Gerke and van Genuchten 1996; Šimůnek *et al.* 2001; Šimůnek *et al.* 2003). Those new features were integrated into the HYDRUS model (Šimůnek *et al.* 2005). The fact that these refinements were needed for their theories and models demonstrates the complicated nature of solute leaching in structured, unsaturated soils during transient water flow.

HYDRUS-1D has been used effectively in recent years to model infiltration in heterogeneous soil profiles with different properties and initial wetness values, on the basis of Mualem's theory and Burdine's model (Mualem 1976; van Genuchten 1980; Šimůnek *et al.* 2003; Šimůnek *et al.* 2005). In HYDRUS-1D, the initial water content θ (or pressure head ψ) was allowed to vary with depth z, and different K, θ (or ψ functions) were assigned to soil layers of different thicknesses. As mentioned in previous chapters, heterogeneity due to macropores is one of the main factors increasing risk of groundwater contamination. HYDRUS-1D has options of a two-region mobile-immobile water model for non-equilibrium solute transport and a one-region model for equilibrium solute transport, but still under single porosity for water flow; and a two region mobile-immobile water model for non-equilibrium solute transport and a one-region model for equilibrium solute transport under dual porosity for water flow (Figure 6.1and Figure 6.2).

The main objectives of this project were to apply HYDRUS-1D to describe water flow and bacterial transport in undisturbed soils (in lysimeters) in field conditions following effluent application and water irrigation, and to determine parameters describing soil hydraulic properties and bacterial and Br transport. This was achieved by inverse modelling to match the measured volumetric water contents at different depths and effluent concentrations (of Br^- and bacteria).

6.2 Theory

6.2.1 Water flow

6.2.1.1 Uniform flow-single porosity flow model

In HYDRUS-1D, one-dimensional uniform water movement is described by a modified form of the Richards' equation, using the assumptions that the air phase plays an insignificant role in the liquid flow process and that water flow due to thermal gradients can be neglected (Šimůnek *et al.* 2005).

Predictions of water and solute movement in the soil are traditionally made using the Richards' equation for variably-saturated water flow, and advection-dispersion type equations for solute movement. For a one-dimensional soil profile the Richards' equation for flow in the x-direction was modified by Šimůnek (1998; 2005):

$$\frac{\partial \theta}{\partial t} = \frac{\partial}{\partial x}\left[K(\frac{\partial h}{\partial x} + \cos\alpha) \right] - S \qquad \textbf{(6.1)}$$

Here θ is the volumetric water content [-], h is the soil water pressure head [L], t is time [T], x is the spatial coordinate [L], S is the sink term [T^{-1}], α is the angle between the flow direction and the vertical axis, and K is the hydraulic conductivity [LT^{-1}] as a function of h or θ given by

$$K(h,x) = K_s(x)K_r(h,x) \qquad \textbf{(6.2)}$$

K_r is the relative hydraulic conductivity and *Ks* the saturated conductivity [L T^{-1}].

HYDRUS implements the soil-hydraulic functions of van Genuchten (1980) who used the statistical pore-size distribution model of Mualem (1976) to obtain a predictive equation for the unsaturated hydraulic conductivity function in terms of soil water retention parameters. The expressions of van Genuchten (1980) are given by

$$\theta(h) = \begin{cases} \theta_r + \dfrac{\theta_s - \theta_r}{[1 + |\alpha h|^n]^m} & h < 0 \\ \theta_s & h \geq 0 \end{cases} \qquad \textbf{(6.3)}$$

$$K(h) = K_s S_e^l [1 - (1 - S_e^{1/m})^m]^2 \qquad \textbf{(6.4)}$$

Where $m = 1 - 1/n, n > 1$ **(6.5)**

The above equations contain five independent parameters: $\theta_r, \theta_s, \alpha$, n, and K_s. θ_r and θ_s denote the residual and saturated volumetric water contents, respectively; *Se* is effective saturation, K_s is the saturated hydraulic conductivity, The pore connectivity parameter l in the hydraulic conductivity function was estimated to be about 0.5 as an average for many soils (Mualem 1976). α, n and m are empirical coefficients.

6.2.1.2 Non-uniform flow-dual-porosity model

Preferential flow in structured media can be described using a variety of dual-porosity models (Gerke and van Genuchten 1993; Šimůnek *et al.* 2005; Jarvis 2007). These accept the coexistence of two separate pore domains, and assume that the two domains are the fractures (or inter-aggregate pores, cracks and macropores) and the matrix (Figure 6.1).

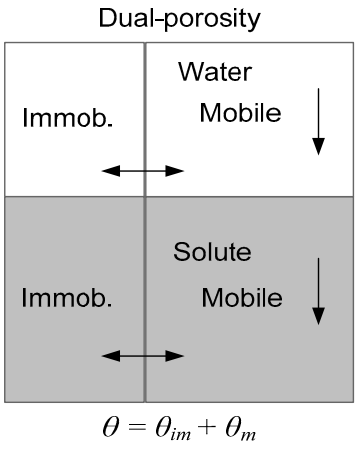

Figure 6.1 **Concept of dual-porosity model on water flow and solute transport (Šimůnek and van Genuchten 2006)**

The dual-porosity formulation for water flow can be based on a mixed formulation of the Richards' equation to describe water flow in the macropores and a mass balance equation to describe moisture dynamics in the matrix as follows (Šimůnek *et al.* 2003):

$$\frac{\partial \theta_m(h_m)}{\partial t} = \frac{\partial}{\partial x_i}\left[K(h_m)(K_{ij}^A \frac{\partial h_m}{\partial x_j} + K_{iz}^A) \right] - S_m(h_m) - \Gamma_w \qquad \textbf{(6.6)}$$

$$\frac{\partial \theta_{im}(h_{im})}{\partial t} = -S_{im}(h_{im}) + \Gamma_w \qquad \textbf{(6.7)}$$

where the subscripts *m* and *im* refer to the mobile and immobile water regions, respectively; $\theta = \theta_m + \theta_{im}$ is the volumetric moisture content [-], S_{im} *and* S_m are sink terms for both regions [T^{-1}], and Γ is the transfer rate for water from the inter- to the intra-aggregate pores [T^{-1}].

The above dual-porosity features were included in the HYDRUS software packages (Šimůnek *et al.* 2003; Šimůnek *et al.* 2005). This option is implemented to permit consideration of physical nonequilibrium transport. The model could be applicable to the case of field soil columns, where large fractures could be represented by the fracture domain and where a matrix containing small-scale fractures might not be considered impermeable and would thus be the second domain (Gerke and van Genuchten 1993). The dual-porosity approach is applicable for variably saturated fluid flow in macropores that are embedded into a porous soil matrix. Such a model can be made quite general by permitting transient variably-saturated flow in the fracture, and simultaneously allowing water to exchange between the fracture and matrix domains (van Genuchten and Šimůnek 2004)

6.2.2 Solute transport

A two-region mobile-immobile model (MIM) (van Genuchten and Wagenet 1989) is included in HYDRUS-1D for simulating solute transport (Figure 6.2). It assumes that water flow and contaminant transport are limited to the mobile water region and that water in the immobile water region is stagnant, with a first-order diffusive exchange process between the two regions (Šimůnek *et al.* 2003; 2005). The following equations are used to simulate solute transport (Šimůnek and van Genuchten 2006):

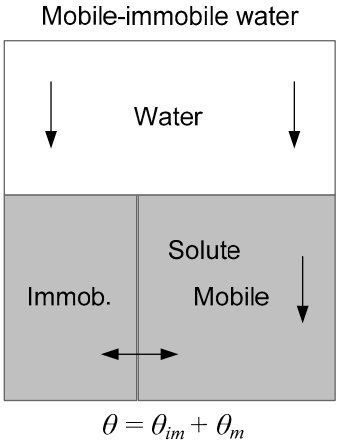

Figure 6.2 **Concept of MIM for water and solute transport (Šimůnek and van Genuchten 2006)**

$$\frac{\partial \theta_m c_m}{\partial t} = \frac{\partial}{\partial x}\left(\theta_m D_m \frac{\partial c_m}{\partial x}\right) - \frac{\partial q\, c_m}{\partial x} - \phi_m - \Gamma_s \qquad \textbf{(6.8)}$$

$$\theta_{im} \frac{\partial c_{im}}{\partial t} = \phi_{im} + \Gamma_s \qquad \textbf{(6.9)}$$

where the subscripts *m* and *im* refer to the mobile and immobile water regions, respectively; *c* is the concentration in the liquid phase [ML^{-3}]; $\theta = \theta_m + \theta_{im}$ is the volumetric moisture content [-]; *D* is the dispersion coefficient [L^2T^{-1}], which is the product of dispersivity ξ [L] and spatial coordinate *x* (i.e., $D = \xi x$); *q* is the water flux [MT^{-1}]; ϕ_m and ϕ_{im} are reactions in the mobile and immobile domains [ML^3T^{-1}], respectively (it is zero for inert tracer), and Γ_s is the solute transfer rate between the two regions [ML^3T^{-1}] governing the rate of solute exchange between the mobile and immobile water regions.

Equations (6.1) - (6.9) were solved numerically using HYDRUS-1D. The governing flow and transport equations are solved numerically using Galerkin-type linear finite element schemes (Šimůnek et al., 2005). HYDRUS also includes a Marquardt-Levenberg type parameter optimization algorithm for inverse estimation of soil hydraulic and/or solute transport and reaction parameters from measured transient or steady-state flow and/or transport data.. HYDRUS-1D was modified for this study to simultaneously assign the same values of optimized parameters to all layers and to keep the mobile water content the

same in all layers. The use of the same parameter values for multiple layers was to reduce the number of parameters to be optimised. This treatment is reasonable as all BTC data were obtained from one sampling point at the bottom of the lysimeters.

6.3 Materials and methods

6.3.1 Leaching experiment

Six experimental soil columns (500 mm x 700 mm) were located in the lysimeter trench at the lysimeter facility of Lincoln University's Centre for Soil and Environmental Quality (CSEQ), with simulated practices of DSE irrigation (spiked with Br^-) and water irrigation, during the 2005/2006 irrigation season (September 2005 to January 2006). The Br^- and FC concentration in effluent were measured. All columns were originally collected from a location used for dairy production more than ten years. These columns were instrumented at four depths (100 mm, 250 mm, 400 mm and 600 mm) with soil moisture sensors (measuring both water content and suction), and temperature sensors. Data were recorded using a datalogger and transferred to computer (refer to Section 3.5 for detail). The data were available from day 45[††]. The DSE application started on day 92, which was set as the transition time between pre-application and post-application simulation. The leaching experiments were carried out for a period of 124 days (refer to Chapter 4, Trial 1 for detail).

6.3.2 Data sets used in modelling

Different measurement sets were used in the inverse optimizations as follows

Water content and pressure head. Daily observed water content θ (measured by TDR probe) and pressure head h data at four depths.

Potential evaporation rate (PE) and potential transpiration rate (PT). Daily potential evapotranspiration (PET) data (mm d^{-1}) were obtained from the Broadfield climate station (about 2 km north of the site), with an adjustment depending on the grass composition health status (e.g. temporary disease). *PET* was divided into *PE* and *PT* for model input. The calculation was on the basis of the following equation (Ritchie 1972):

[††] Days were counted from 1 July 2005 (day 1), and installation of all sensors was completed on 14 Aug. 2005 (day 45), then DSE was applied on 30 Sept.2005 (day 92)

$$PE = PET * \exp(-rExtinct * LAI) \quad \textbf{(6.10)}$$

$$PT = PET - PE \quad \textbf{(6.11)}$$

Here, *rExtinct* is a canopy extinction coefficient, which is 0.60 (Hay and Porter 2006). LAI is Leaf Area Index. For grassland, LAI is generally 3.

Soil texture, water retention and bulk density data. After the leaching experiments, all six soil columns were destructively sampled by layer (following the depths used for sensor installation) for soil particle size distribution (PSD), pore size distribution and bulk density measurement (refer to Section 3.15).

Precipitation: Weather data and rainfall were recorded automatically at the experimental site using a tipping bucket system connected to a data logger (Campbell Scientific, USA). Those data together with irrigation data provided variable boundary condition data.

6.3.3 Description of the simulation

HYDRUS-1D has a maximum capacity of 15 adjustable parameters. In order to simplify the simulation process and decrease the number of estimated parameters, two similar soil layers were combined into one layer. 'Similarity' depended on comparisons of both water content plots and textural composition of the layers. So the required optimized parameters were 15 in total (i.e. three sets of $\theta_r, \theta_s, \alpha,$ n and K_s). The combined layer varied between lysimeters.

The steps used in the modelling can be described as follows.

6.3.3.1 Pre-application simulation (before DSE application) of water flow

Initial soil hydraulic parameters (van Genuchten parameter values) were estimated by pedotransfer functions (PTFs) from soil texture data (measured particle size distribution and bulk density), using the Rosetta package (Schaap *et al.* 2001), which is embedded in HYDRUS-1D; or from measured water retention data (i.e. pairs of pressure head/suction and water content data) using RETC (van Genuchten *et al.* 1991). Some of those parameters were also adjusted on the basis of the dye study.

Initial and boundary conditions were set up using the measured soil water content, rainfall data, irrigation treatment and ET data.

The inverse method available within HYDRUS-1D was then used to determine soil hydraulic parameters simultaneously. This method is based on minimization of an

objective function ϕ (Šimůnek *et al.* 1998), which expresses the difference between the observed and predicted values of soil water content θ, starting with different initial estimates:

$$\phi(b) = \sum_{j=1}^{m} \sum_{i-1}^{n} w_{ij} \left[O_j(z,t_i) - E_j(z,t_j,b) \right]^2 \qquad \textbf{(6.12)}$$

Here m is the number of different sets of measurements, n is the number of observations in a particular measurement set, $O_j\ (z,\ t_i)$ represents observations at time t_i for the *jth* measurement set at location (z), E_m ($x,\ t_i,\ b$) are the corresponding estimated space-time variables for the vector of optimized van Genuchten (1980) parameters (e.g., $\theta_r, \theta_s, \alpha,\ n$ and K_s). w_{ij} are weighting factors that were calibrated in repeated inverse simulation runs until similar contributions were achieved for all observation sets to the weighted least squares of residuals between observations and model estimates. The Levenberg - Marquardt algorithm was applied to minimize the objective function (Šimůnek *et al.* 1998).

6.3.3.2 Post-application simulation (after DSE application) of water flow

There were two ways to estimate initial input parameters for the post application period.

- The pre-application parameters were used as inputs for the post-application, with direct running of the model to test the validity of the fitted parameters.
- Or they were estimated from soil texture data, using the Rosetta package.

The van Genuchten uniform flow (single pore domain) model was also employed in this stage, as in the pre-application simulation. The parameters were optimized simultaneously.

6.3.3.3 Dual-porosity simulation

For those lysimeters for which the uniform flow model could not achieve good fit, the dual-porosity version of HYDRUS-1D was used for post-application simulation. In this research, two lysimeters with fast leaching ability were simulated by the dual-porosity model (refer Section 6.2.1.2).

6.3.3.4 Experimental conditions and boundary conditions

The bottom of each lysimeter has an added 20-30 mm thick layer of gravel. The base is sealed except for the centre hole, open to the atmosphere, for collecting drainage samples. No suction was applied to the base when samples were taken. Thus it only gets water when the bottom is saturated. Mathematically, it is a seepage face (Flury *et al.* 1999).

The root zone depth was developed to *c.* 400 mm, with most roots between 5 and 10 cm. Root-uptake was modelled using a linear root distribution (from 1 to 0 from top to bottom of the root zone), with uptake decreasing linearly with depth *h*. This would allow more loss at the surface and no root uptake at the bottom of the root zone. The function of Feddes (1978) was employed in HYDRUS-1D (Šimůnek *et al.* 1998; Šimůnek *et al.* 2001; Šimůnek *et al.* 2005)

6.3.3.5 Solute (Br^-) and FC transport

A two-region mobile-immobile model (MIM) (van Genuchten and Wagenet 1989) was used to simulate transport of Br^- and bacteria (see Section 6.2.2.and Equations 6.8 and 6.9). Values of ξ, θ_m (via θ_{im}), and α were optimized for Br^- data, while ξ, θ_m (again via θ_{im}), *SinkL* and α were optimized for bacteria data. Single values of ξ, θ_m, α, and *SinkL* (only for FC) were assigned for all layers.

The parameters were obtained by an inverse method, i.e. by simultaneous optimization of the fit of modeled and measured bromide and FC effluent data. The distinctive transport patterns of Br^- and the microbial tracers, as a result of size-exclusion in microbial transport, meant that ξ and θ_m for microbes had to be independently estimated from Br^-.

The inactivation rate for the bacteria in the liquid phase was determined by fitting the die-off experimental data (carried out by auther) with an exponential function $c = c_o \exp(-\mu t)$, using the Solver function of the Excel spreadsheet (where c_o is the influent concentration). See Appendix 1.

6.3.3.6 Goodness of model fit

The goodness of fit of the models was measured by evaluating the sum of squares (*SSQ*) of a nonlinear regression (Marquardt-Levenberg optimization) and a R^2 value (regression of observed vs. fitted values). The best-fit parameters were obtained by minimizing the sum of squares of a linear regression function and maximum R^2 (a value of 1 indicating a perfect correlation between the fitted and observed values). (Šimůnek and Hopmans 2002; Šimůnek *et al.* 2005). Using different initial values of parameters (including the five van Genuchten parameters and solute parameters), *SSQ* and R^2 values were compared to test for rubstness of the optimisation. The constraint for optimized parameters may need to be defined, if necessary, on the basis of values from the literature, or from measurement, in order to get realistic values.

Visual comparison of simulated and observed hydrographs provides a quick and often comprehensive means of assessing the accuracy of model output, including curve match of breakthrough, and curve pattern (Green and Stephenson 1986)

6.4 Results and discussion

6.4.1 Soil properties

Table 6.1 shows the selected soil properties for the lysimeters. There was great variety between layers in one single lysimeter and between lysimeters in soil texture and also porosity. The textural class varied from sandy loam to silt loam and finer to coarser from the surface to the bottom. The organic matter and pH were measured only for the upper 50 mm of the soil, and they ranged from 6.07 % to 7.24 % and from 4.11 to 5.75 respectively.

Table 6.1 Soil properties for the six lysimeters (A – F)

Lysimeter	Depth (mm)	Clay (%)	Silt (%)	Sand (%)	Bulk density (g cm^{-3})	Porosity (%)	Textural Class*	Organic matter (%)	pH
	0-200	19.85	49.51	30.30	1.09	0.58	Silt loam	6.72	4.41
	200-350	16.75	50.11	32.90	1.19	0.55	Silt loam		
	350-500	9.69	58.13	32.18	1.42	0.46	Silt loam		
A	500-700	5.84	46.50	47.66	1.46	0.45	Sandy loam		
	0-200	7.34	55.69	36.97	1.27	0.51	Silt loam	6.21	4.97
	200-350	7.93	51.67	40.41	1.23	0.53	Silt loam		
	350-500	5.55	40.29	54.16	1.44	0.46	Sandy loam		
B	500-700	3.37	33.12	63.52	1.45	0.45	Sandy loam		
	0-200	19.78	54.67	25.12	1.22	0.53	Silt loam	7.24	5.75
	200-350	9.18	56.26	34.55	1.28	0.52	Silt loam		
	350-500	8.96	55.95	35.09	1.43	0.46	Silt loam		
C	500-700	4.82	33.34	61.84	1.54	0.42	Sandy loam		
	0-200	9.32	57.47	33.22	1.19	0.54	Silt loam	7.18	4.72
	200-350	14.10	66.41	19.58	1.20	0.55	Silt loam		
	350-500	9.92	54.69	35.40	1.59	0.40	Silt loam		
D	500-700	10.48	48.88	40.64	1.53	0.42	Loam		
	0-200	9.63	57.40	32.97	1.17	0.55	Silt loam	6.30	4.66
	200-350	8.72	55.83	35.46	1.16	0.56	Silt loam		
	350-500	6.09	41.69	52.22	1.40	0.47	Sandy loam		
E	500-700	5.98	47.99	46.03	1.32	0.50	Sandy loam		
	0-200	8.96	54.91	36.13	1.03	0.60	Silt loam	6.07	4.11
	200-350	8.48	53.60	37.92	1.25	0.53	Silt loam		
	350-500	9.52	54.92	35.56	1.54	0.42	Silt loam		
F	500-700	6.65	46.45	46.90	1.48	0.44	Sandy loam		

* McLaren (1996)

6.4.2 van Genuchten model - inverse analysis

6.4.2.1 Pre- and post- DSE application simulations

Pre-application stage

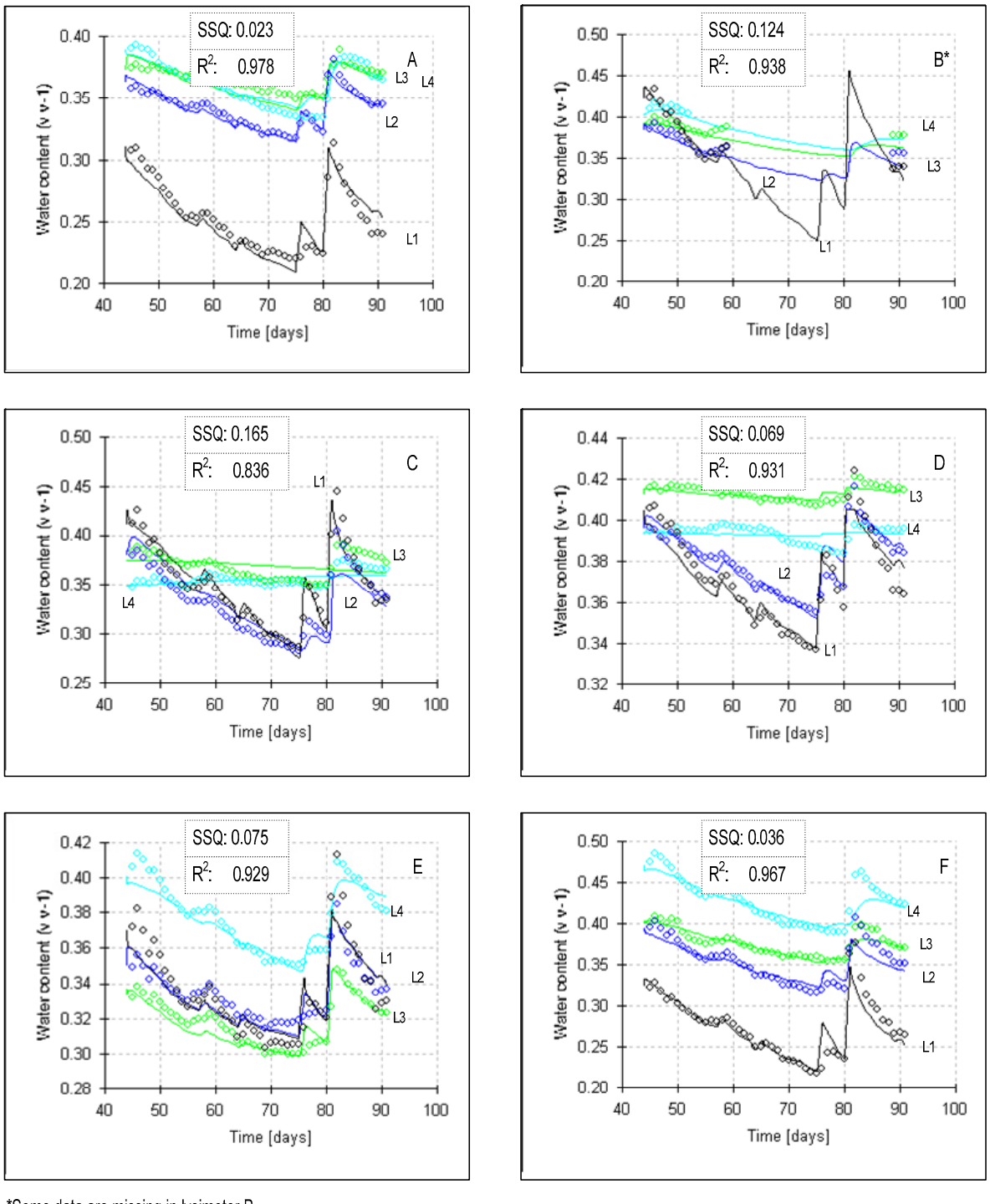

*Some data are missing in lysimeter B

Figure 6.3 Pre-application simulation of water flow in the six lysimeters between days 45 and 92. Lines show predicted values and circles show observations. L1 to L4 represent the four measurement depths (100, 250, 400 and 600 mm).

Figure 6.3 shows the results of the pre-application simulation for water content. All lysimeters gave good fit with the uniform van Genuchten water flow model, based on the statistical functions (*SSQ and* R^2 see Figure 6.3 and Table 6.2). The linear least squares for the pre-application stage are below 0.165 and R^2 are more than 0.836 between measured and predicted water contents, corresponding to Figure 6.3. There is good agreement

between predicted and measured values. During this period, no irrigation was applied, only natural precipitation. Minor preferential flow is expected without irrigation (Chen *et al.* 2002).

The pressure head simulation results (not shown here) were not as good as those for water content. As soil water suction was measured by tensiometer in a smaller soil volume, it may be associated with larger variability and uncertainty than water content, which was averaged over a larger soil volume using TDR-probes. In addition, external factors such as variation in temperature and the long capillary tubes between ceramic cup (Figure 3.3) and pressure transducer may result in larger uncertainties of the pressure head measurements (Jacques *et al.* 2002).

In the pre-application period, the dual-porosity model was also applied. However, it did not fit very well, compared with the uniform flow simulation (results not shown here).

Post-application stage

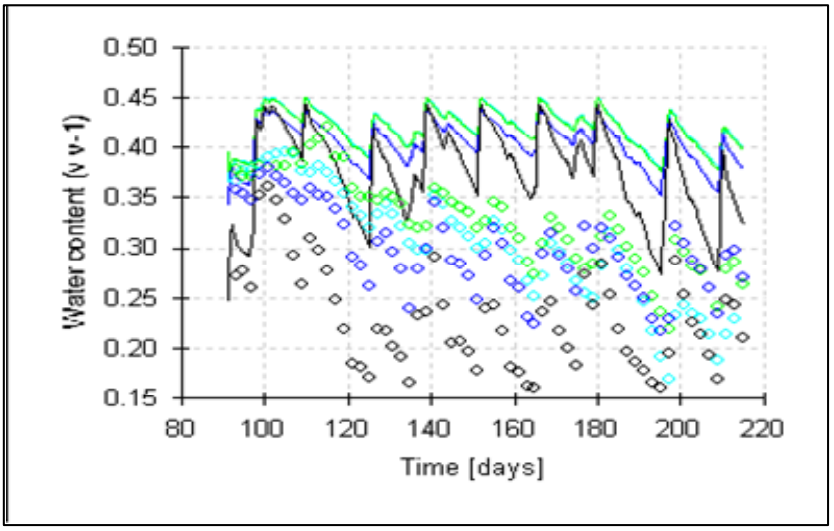

Figure 6.4 Predicted vs. observed values with pre-application parameters in post-application in lysimeter A. Lines show the predicted values and circles show the observed values (black-layer 1, blue-layer 2, light blue-layer 3 and green-layer 4)

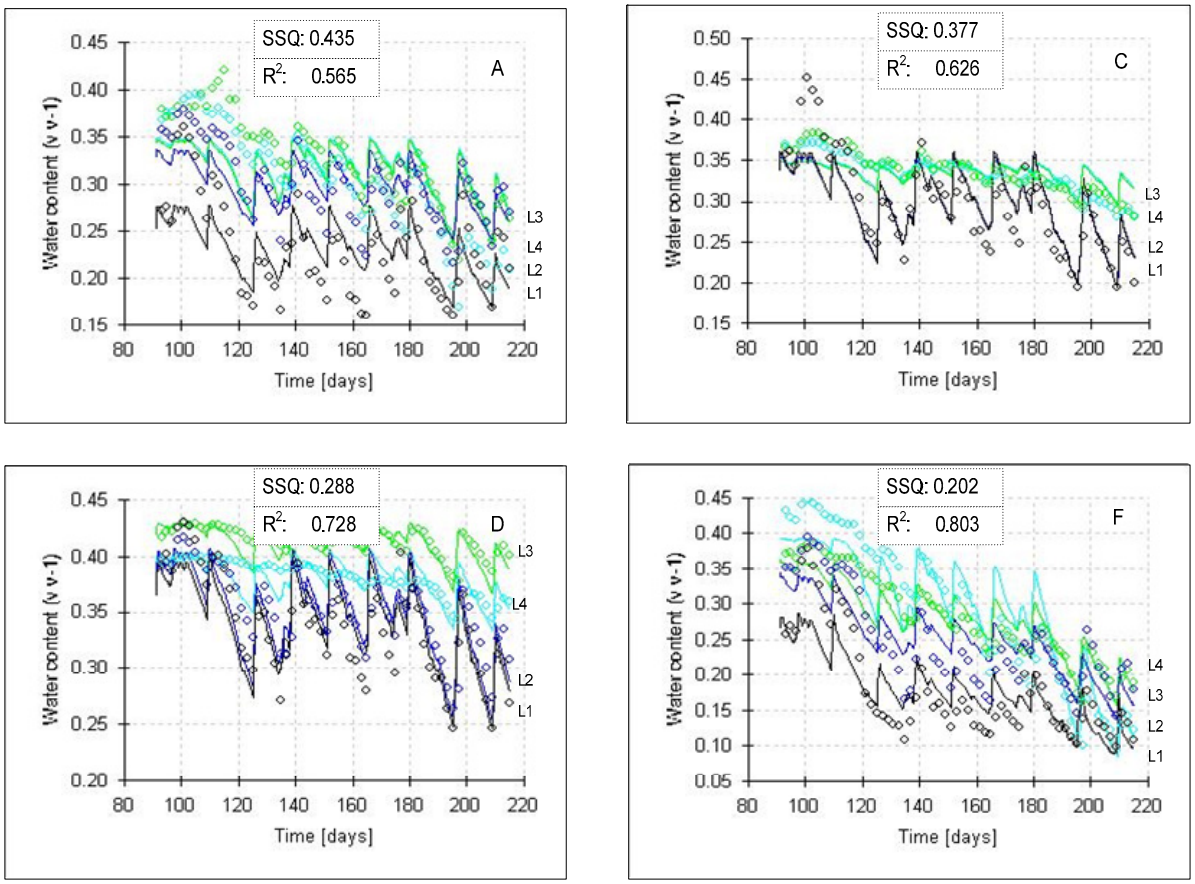

Figure 6.5 Post-application simulation of water flow in four of the lysimeters (A, C, D and F) between days 92 and 215, Lines show predicted values and circles show observations

Post-application simulation of water flow in four of the lysimeters (A, C, D and F) between days 92 and 215, Lines show predicted values and circles show observations Direct (forward) running of the model with pre-application parameters as inputs showed that all predicted values of water content were higher than observed values (Figure 6.4), indicating that more macropores were developed, especially near the surface as the weather was getting warm and dry (refer to Figure 4.4 for corresponding season). Much of water went through preferential flow, bypassed the matrix and drained when irrigation water was applied, resulting in the water content in the soil profile lower than predicted.

The inverse solution was then used to optimize the parameters for post-application. However, not all lysimeters gave good fit using the uniform flow model with a single van Genuchten function. Moreover, in post-application simulations, the goodness of fit was poorer than for pre-application simulation. Figure 6.4 shows the results of post-application simulation, which are considered to be good fits, with linear least squares values below 0.435 and R^2 above 0.565, but the *SSQ* values are very much higher and R^2 values lower than those of pre-application stage. One reason is that the post-application stage was longer

(124 days) than the pre-application (47 days), which correspondingly increased the *SSQ* and reduced R^2 values. Also, during post-application, the irrigation was applied, which is more likely to generate preferential flow compared to rainfall (Chen *et al.* 2002); and also the weather was hotter and drier, which promoted the formation of macropores (Brown *et al.* 2000; Jarvis 2007).

Table 6.2 Hydraulic parameters optimized by the HYDRUS uniform water flow model for the pre- and post- DSE application stages, for lysimeters A, C, D and F.

	Pre-application							Post-application						
Lys.	θ_r ($v\,v^{-1}$)	θ_s ($v\,v^{-1}$)	α (m^{-1})	*n*	*Ks* ($m\,d^{-1}$)	*SSQ*	R^2	θ_r ($v\,v^{-1}$)	θ_s ($v\,v^{-1}$)	α (m^{-1})	*n*	*Ks* ($m\,d^{-1}$)	*SSQ*	R^2
	0.034	0.446	0.221	1.372	7.128	0.023	0.978	0.042	0.308	1.340	1.300	6.339	0.435	0.565
	0.099	0.439	0.208	1.202	6.606			0.103	0.348	0.800	1.305	7.128		
A	0.000	0.450	0.227	1.123	0.172			0.000	0.349	0.286	1.415	1.993		
	0.076	0.450	2.479	1.697	0.121	0.165	0.836	0.058	0.382	0.634	1.788	1.168	0.377	0.626
	0.051	0.415	5.623	1.338	0.223			0.065	0.366	0.600	1.829	7.000		
C	0.001	0.375	5.512	2.423	0.000			0.128	0.350	0.267	1.606	3.370		
	0.059	0.405	0.530	2.571	0.011	0.069	0.931	0.027	0.418	0.601	1.788	7.000	0.288	0.728
	0.014	0.416	0.163	1.898	2.527			0.173	0.430	0.343	1.959	0.268		
D	0.041	0.394	0.111	1.955	0.001			0.202	0.404	0.617	1.654	0.313		
	0.000	0.365	0.785	3.105	0.026	0.036	0.967	0.049	0.358	1.428	2.638	1.405	0.202	0.803
	0.032	0.414	0.727	2.190	0.011			0.007	0.368	1.045	2.298	1.989		
F	0.022	0.485	1.122	1.663	0.041			0.014	0.393	1.255	3.714	0.484		

Simulations of water flow for the post-DSE period generated decreased saturated water contents (θ_s) in comparison with the pre-DSE period, suggesting the presence of macropore flow, which could be enhanced by irrigation (Table 6.2).

The parameters that best describe flow under one set of conditions may not be optimal for another set because the flow geometry may change, especially for short times following the initial water input period. Discrepancies could be seen in the short initial stage, e.g. for lysimeter F or C in Figure 6.4.

6.4.2.2 Br^- and FC transport

Figure 6.6 shows Br^- transport simulation results for lysimeters A, C, D and F. The optimized parameters are displayed in Table 6.3. ξ stands for dispersivity; θ_{im} is the immobile water content*, and* α is mass transfer coefficient for solute exchange between mobile and immobile liquid regions (Table 6.3).

Figure 6.7 shows FC transport simulation results. The regular solute transport model was used with optimisation of three parameters: dispersivity ξ, *SinkL* (representing lumped effects of die-off, plus entrapment in liquid and air-water interfaces,), and α for exchange between mobile and immobile water (see Table 6.3, Section 6.2.2 and 6.3.3.5.)

There were significantly higher normalized concentrations (C/C_0) of FC during the rising limb of the BTC, and the predicted FC obviously were underestimated in the initial stage (in less than an hour) (Figure 6.7). This suggested FC took short-circuit by preferential flow, which is also consistent with the theory of pore size exclusion (Ginn 2002; Sinton *et al.* 2005). Actually, there were under predictions in the initial-stage simulations of water flow (for water content), and most of Br^- and all of FC (for normalized concentrations). This discrepancy may result from the dynamic of structure change of soils, while the mobile and immobile regions are considered by the model to be constant in the whole process (Mitchell and van Genuchten 1991). There have been many evidences indicating that irrigation, when initialized from dry conditions, (especially on the surface), and before the soil can wet up and swell, makes soil prone to have more preferential or non-equilibrium flow, due to prior shrinkage and water repellence (Edwards *et al.* 1993b; Jarvis 2007).

Comparing the parameters in the same lysimeter, the dispersivity ξ for Br^- transport is greater than that for FC transport; and similarly for α (exchange coefficient). That means that FC had less mass exchange between the two regions. Small dispersivity derived from FC data is a result of pore-size exclusion in FC transport, i.e., FC travelled through a narrower range of pore-network. These are the expected trends in the properties of FC and Br^-(Table 6.3).

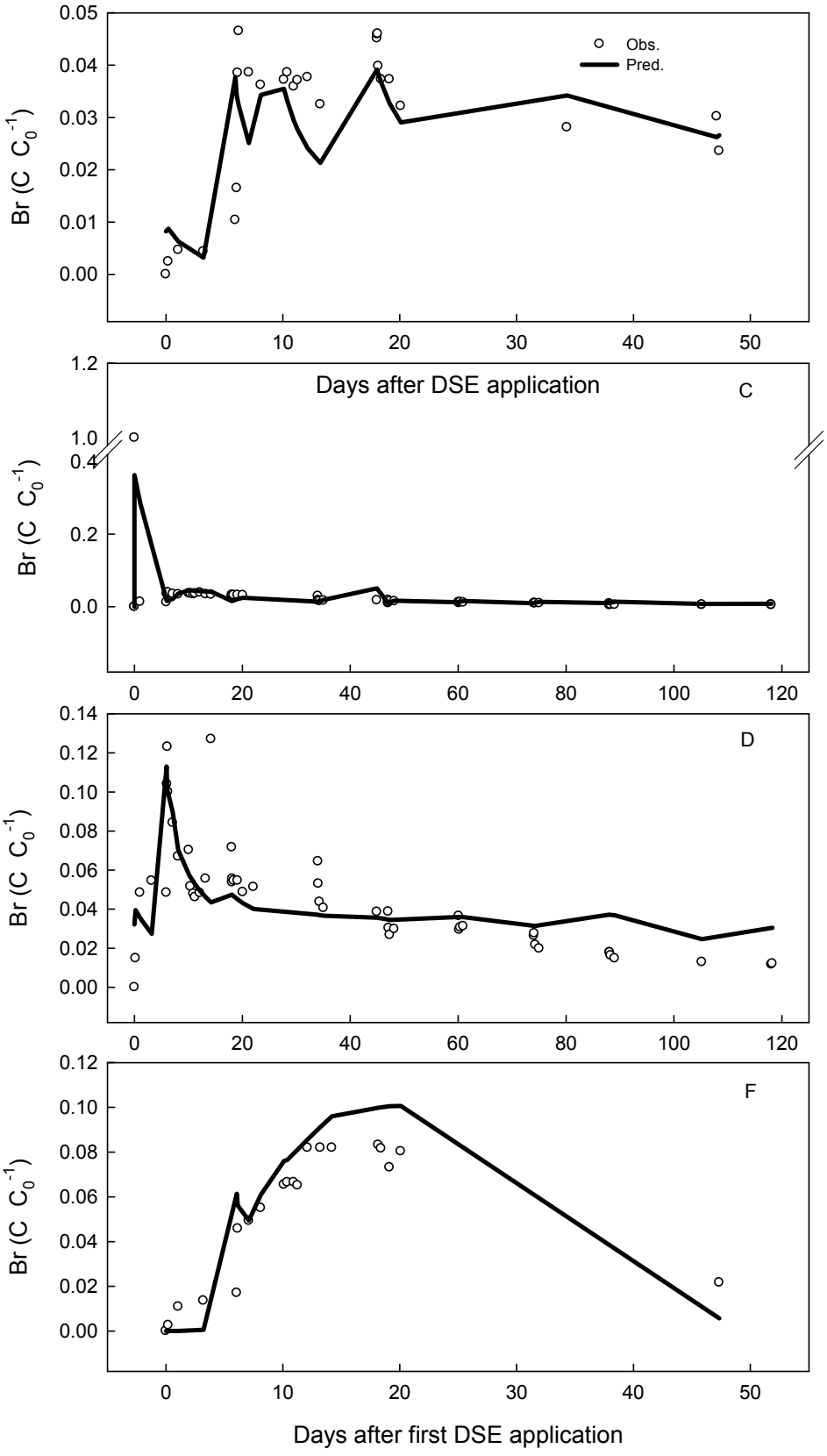

Figure 6.6 Measured (Obs.) and simulated (Pred.) Br^- concentration (normalised) in drainage from lysimeters A, C, D and F

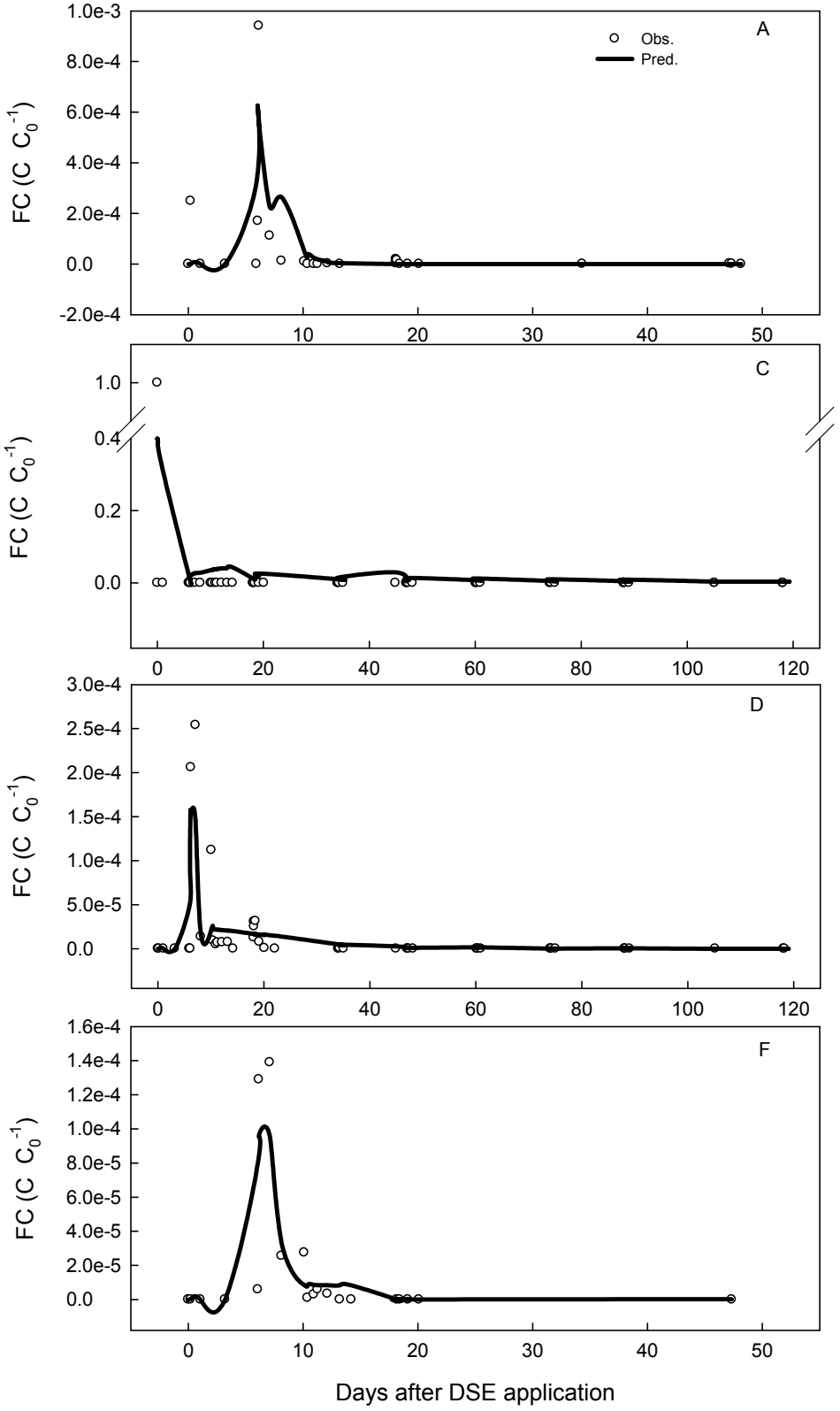

Figure 6.7 Measured (Obs.) and simulated (Pred.) FC concentrations (normalised) in drainage from lysimeters A, C, D and F

Table 6.3 Parameters optimized by the HYDRUS MIM model for Br^- and FC transport, for lysimeters A, C, D and F using uniform flow model

Lysimeter	Br					FC					
	ξ (m)	θ_{im} ($v\ v^{-1}$)	α	SSQ	R^2	ξ (m)	θ_{im} ($v\ v^{-1}$)	SinkL	α	SSQ	R^2
A	0.016	0.245	0.026	0.437	0.581	0.006	0.181	0.753	0.026	0.470	0.530
C	0.547	0.335	0.037	0.501	0.559	0.254	0.330	0.359	0.013	0.518	0.498
D	0.179	0.316	0.014	0.537	0.468	0.004	0.353	0.064	0.000	0.445	0.556
F	0.031	0.254	0.403	0.324	0.892	0.000	0.229	21.573	0.001	0.287	0.717

6.4.2.3 Dual-porosity Model

Based on observations during the destructive sampling of lysimeters, macro-pores were developed to *c*. 400 mm depth, and most had worm channels down to *c*. 400 mm, and a few even deeper. Therefore, the dual-porosity model probably is more realistic to describe water flow and Br^- and FC transport processes. In this research, the dual-porosity model (refer to Section 6.2.1.2) was applied for simulation post-application in lysimeters B and E, which failed to be simulated by the uniform model. B and E were also the two lysimeters with the highest effective conductivity (K_{eff}, refer to Chapter 4) under surface-ponded conditions. For lysimeter E, the hydraulic parameters were optimized for the pre-application stage using the dual porosity model and these acted as initial values for post-application simulation. Lysimeter B had some missing data for the pre-application period, so simulation started from the post-application period.

Using the measured water retention datasets (for suctions 0-1000 mm), RETC was employed to develop the hydraulic parameters. However, the values obtained were not useful for hydraulic parameter estimation, probably because of insufficient pressure head measurement range.

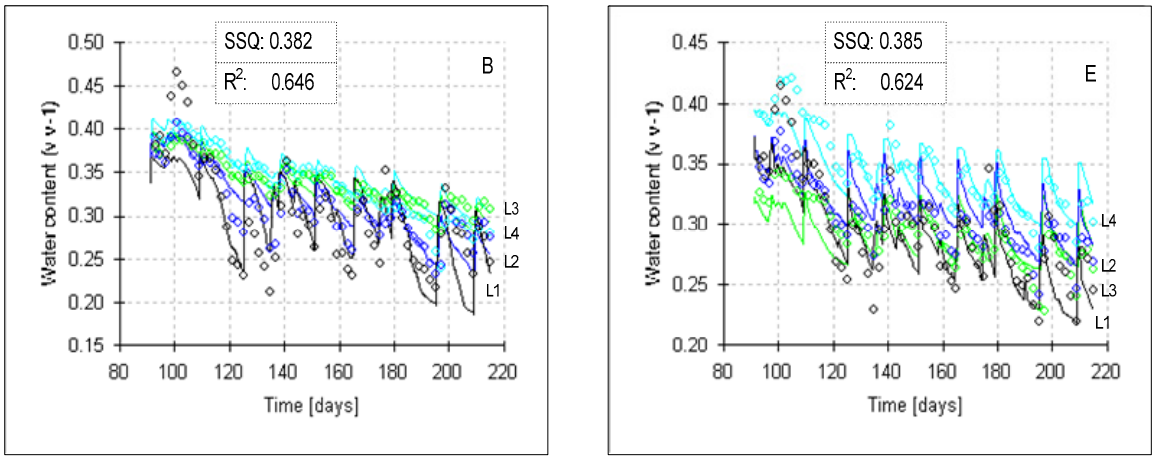

Figure 6.8 Post-application simulation by the dual-porosity model of water content in lysimeters B and E. Lines show predicted results and circles show the observed values)

Simulation results are shown in Figure 6.8 (water flow), Figure 6.9 (Br^- transport), and Figure 6.10 (FC transport). The optimized parameters are listed in Table 6.4, and Table 6.5. The average mobile water content proportion in simulation results is 0.081, which is close to the 0.108 (i.e. 10.8%), the average porosity (from all six lysimeter) of pores with diameter >750μm.

Table 6.4 Hydraulic parameters optimized by dual-porosity model for lysimeters B and E

Lysimeter (layers) \ Variable		θ_m ($v\ v^{-1}$)	*Alpha* (m^{-1})	*n*	*Ks* ($m\ day^{-1}$)	ω	*SSQ*	R^2
B	L_1	0.091	0.010	0.388	8.744	0.003	0.382	0.646
	L_2	0.075	0.255	10.000	2.168	0.003		
	L_3	0.069	1.355	2.170	2.140	0.008		
E	L_1	0.083	1.816	1.846	1.136	0.003	0.385	0.624
	L_2	0.090	10.849	1.207	0.498	0.014		
	L_3	0.076	1.989	1.773	1.101	0.011		

In general, there is good agreement in bromide transport simulation (Figure 6.9), although the observed Br^- concentration drops much faster than predicted using the dual-porosity, mobile-immobile flow model. This indicates that there may be hysteresis in Br^- transfer between mobile and immobile water.

Figure 6.10 shows FC simulation results. Lysimeter B fits very much better than lysimeter E. For E, there were abnormal rises between days 40-60 (4th water irrigation, refer to Chapter 4) resulting from unknown and uncertain reasons, and beyond what the model can do. That produced higher *SSQ* and lower R^2. The α parameter (exchange rate) turned out to be very large, suggesting that FC were multiplying in the soil (Table 6.5).

Table 6.5 Parameters optimized by the HYDRUS MIM model for Br^- and FC transport, for lysimeters B and E using dual-porosity flow model

Lysimeter	Br					FC				
	ξ (m)	*SinkG1`*	*α*	*SSQ*	R^2	*ξ (m)*	*SinkL*	*α*	*SSQ*	R^2
B	0.024	0.109	0.039	0.579	0.422	0.025	0.466	0.040	0.284	0.717
E	0.004	0.092	0.073	0.551	0.638	2.32E-04	0.733	0.562	0.930	0.169

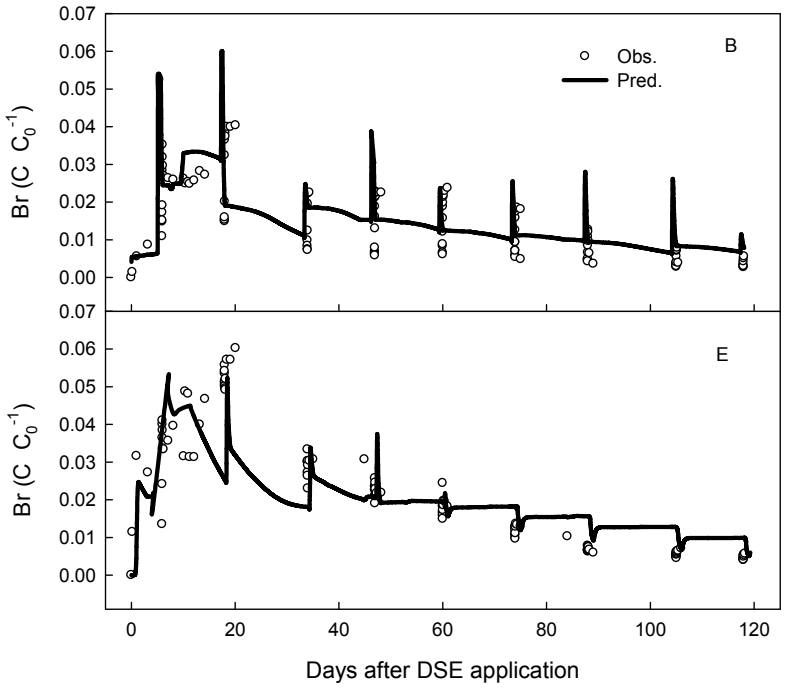

Figure 6.9 Bromide transport simulation for lysimeters B and E in Trial 1, using the dual-porosity (mobile-imobile, head transfer) flow model

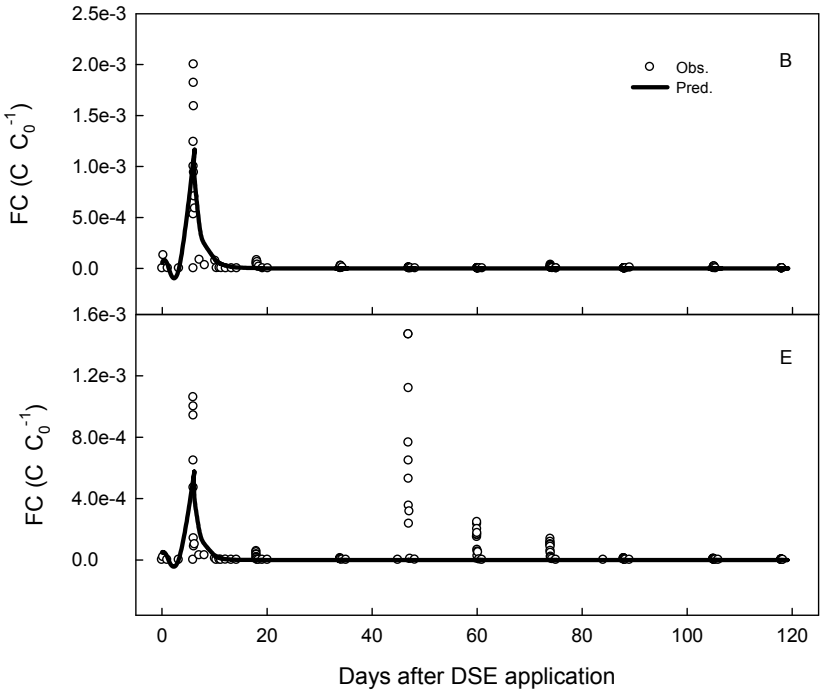

Figure 6.10 Simulations of bacterial transport simulation for lysimeter B and E in Trial 1, using the dual-porosity (mobile-immobile, head transfer) flow model

6.5 Conclusions and recommendations

We applied the inverse method to simultaneously optimize the hydraulic and Br^- and FC transport parameters needed to describe the field-scale water flow and solute transport under transient flow conditions. The uniform flow (single pore domain) model could successfully describe the water flow processes in the pre-DSE application period in all six lysimeters, and in the post-application period in four lysimeters. The fitting results for volumetric water content in the pre-application period are more satisfactory than in the post-application period. Values of the fitted saturated θ_s parameter decreased in the post-application period. Two lysimeters were described by applying the dual-porosity flow model. The Br^- and FC transport could be reasonably described by applying the two-region mobile-immobile model. However, the applied model failed to describe some specific features such as the initial breakthrough feature of FC transport. The introduction of DSE application followed by water irrigation, and the increases of temperature and evapotranspiration in summer, enhanced the preferential flow, which contributed to the

higher FC concentration in effluent. That is probably the main reason for the unfitness of simulation.

Transient flow processes in field conditions may significantly complicate the parametric description of the FC transport processes, especially in the long term with changes in weather, and in physical (e.g. pore geometry), chemical (e.g. reaction), and biological (e.g. bacterial die-off or growing) conditions.

The implication of this research is that preferential flow in the soil facilitated rapid transport of FC from DSE, which has the potential to impair ground water quality. Clearly, management strategies to reduce FC contamination following application of DSE in these soils must aim to decrease preferential flow by adjusting irrigation schemes. Attention needs to be given to decrease irrigation rates at the beginning of each irrigation event.

Chapter 7 Conclusions and Recommendations for Future Work

7.1 Introduction

The ongoing expansion of dairy farming in NZ and the associated increase in DSE land application has the potential to increase the risk of pathogen contamination by leaching from free-draining soils under irrigation. This in turn will influence the long-term environmental sustainability of dairy farming in NZ. While there is some information on N, P and pesticide leaching from pastures in New Zealand, little data is available on the impacts of application of DSE on the bacterial leaching from grassland soils under irrigation. Accordingly, the major objectives of this study were to: understand the processes of bacterial transport, investigate the role and the controlling factors of preferential flow, and extrapolate the relationship between soil properties (like soil structure, texture) and physical status (soil water potential and volumetric water content), and bacterial transport associated with the DSE and water irrigation in a Templeton soil.

7.2 Summary

7.2.1 Field lysimeter experiment

This experiment investigated bacterial transport from land-applied dairy shed effluent, via six field lysimeters, using two irrigation methods with contrasting application rates, through the 2005-06 irrigation season. Transient water flow and bacterial transport were studied, and the factors controlling faecal coliform transport are discussed. Two trials were carried out in summer and autumn seasons, with an introduced bacterial indicator and inert chemical tracers added to the DSE. Leachates were collected after each water irrigation or heavy rainfall (when applicable) for concentration measurement. All lysimeters were instrumented at four depths (100, 250, 450 and 600 mm) for monitoring soil volumetric water content (θ), matric potential (ψ) and temperature.

The lysimeter experiments showed that bacteria could readily penetrate through 700 mm deep soil columns to the bottom. In the summer trial, FC concentration in leachate similar to concentration of DSE was detected in one lysimeter with higher clay content in topsoil immediately after DSE application, and before any water irrigation. This indicated that

applied DSE leached through preferential flow paths without any dilution. The highest post-water-irrigation concentration was 3.4×10^3 cfu 100 mL^{-1} under flood irrigation. Flood irrigation resulted in more bacteria and Br^- leaching than spray irrigation. Trial 2 (autumn) results also showed large differences between irrigation treatments in lysimeters sharing similar drainage class (moderate or moderately rapid), and flood irrigation again gave more bacteria and tracer (Cl^-) leaching. Bacterial concentration in the leachate was positively correlated with both θ and ψ, and sometimes drainage rate. Greater bacterial leaching was found in the lysimeter with rapid whole-column effective hydraulic conductivity, K_{eff} , for both flood and spray treatments. The 'seasonal condition' of the soil (including variation in initial water content) also influenced bacterial leaching, with less risk of leaching in autumn than in summer.

7.2.2 Characterizing soil structure of lysimeters

The measurement of infiltration and a dye study were accomplished for the investigation of soil structure, to connect with the leaching experiment performance. Disc tension infiltrometers were used. Zero and 40 mm suction were applied in order to measure the saturated conductivity K_{sat} and unsaturated conductivity $K\text{-}_{40mm}$. The contribution of macropores with diameters > 0.75 mm to conductivity (macropore flow) in each lysimeter was thus determined from the difference between the two infiltration rates. The results showed in most cases,a correlation between the proportion of bacteria leached and the flow contribution of these macropores. The greater the K_{sat}, the greater the amount of drainage and bacterial leaching obtained. This research also found that this technique may exclude the activity of some continuous macropores (e.g., cracks) due to the difference of initial wetness, which could substantially change the conductivity and result in more serious bacterial leaching in this Canterbury fine sandy loam soil.

The dye infiltration experiment was conducted after the disc infiltration measurements. An image analysis technique – the Robolab software package (2.5.4 c) – was used to determine two-dimensional dye distributions. Our results suggest that, following flooding of the lysimeters with dye solution, there was considerable variation between lysimeters in the pattern of water flow, as indicated by the distribution of dye in both vertical and horizontal directions, and most of the flow reaching deeper than 50 cm resulted from macropores, mainly visible cracks.

7.2.3 Modelling water flow and bacterial (or Br-) transport

Transient water flow was simulated separately for pre- and post-DSE application periods by HYDRUS-1D .We applied the inverse method to simultaneously optimize the hydraulic and Br^- and FC transport parameters needed to describe the field-scale water flow and solute transport under transient flow conditions. The uniform-flow (single pore domain) model could successfully describe the water flow processes in the pre-DSE application period in all six lysimeters, and in the post-application period in four lysimeters. The fitting results for volumetric water content in the pre-application period were more satisfactory than in the post-application period. Values of the fitted saturated θ_s parameter decreased in the post-application period, suggesting the presence of macropore flow, which could be enhanced by irrigation. Flow in two of the lysimeters was described by applying the dual-porosity flow model. The Br^- and FC transport could be reasonably well described by applying the two-region mobile-immobile model. However, the applied model failed to describe some specific features such as the initial breakthrough feature of FC transport. Bacterial concentrations were under-predicted at the very initial stage in all simulations, indicating that non-equilibrium processes were dominant during those short periods, and suggesting that there were strong dynamic processes involving change in structure change and subsequently flow paths.

The introduction of DSE application followed by water irrigation, and the increases of temperature and evapotranspiration in summer, enhanced the preferential flow, which contributed to the higher FC concentration in effluent. That is probably the main reason for the poorer performance of the simulation.

7.3 Main conclusions

- Current practices for land-applied DSE may cause shallow groundwater contamination by microbes where strongly structured, fine-textured soils directly connect with shallow groundwater, especially in dry conditions. In this study FC could readily penetrate through 700 mm deep soil columns to the bottom when DSE and water irrigation were applied in ways representative of general practice. For one lysimeter (C), the immediate leachate after DSE application contained the maximum bacterial concentration.
- Flood irrigation resulted in one order of magnitude more bacterial leaching than spray irrigation, in lysimeters in the same drainage class. For lysimeters with

rapid K_{eff}, there were no obvious effects of the irrigation schemes. High risk of bacterial contamination occurred in both flood and spray treatments, especially in the summer season.

- In the summer, the irrigation posed more threat for shallow groundwater contamination by bacteria than in autumn due to the drier condition of soil columns, especially for those with more clay content in topsoil, when shrinkage cracks could form, promoting preferential flow and facilitating bacterial leaching.
- This study demonstrated that the soil pore system (or structure) is a dynamic system. The relative proportions of macropore and less permeable matrix pores changes with environmental conditions, e.g. the initial water content, water application rate and amount, and soil surface contributing area.
- Dynamic changes in soil structure with time can result in significantly large differences in bacterial leaching. For this field lysimeter study, this is an important factor.
- Our results suggest that bacterial leaching was not interrelated with total porosity. Pore sizes, pore space heterogeneity and continuity are clearly more important for leaching. In this longer-term field trial, multi-factorial interactions complicated the research, so that observations revealed trends rather than results with strong statistical significance.
- Regarding development of BMPs, one problem which needs to be solved by improved soil and water management is to minimise macropore flow and hence K_{sat}. Therefore, practical measures are required to protect groundwater from pathogen contamination, including:

  1) to apply spray irrigation instead of flood irrigation;

  2) to monitor soil water content and schedule irrigation to avoid soil getting extremely dry, especially in summer;

  3) to decrease the DSE application *depth* by increasing irrigator groundspeed, or improve irrigator design to increase application spatial uniformity;

  4) to reduce the application rates of both DSE and water especially at the initial stage of irrigation to allow soil to have enough time to wet up. This

could reduce the risk of leaching in seasons with high risk of crack formation.

7.4 Recommendations for future work

- In this research we were unable to investigate the interactive effect of management factors such as irrigation method and soil surface structure on the relative contribution of macropores to water flow, due to the limited number (six) of lysimeters and their variability. That can be a suggested topic for further research.
- Effluent discharge consents are currently based on N loadings or some farmers now base their effluent loading calculations on potassium levels. It would be useful to determine any correlation between N or K and bacterial loadings for effluent. This would tell us how well the current conditions reflect the risk of microbial leaching.
- There are high degrees of temporal and spatial variations in soil structure, even within soils with identical textures. When investigating structure control of contaminant leaching, a main concern when designing experimental methods or instruments should be keeping the conditions consistent.
- Although the effects of macropore and preferential flow paths on microbial transport in intact soils are well known, seasonal dynamics of soil structure changes need some attention and further research is suggested

References

Abdou HM, Flury M (2004) Simulation of water flow and solute transport in free-drainage lysimeters and field soils with heterogeneous structures. *European Journal of Soil Science* **55**, 229-241.

Abu-ashour J, Joy DM, Lee H, Whiteley HR, Zelin S (1994) Transport of microorganisms through soil. *Water, Air and Soil pollution* **75**, 141-158.

Aislabie J, Smith JJ, Fraser R, McLeod M (2001) Leaching of bacterial indicators of faecal contamination through four New Zealand soils. *Australian Journal of Soil Research* **39**, 1397-1406.

Albinger O, Biesemeyer BK, Arnold RG, Logan BE (1994) Effect of bacterial heterogeneity on adhesion to uniform collectors by monoclonal populations. *Fems Microbiology Letters* **124**, 321-326.

American Public Health Association, American Water Works Association, Federation WE (1998) 'Standard methods for the examination of water and waste water.' (American Public Health Association: Washington, DC).

Ankeny MD, Ahmed M, Kasper TC, Horton R (1991) Simple field methhod for determining unstaturated hydraulic conductivity. *Soil Science Society of America Journal* **55**, 467-470.

Auckland Regional Council (1999) Regional Plan: farm dairy dischargesAuckland, NZ).

Baker RS, Hillel D (1990) Laboratory tests of a theory of fingering during infiltration into layered soils. *Soil Science Society of America Journal* **54**, 20-30.

Ball A (2006) Estimation of the burden of water-borne disease in New Zealand: Preliminary report. Institute of Environmental Science and Research Ltd., Wellington, NZ.

Banning N, Toze S, Mee BJ (2002) *Escherichia coli* survival in groundwater and effluent measured using a combination of propidium iodide and the green fluorescent protein. *Journal of Applied Microbiology* **93**, 69-76.

Barkle GF (2001) The fate of carbon and nitrogen from an organic effluent irrigated onto soil : process studies, model development and testing. PhD Thesis Lincoln University

Becker MW, Collins SA, Metge DW, Harvey RW, Shapiro AM (2004) Effect of cell physicochemical characteristics and motility on bacterial transport in ground water. *Journal of Contaminant Hydrology* **69**, 195-213.

Bejat L, Perfect E, Quisenberry VL, Coyne MS, Haszler GR (2000) Solute transport as related to soil structure in unsaturated intact soil blocks. *Soil Science Society of America Journal* **64**, 818-826.

Beven K (1981) Micro-. meso-, Macro-porosity and channeling flow phenomena in soils. *Soil Science Society of America Journal* **45**, 1245.

Beven K, Germann P (1981) Water flow in soil macropores II. A combined slow model. *Journal of Soil Science* **32**, 15-29.

Beven K, Germann P (1982) Macropores and water flow in soils. *Water Resources Research* **18**, 1311-1325.

Bidwell V, Cameron KC (2001) Methods for the management of nitrogen loading rates from animal effluent onto land. Lincoln Environmental, Lincoln Ventures Ltd. 4466/1, Canterbury.

Blakemore LC, Searle PL, Daly BK (1987) Methods for chemical analysis of soils. NZ soil bureau Scientific Report 80.

Blue KA, Logan BE, Arnold RG (1995) Modeling bacterial detachment during transport through porous media as a residence-time-dependent process. *Water Resources Research* **31**, 2649-2658.

Bogosian G, Sammons LE, Morris PJ, Neil JPO, Heitkamp MA, Weber DB (1996) Death of the *Escherichia coli* K-12 Strain W3110 in soil and water. *Applied and Environmental Microbiology* **62**, 4114-4120.

Bond WJ (1998) Effluent irrigation - an environmental challenge for soil science. *Australian Journal of Soil Research* **36**, 543-555.

Bouma J (1982) Measuring the hydraulic conductivity of soil horizons with continuous macropores. *Soil Science Society of America Journal* **46**, 438-441.

Bouma J (1991) Influence of soil macroporosity on environmental quality. *Advances in Agronomy* **46**, 1-37.

Bouma J, Baker FG, Veneman PLM (1974) Measurement of water movement in soil pedons above the water table. *Information circular* **No. 27**.

Bouma J, Belmans CFM, Dekker LW (1982) Water infiltration and redistribution in a silt loam subsoil with worm channel. *Soil Science Society of America Journal* **46**, 917-921.

Bouma J, Dekker LW (1978) A case study on infiltration into dry clay soil I. Morphological observation. *Geoderma* **46**, 3-13.

Bouma J, Wosten JHM (1979) Flow patterns during extended saturated flow in two, undisturbed swelling clay soils with different macrostructures. *Soil Science Society of America Journal* **43**, 16-22.

Bouwer EJ, Rittmann BE (1992) Comment on "Use of colloid filtration theory in modelling movement of bacteria through contaminated sandy aquifer". *Environmental Science and Technology* **26**, 400-401.

Bowler DG (1980) 'The drainage of wet soil.' (Hodder and Stoughton: Auckland, New Zealand).

Brewer R (1964) 'Fabric and Mineral Analysis of Soils.' (Wiley, NY).

Brown CD, Hollis JM, Bettinson RJ, Walker A (2000) Leaching of pesticides and a bromide tracer through lysimeters from five contrasting soils. *Pest Management Science* **56**, 83-93.

Cameron KC, Buchan GD (2002) Porosity and pore-size distribution. In 'Encyclopedia of Soil Science'. (Ed. R Lal) pp. 1031-1034. (Marcel Dekker, Inc.: NY).

Cameron KC, Di HJ (2004) Nitrogen leaching losses from different forms and rates of farm effluent applied to a Templeton soil in Canterbury, New Zealand. *New Zealand Journal of Agricultural Research* **47**, 429-437.

Cameron KC, Di HJ, McLaren RG (1997) Is soil an appropriate dumping ground for our wastes? *Australian Journal of Soil Research* **35**, 995-1035.

Cameron KC, Smith NP, Mclay CDA, Fraser PM (1992) Lysimeters without edge flow: An improved design and sampling procedure. *Soil Science Society of America Journal* **56**, 1625-1628.

Cameron M, Trenouth C (1999) 'Are desired environmental outcomes being achieved at least cost? : a case study of farm dairy effluent management.' (Ministry for the Environment: Wellington, NZ).

Carr G (2006) The Compliance Status of Dairy Shed Effluent Discharges to Land in the Canterbury Region for the 2005/2006 Season.Report No. R06/39, Christchurch, NZ.

Chen C, Roseberg RJ, Selker JS (2002) Using microsprinkler irrigation to reduce leaching in a shrink/swell clay soil. *Agricultural Water Management* **54**, 159-171.

Chen S, Franklin RE, Quisenberry VL, Dang P (1999) The effect of preferential flow on the short and long-term spatial distribution of surface applied solutes in a structured soil. *Geoderma* **90**, 229-241.

Chu Y, Jin Y, Baumann T, Yates MV (2003) Effect of soil properties on saturated and unsaturated virus transport through columns. *Journal of Environmental Quality* **32**, 2017-2025.

Close M, Dann R (2005) Pathogen pathways-update on groundwater contamination. Ministry of Agriculture and Forestry. Rep. No. 0-478-07835-8 Christchurch, NZ.

Close M, Dann R, Ball A, Pirie R, Savill M, Smith Z (2008) Microbial groundwater quality and its health implications for a border-strip irrigated dairy farm catchment, South Island, New Zealand. *Journal of Water and Health* **6**, 83-98.

Clothier BE, White I (1981) Measurement of sorptivity and soil water diffusivity in the field. *Soil Science Society of America Journal* **45**, 241-245.

Collins R (2002) Management Strategies to Mitigate Faecal Contamination Inferred from Analysis of Data from the Waikato Region. Wellington, NZ.

Conboy MJ, Goss MJ (2000) Natural protection of groundwater against bacteria of faecal origin. *Journal of Contaminant Hydrology* **43**, 1-24.

Cools D, Merckx R, Vlassak K, Verhaegen J (2001) Survival of *E. coli* and *Entercoccus spp*. derived from pig slurry in soils of different texture. *Applied Soil Ecology* **17**, 53-62.

Corapcioglu MY, Choi H (1996) Modeling colloid transport in unsaturated porous media and validation with laboratory column data. *Water Resources Research* **32**, 3437-3449.

Corapcioglu MY, Haridas A (1985) Microbial transport in soils and groundwater: A numerical model. *Advances in Water Resources* **8**, 188-200.

Cox JE (1978) Soils and Agriculture of Part Paparua County.N.Z. Soil Bureau Bulletin 34, Canterbury, New Zealand.

Crane SR, Moore JA (1986) Modeling enteric bacterial die-off : A review. *Water, Air and Soil pollution* **27**, 411-439.

Dairying and the Environment Committee (1996) Dairying and the Environment: Managing Farm Dairy Effluent. Dairy Research Institute, Palmerston North, NZ.

Deely JM, Bruere AC, Mclntosh JJ (1998) Little Waihi Catchment Farm Dairy Shed Impact Report. Environment B. O. P.Environmental Report 98/17, Whakatana, NZ.

Dekker LW, Ritsema CJ (1996) Preferential flow paths in a water repellent clay soil with grass cover. *Water Resources Research* **32**, 1239-1249.

Deshpande PA, Shonnard DR (1999) Modeling the effects of systematic variation in ionic strength on the attachment kinetics of Pseudomonas fluorescens UPER-1 in saturated sand columns. *Water Resources Research* **35**, 1619-1627.

Di HJ, Cameron KC (2005) Reducing environmental impacts of agriculture by using a fine particle suspension nitrification inhibitor to decrease nitrate leaching from grazed pastures. *Agriculture, Ecosystems and Environment* **109**, 202-212.

Di HJ, Cameron KC, Moore S, Smith NP (1998) Nitrate leaching from dairy shed effluent and ammonium fertiliser applied to a free-draining pasture soil under spray or flood irrigation. *New Zealand Journal of Agricultural Research* **41**, 263-270.

ECan (2001) 'Environmental Guidelines for Dairy Farming in Canterbury.' (Christchurch, NZ).

ECan, Dexcel Ltd. (2004) A Guide to Managing Farm Dairy Effluent. Christchurch, NZ.

Edwards WM, Shipitalo MJ, Owens LB (1993a) Gas, water and solute transport in soils containing macropores: a review of methodology. *Geoderma* **57**, 31-49.

Edwards WM, Shipitalo MJ, Owens LB, Dick WA (1993b) Factors affecting preferential flow of water and atrazine through earth-worm burrows under continuous no-till corn. *Journal of Environmental Quality* **22**, 453-457.

Ersahin S, Papendick RI, Smith JL, Keller CK, Manoranjan VS (2002) Macropore transport of bromide as influenced by soil structure differences. *Geoderma* **108**, 207-223.

EWRC, Dexcel Ltd. (2005) A Guide to Managing Farm Dairy Effluent.

Feigin A, Ravina I, Shalhevet J (1991) 'Irrigation with treated sewage effluent : management for environmental protection.' (Springer-Verlag: Berlin ; New York).

Ferguson C, Husman AMD, Altavilla N, Deere D, Ashbolt N, de RHAM (2003) Fate and transport of surface water pathogens in watersheds. *Critical Reviews in Environmental Science and Technology* **33**, 299-361.

Flury M (1996) Experimental evidence of transport of pesticides through field soils-A review. *Journal of Environmental Quality* **25**, 25-45.

Flury M, Flühler H (1994) Brilliant Blue FCF as a dye tracer for solute transport studies - a toxicological overview. *Journal of Environmental Quality* **23**, 1108-1112.

Flury M, Flühler H (1995) Tracer characteristics of Brilliant Blue FCF. *Soil Science Society of America Journal* **59**, 22-27.

Flury M, Flühler H, Jury WA, Leuenberger J (1994) Susceptibility of soils to preferential flow of water - a field study. *Water Resources Research* **30**, 1945-1954.

Flury M, Wai NN (2003) Dyes as tracers for vadose zone hydrology. *Reviews of Geophysics* **41**, 1-37.

Flury M, Yates MV, Jury WA (1999) Numerical analysis of the effect of the lower boundary condition on solute transport in lysimeters. *Soil Science Society of America Journal* **63**, 1493-1499.

Fontes DE, Mills AL, Hornberger GM, Herman JS (1991) Physical and chemical factors influencing transport of microorganisms through porous media. *Applied and Environmental Microbiology* **57**, 2473-2481.

Francis GS, Cameron KC, Kemp RA (1988) A comparison of soil porosity and solute leaching after six years of direct drilling or conventional cultivation. *Australian Journal of Soil Research* **26**, 637-649.

Gagliardi JV, Karns JS (2000) Leaching of *Escherichia coli* O157 :H7 in diverse soil under various agricultural management practices. *Applied and Environmental Microbiology* **66**, 877-883.

Gerba CP, Bitton G (1984) Microbial pollutants: their survival and transport pattern to groundwater. In 'Groundwater Pollution Microbiology' pp. 65-88. (John Wiley & Sons, NY.

Gerba CP, James E. Smith J (2005) Sources of pathogenic microorganisms and their fate during land application of wastes. *Journal of Environmental Quality* **34**, 42-48.

Gerba CP, Wallis C, Melnick JL (1975) Fate of wastewater bacteria and viruses in soil. *Journal of the Irrigation and Drainage Division* **101**, 157-174.

Gerke HH, van Genuchten MT (1993) A dual-porosity model for simulating the preferential movement of water and solutes in structured porous media. *Water Resources Research* **29**, 305-320.

Gerke HH, van Genuchten MT (1996) Macroscopic representation of structural geometry for simulating water and solute movement in dual-porosity media. *Advances in Water Resources* **19**, 343-351.

German-Heins J, Flury M (2000) Sorption of Brilliant Blue FCF in soils as affected by pH and inonic strength. *Geoderma* **97**, 87-101.

Germann P, Beven K (1981) Water flow in soil macropores I. An experimental approach. *Journal of Soil Science* **32**, 1-13.

Ginn TR (2002) A travel time approach to exclusion on transport in porous media. *Water Resources Research* **38**, 12.01-12.12.

Ginn TR, Wood BD, Nelson KE, Scheibe TD, Murphy EM, Clement TP (2002) Processes in microbial transport in the natural subsurface. *Advances in Water Resources* **25**, 1017-1042.

Gish TJ, Isensee AR, Nash RG, Helling CS (1991) Impact of pesticides on shallow groundwater quality. *Transactions of the ASAE.* **34**, 1745-1753.

Golabi MH, Radcliffe DE, Hargrove WL, Trollner EW (1995) Macro effects in conventional tillage and no-tillage soils *Journal of Soil and Water Conservation* **50**, 205-210.

Goss MJ, Howse KR, Lane PW, Christian DG, Harris GL (1993) Losses of nitrate-nitrogen in water draining from under autumn-sown crops established by direct drilling or mouldboard ploughing. *Journal of Soil Science* **44**, 35-48.

Green IRA, Stephenson D (1986) Criteria for comparison of single event models. *Hydrological Sciences* **31**, 395-411.

Hallberg GG, Baker JL, Randall GW (1986) Utility of tile-line effluent studies to evaluate the impact of agricultural practice on ground water In 'Proceedings of Conference on Agricultural Impacts on Ground Water'. Omaha, NE pp. 298-326. (National Water Well Assoc. Dublin, OH).

Hamdi M, Durnford D, Loftis J (1994) Bromide transport under sprinkler and ponded irrigation. *Journal of Irrigation and Drainage Engineering-ASAE* **120**, 1086-1097.

Harris RF (1981) Water Potential on Microbial Growth and Activity. In 'Water Potential Relations in Soil Microbiology'. (Eds JF Parr, WR Gardner, LF Elliot) pp. 23-95. (Soil Science Society of America: WI).

Harvey RW (1991) Parameters involved in modeling movement of bacteria in groundwater. In 'Modeling the Environmental Fate of Microorganisms'. (Ed. CJ Hurst) pp. Chapter 5, 89-114. (The American Society for Microbiology: Washington, D. C.).

Harvey RW (1997) Microorganisms as tracers in groundwate injection and recovery experiments: a review. *FEMS microbiological Reviews* **20**, 461-472.

Harvey RW, Garabedian SP (1991) Use of colloid filtration theory in modeling movement of bacteria through a contaminated sandy aquifer. *Environmental Science and Technology* **25**, 178-185.

Harvey RW, Geoge LH, Smith RL, LeBlanc DR (1989) Transport of microspheres and indigenous bacteria through a sandy aquifer: results of natural and forced-gradient tracer experiments. *Environmental Science and Technology* **23**, 51-56.

Hawke RM, Summers SA (2003) Land application of farm dairy effluent: results from a case study, Wairarapa, New Zealand. *New Zealand Journal of Agricultural Research* **46**, 339-346.

Hay RKM, Porter JR (2006) 'The Physiology of Crop Yield ' (Ames, Iowa : Blackwell Pub.: Oxford, UK).

Heathwaite AL, Dils RM (2000) Characterising phosphorus loss in surface and subsurface hydrological pathway. *The Science of the Total Environment* **251**, 523-538.

Heatley P (Ed.) (1996) 'Dairying and the Environment,Managing Farm Dairy Effluent.' (Dairying and the Environment Committee: Palmerston North).

Hegde P, Kanwar RS (1997) Impact of manure application on groundwater quality? In 'ASAE Annual International Meeting,' pp. Paper No. 97-2144. (AWE, Minneapolis, MI.).

Hillel D (1998) 'Environmental Soil Physics.' (Academic Press: London, UK).

Hornberger GM, Beven KJ, Germann PF (1990) Inferences about solute transport in macroporous forest soils from time series models. *Geoderma* **46**, 249-262.

Horton RE (1942) Remarks on hydrologic terminology. *Eos Trans. AGU* **23**, 479-482.

Howell JM, Coyne MS, Cornelius P (1995) Fecal bacteria in agricultural waters of the bluegrass region of Kentucky. *Journal of Environmental Quality* **24**, 411-419.

Hussen AA, Warrick AW (1993) Algebraic models for disc matric suction infiltrometers. *Water Resources Research* **29**, 2779-2786.

Hutson JL, Wagenet RJ (1995) A multi-region model describing water flow and solute transport in heterogeneous soils. *Soil Science Society of America Journal* **59**, 743-751.

Jacques D, Šimůnek J, Timmerman A, Feyan J (2002) Calibration of Richards' and convection-dispersion equations to field-scale water flow and solute transport under rainfall conditions. *Journal of Hydrology* **259**, 15-31.

Jamieson RC, Gordon RJ, Sharples KE, Stratton GW, Madani A (2002) Movement and persistence of fecal bacteria in agricultural soils and subsurface drainage water: a review. *Canadian Biosystems Engineering* **44**, 1.1-1.9.

Jarvis NJ (2007) A review of non-equilibrium water flow and solute transport in soil macropores:principles, controlling factors and consequences for water quality. *European Journal of Soil Science* **58**, 523-546.

Jiang G (2005) Bacterial transport and deposition in an intact soil lysimeter and packed sand columns. Master Thesis, Lincoln University.

Jiang G, Noonan MJ, Buchan GD, Smith N (2005) Transport and deposition of *Bacillus subtilis* through an intact soil column. *Australian Journal of Soil Research* **43**, 695-703.

Jiang G, Noonan MJ, Buchan GD, Smith N (2007) Transport of *Escherichia coli* through vairably saturated sand columns and modeling approaches. *Journal of Contaminant Hydrology* **93**, 2-20.

Jiang X, Morgan J, Doyle MP (2002) Fate of *Escherichia coli* 0157:H7 in manure-amended soil. *Applied and Environmental Microbiology* **68**, 2605-2609.

Joergensen RG, Küntzel H, Scheu S, Seitz D (1998) Movement of fecal indicator organisms in earthworm channel under a loamy arable and grassland soil. *Applied Soil Ecology* **8**, 1-10.

Jones DL (1999) Potential health risks associated with the persistence of *Escherichia coli* O157 in agricultural environments. . *Soil Use and Management* **15**, 76-83.

Kätterer T, Schmied B, Abbaspour KC, Schulin R (2001) Single- and dual-porosity modelling of multiple tracer transport through soil columns: effects of initial moisture and mode of application. *European Journal of Soil Science* **52**, 25-36.

Keswick BH, Wang D-s, Gerba CP (1982) The use of microorganisms as ground-water tracers: A review. *Ground Water* **20**, 142-149.

Kim JG, Chon C-M, Lee J-S (2004) Effect of structure and texture on infiltration flow pattern during flood irrigation. *Environmental Geology* **46**, 962-969.

Kladivko EJ, Van Scoyoc G, Monke EJ, Oates KM, Pask W (1991) Pesticide and nutrient movement into subsurface tile drains in a silt loam soil in Indiana. *Journal of Environmental Quality* **20**, 264-270.

Kluitenberg GJ, Horton R (1990) Effect of solute application method on preferential transport of solutes in soil. *Geoderma* **46**, 283-297.

Kool JB, Genuchten MTV (1991) HYDRUS. One-dimensional variably saturated flow and transport model including hysteresis and root water uptake. U. S. Salinity Lab., Riverside, CA.

Kutilek M (1996) Water relation and water management of Vertisols. Elsevier Science Publishers, Amsterdam.

Lin HS, McInnes KJ (1995) Water flow in clay soil beneath a tension infiltrometer. *Soil Science* **159**, 375-382.

Livestock Improvement Ltd., Dairy InSight NZ (2004-2005) Dairy statistics 2004-2005.

Livestock Improvement Ltd., Dairy InSight NZ (2005-2006) Dairy statistics 2005-2006.

Longhurst RD, Roberts AHC, O'connor MB (2000) Farm dairy effluent: A review of published data on chemical and physical characteristics in New Zealand. *New Zealand Journal of Agricultural Research* **43**, 7-14.

Luxmoore RJ (1981) Micro-, meso-, and Macro-porosity of soil. *Soil Science Society of America Journal* **45**, 671-672.

McCaulou DR, Bales RC (1995) Effect of temperature-controlled motility on transport of bacteria and microspheres through saturated sediment. *Water Resources Research* **31**, 271-280.

McCaulou DR, Bales RC, McCarthy JF (1994) Use of short-pulse experiments to study bacteria transport through porous media. *Journal of Contaminant Hydrology* **15**, 1-14.

McDowell-Boyer LM, Hunt JR, Sitar N (1986) Particle transport through porous media. *Water Resources Research* **22**, 1901-1921.

McGechan MB, Vinten AJA (2003) Simulation of transport through soil of *E. coli* derived from livestock slurry using the MACRO model. *Soil Use and Management* **19**, 321-330.

McGechan MB, Vinten AJA (2004) Simulating transport of *E. coli* derived from faeces of grazing livestock using the MACRO model. *Soil Use and Management* **20**, 195-202.

McIndoe I (1998) Testing of Irrigation Best Management Guidelines. MAF Technical Paper No. 00/06, Wellington, NZ.

McInerney MJ (1991) Use of models to predict bacterial penetration and movement within a subsurface matrix. (Ed. CJ Hurst) pp. 115-131.

McIntosh J, Gordon DA, Environment BOP. (2002) Land Application of Dairy Shed Effluent and Effects on Groundwater Quality. Environment BOP, Whakatane, N.Z.

McLaren RG, Cameron. KC (1996) 'Soil Science: Sustainable Production and Environmental Protection.' (Oxford University Press: Auckland, NZ).

McLeod M, Aislabie J, Ryburn J, McGill A (2004) Microbial and chemical tracer movement through Granular, Ultic and Recent Soils. *New Zealand Journal of Agricultural Research* **47**, 557-563.

McLeod M, Aislabie JM, Ryburn J, McGill A, Taylor MD (2003) Microbial and chemical tracer movement through two Southland soils, New Zealand. *Australian Journal of Soil Research* **41**, 1163-1169.

McLeod M, Aislabie JM, Smith J, Fraser RH, Robert A, Taylor MD (2001) Viral and chemical tracer movement through contrasting soil. *Journal of Environmental Quality* **30**, 2134-2140.

McLeod M, Schipper LA, D TM (1998) Preferential flow in a well drained and a poorly drained soil under different overhead irrigation regimes. *Soil Use and Management* **14**, 96-100.

Medema GJ, Bahar M, Schets FM (1997) Survival of *Cryptosporidium parvum*, *E. coli*, fecal enterococci and *Clostridium perfringens* in River water - influence of temperature and autochthonous microorganism. *Water Science and Technology* **35**, 249.

Mitchell AR, van Genuchten MT (1991) Deterministic modeling of preferential flow in a cracked soil during flood irrigation. . In 'Preferential Flow'. (Eds TJ Gish, A Shirmohammadi) pp. 278-287. (Am. Soc. Agric. Eng.: St. Joseph, MI).

Mon J, Flury M, Harsh JB (2006) Sorption of four triarylmethane dyes in a sandy soil determined by batch and column experiments. *Geoderma* **133**, 217-224.

Monaghan RM, Smith LC (2004) Minimizing surface water pollution resulting from farm-dairy effluent application to mole-pipe drained soils. II. The contribution of preferential flow of effluent to whole-farm pollutant losses in subsurface drainage from a West Otago Dairy farm. *New Zealand Journal of Agricultural Research* **47**, 417-428.

Mualem Y (1976) A new model for prediction of the hydraulic conductivity of unsaturated porous media. *Water Resources Research* **12**, 513-522.

Mubiru DN, Coyne MS, Grove JH (2000) Mortality of *E. coli* O157:H7 in two soils with different physical and chemical properties. *Journal of Environmental Quality* **29**, 1821-1825.

Natsch A, Keel C, Troxler J, Zala M, Albertini NV, Defago G (1996) Importance of preferential flow and soil management in vertical transport of a biocontrol strain of *Pseudomonas fluorescens* in structured field soil. *Applied and Environmental Microbiology* **62**, 33-40.

Newby DT, Pepper IL, Maier RM (2000) Microbial transport. In 'Environmental Microbiology'. (Eds RM Maier, IL Pepper, CP Gerba). (Academic: San Diego, California; London).

Nielsen DR, Biggar JW, Erh KT (1973) Spatial variability of field-measured soil-water properties. *Hilgardia* **42**, 215-219.

Nobles MM, Wilding LP, McInnes KJ (2004) Pathways of dye tracer movement through structured soils on a macroscopic scale. *Soil Science* **169**, 229-242.

Otago Regional Council (2001) 'Environmental Considerations for Dairy Farming in Otago.' (Otago, NZ).

Pang L, Mcleod M, Aislabie J, Simunek J, Close M, Hector R (2008) Modeling transport of microbes in ten undisturbed soils under effluent irrigation. *Vadose Zone Journal* **7**, 97-111.

Paterson E, Kemp JS, Gammack SM, FitzPatrick EA, Cresser MS, Mullins CE, Killham K (1993) Leaching of genetically modified *Pseudomonas fluorescens* through intact soil microcosms: Influence of soil type. *Biology and fertility of soils* **15**, 308-314.

Peterson TC, Ward RC (1989) Development of a bacterial transport model for coarse soils. *Water Resources Bulletin* **25**, 349-357.

Powelson DK, Mills AL (1998) Water saturation and surfactant effects on bacterial transport in sand columns. *Soil Science* **163**, 694-704.

Quinton JN, Tyrrel SF, Ramos MC (2003) The effect of incorporating slurries on the transport of faecal coliforms in overland flow. *Soil Use and Management* **19**, 185-186.

Reddy KR, Khaleel R, Overcash MR (1981) Behavior and transport of microbial pathogens and indicator organisms in soils treated with organic wastes. *Journal of Environmental Quality* **10**, 255-266.

Reynolds WD, Elrick DE (1991) Determination of hydraulic conductivity using a tension infiltrometer. *Soil Science Society of America Journal* **55**, 633-639.

Ritchie H (1999) Option for the management of non-point source discharges from Waikato Dairy Farms. North Canterbury Catchment Board TR: 99/17, Christchurch, NZ.

Ritchie JT (1972) Model for predicting evaporation from a row crop with incomplete cover *Water Resources Research* **8**, 1204-1213.

Roslev P, Bjergbaek LA, Hesselsoe M (2004) Effect of oxygen on survival of faecal pollution indicators in drinking water. *Journal of Applied Microbiology* **96**, 938-945.

Ross PJ (1990) 'SWIM: A Simulation Model for Soil Water Infiltration and Movement. Reference Manual, .' (CSIRO Division of Soils: Townsville, Australia).

Schaap MG, Leij FJ, van Genuchten MT (2001) Rosetta: a computer program for estimating soil hydraulic parameters with hierarchical pedotransfer functions. *Journal of Hydrology* **251**, 163-176.

Schafer A, Ustohal P, Harms H, Struffer F, Dracos T, Zehnder AJB (1998) Transport of bacteria in unsaturated porous media. *Journal of Contaminant Hydrology* **33**, 149-169.

Scheibe TD, Chien Y-J, Radtke JS (2001) Use of quantitative models to design microbial transport experiments in a sandy aquifer. *Ground Water* **39**, 210-222.

Schijven JF, Hassanizadeh SM (2000) Removal of viruses by soil passage: Overview of modeling, processes and parameters. *Critical Reviews in Environmental Science and Technology* **30**, 49-127.

Schijven JF, Hoogenboezem W, Hassanizadeh SM, Peters JH (1999) Modeling removal of bacteriophages MS2 and PRD1 by dune recharge at Castricum, Netherlands. *Water Resources Research* **35**, 1101-1111.

Shein EV, Polyanskaya LM, Devin BA (2002) Transport of microorganisms in soils: Physicochemical approach and mathematical modeling. *Eurasian Soil Science* **35**, 500-508.

Shiptitalo MJ, Edwards WM (1996) Effects of initial water content on macropore/matrix flow and transport of surface-applied chemicals. *Journal of Environmental Quality* **25**, 662-670.

Silliman SE, Dunlap R, Fletcher M, Schneegurt MA (2001) Bacterial transport in heterogeneous porous media: Observations from laboratory experiments. *Water Resources Research* **37**, 2699-2707.

Silva RG (1999) Effect of urinary nitrogen, dairy shed effluent and nitrogen fertiliser on nitrate leaching from a pasture soil PhD Thesis, Lincoln University.

Silva RG, Cameron KC, Di HJ, Hendry T (1999) A lysimeter study of the impact of cow urine, dairy shed effluent, and nitrogen fertiliser on nitrate leaching. *Australian Journal of Soil Research* **37**, 357-369.

Silva RG, Cameron KC, Di HJ, Smith NP, Buchan GD (2000) Effect of macroporeflow on the transport of surface-applied cow urine through a soil profile. *Australian Journal of Soil Research* **38**, 13-23.

Šimůnek J, Hopmans JW (2002) Parameter optimization and nonlinear fitting. In 'Methods of Soil Analysis, Part 4, Physical Methods'. (Eds JH Dane, GC Topp) pp. 139-157. (Soil Science Society of America, Inc.: Madison, Wisconsin, USA).

Šimůnek J, Jarvis NJ, van Genuchten MT, Gärdenäs A (2003) Review and comparison of models for describing non-equilibrium and preferential flow and transport in the vadose zone. *Journal of Hydrology* **272**, 14-35.

Šimůnek J, Sejna M, Van Genuchten MT (1998) The *HYDRUS-1D* software package for simulating the one-dimensional movement of water, heat, and multiple solutes in variably-saturated media: version 2.0. *IGWMC-TPS-70*. International Ground Water Modeling Center, Colorado School of Mines, Golden.

Šimůnek J, van Genuchten MT (2006) Contaminant Transport in the Unsaturated Zone Theory and Modeling. In 'The Handbook of Groundwater Engineering'. (Ed. JW Delleur) pp. 22.21-22.46. (CRC Press Boca Raton, FL).

Šimůnek J, Van Genuchten MT, Sejna M (2005) 'The HYDRUS-1D software package for simulating the one-dimensional movement of water, heat and multiple solutes in variably-saturated media.' (Department of Environmental Sciences, University of California Riverside , Riverside, California: California).

Šimůnek J, Wendroth O, Wypler N, van Genuchten MT (2001) Non-equilibrium water flow characterized by means of upward infiltration experiments. *European Journal of Soil Science* **52**, 13-24.

Singh P, Kanwar RS (1991) Preferential solute transport through macropores in large undisturbed saturated soil columns. *Journal of Environmental Quality* **20**, 295-300.

Sinton LW (1980) Two antibiotic resistant strains of *E. coli* for tracing the movement of sewage in groundwater. *Journal of Hydrology* **19**, 119-130.

Sinton LW, Braithwaite RR, Hall CH, Pang L, Close ME, Noonan MJ (2005) Tracing the movement of irrigated effluent into an alluvial gravel aquifer. *Water, Air, and Soil Pollution* **166**, 287-301.

Sinton LW, Finlay RK, Lynch AP (1999) Sunlight inactivation of fecal bacteriophages and bacteria in sewage-polluted sweater. *Applied and Environmental Microbiology* **65**, 3605-3613.

Smettem KRJ, Bristow KL (1999) Obtaining soil hydraulic properties for water balance and leaching models from survey data. 2. Hydraulic conductivity. *Australian Journal of Agricultural Research* **50**, 1259-1262.

Smettem KRJ, Collis-George N (1985) The influence of cylindrical macropores on steady-state infiltration in a soil under pasture. *Journal of Hydrology* **79**, 107-114.

Smettem KRJ, Oliver YM, Heng LK, Bristow KL, Ford EJ (1999) Obtaining soil hydraulic properties for water balance and leaching models from survey data. 1. Water retention. *Australian Journal of Agricultural Research* **50**, 283-289.

Smith MS, Thomas GW, White RE, Ritonga D (1985) Transport of *Escherichia coli* through intact and disturbed soil columns. *Journal of Environmental Quality* **14**, 87-91.

Statistics New Zealand (2007) Agricultural Production Statistics 2006. In 'Agricultural production statistics'. (Statistics New Zealand: Wellington, NZ).

Steenhuis TS, W. Staubitz MS, Andreini J, Surface TL (1990) Preferential movement of pesticides and tracers in agricultural soils. *Journal of Irrigation and Drainage Engineering* **116**, 50-66.

Stevik TK, Ausland G, Hanssen JF, Jenssen PDl (1999) The influence of physical and chemical factors on the transport of *E. Coli* through biological filters for wastewater purification. *Water Research* **33**, 3701-3706.

Stirk GB (1954) Some aspect of soil shrinkage and the effect of cracking upon water entry into soil. *Australian Journal of Agricultural Research* **5**.

Stoddard CS, Coyne MS, Gove JH (1998) Fecal bacterial survival and infiltration through a shallow agricultural soil : timing and tillage effects. *Journal of Environmental Quality* **27**, 1516-1523.

Tan Y, Ganon JT, Baveye P, Alexander M (1994) Transport of bacteria in an aquifer sand : Experiments and model simulations. *Water Resources Research* **30**, 3243-3252.

Taranaki Regional Council (1995) Priority Taranaki Streams for Strategic Enhancement of Protection Measures. Stratford, NZ.

Taranaki Regional Council. (1995) 'The Strategy for the Management of Dairyshed Effluent.' (Taranaki Regional Council: Stratford N.Z.).

Tawfik A, Klapwijk B, Buuren JV, Gohary FE-, Lettinga G (2004) Physico-chemical factors affecting the *E. coli* removal in a rotating biological contactor (RBC) treating UASB effluent. *Water Research* **38**, 1081-1088.

Thomas GW, Phillips RE (1979) Consequences of water movement in macropores. *Journal of Environmental Quality* **8**, 149-152.

Toor GS (2002) Phosphorus leaching losses from an irrigated free-draining soil under dairying PhD thesis, Lincoln University. New Zealand.

Toor GS, Condron LM, Cade-menun BJ, Di HJ, Cameron KC (2005) Preferential phosphorus leaching from an irrigated grassland soil. *European Journal of Soil Science* **56**, 155-167.

Toor GS, Condron LM, Di HJ, Cameron KC (2004a) Seasonal fluctuations in phosphorus loss by leaching from a grassland soil. *Soil Science Society of America Journal* **68**, 1429-1436

Toor GS, Condron LM, Di HJ, Cameron KC, Sims JT (2004b) Impact of farm-dairy effluent application on the amounts and forms of phosphorus loss by leaching from irrigated grassland. *New Zealand Journal of Agricultural Research* **47**, 479-490.

Trojan MD, Linden DR (1992) Microrelief and rainfall effects on water and solute movement in earthworm burrows. *Soil Science Society of America Journal* **56**, 727-733.

Trojan MD, Linden DR (1998) Maroporosity and hydraulic properties of earthworm-affected soils and influenced by tillage and residue management. *Soil Science Society of America Journal* **62**, 1687-1692.

Tyrrel SF, Quinton JN (2003) Overland flow transport of pathogens from agricultural land receiving faecal wastes. *Journal of Applied Microbiology* **94**, 87S-93S.

Unc A, Goss MJ (2003) Movement of faecal bacteria through the vadose zone. *Water, Air and Soil pollution* **149**, 327-337.

van Elsas JD, Trevors JT, van Overbeek LS (1991) Influence of soil properties on the vertical movement of genetically-marked *Pseudomonas fluorescens* through large soil microcosms. *Biology and fertility of soils* **10**, 249-255.

van Genuchten MT (1980) A closed-form equation for predicting the hydraulic conductivity of unsaturated soils. *Soil Science Society of America Journal* **44**, 892-898.

van Genuchten MT, Leij FJ, Yates SR (1991) The RETC Code for Quantifying the Hydraulic Functions of Unsaturated Soils. Version 1.0. U.S. Salinity Laboratory,EPA Report 600/2-91/065, USDA, ARS, Riverside, CA.

van Genuchten MT, Šimůnek J (2004) Integrated modeling of vadose-zone flow and transport processes. In 'Unsaturated- Zone Modeling; Progress, Challenges and Applications, Wageningen UR Frontis Series'. (Eds RA Feddes, GHd Rooij, JCv Dam) pp. 37-69, x-xi. (Kluwer Academic Publishers: Dordrecht, The Netherlands).

van Genuchten MT, Wagenet RJ (1989) Two-site/two-region models for pesticide transport and degradation: Theoretical development and analytical solutions. *Soil Science Society of America Journal* **53**, 1303-1310.

Verburg K, Ross PJ, Bristow KL (1996) SWIM v2.1 User Manual, CSIRO Australia Division of Soils. Divisional Report No. 130.

Vinten AJA, Lewis DR, Fenlon DR, Leach KA, Howard R, Svoboda I, Ogden I (2002) Fate of *Escherichia coli* and *Escherichia coli* O157 in soils and drainage water following cattle slurry application at 3 sites in southern Scotland. *Soil Use and Management* **18**, 223-231.

Watt JPC, Burgham SJ (1992) 'Physical properties of eight soils of the Lincoln area, Canterbury.' (Wellington, NZ).

Weiler M, Naef F (2003) Simulating surface and subsurface initiation of macropore flow. *Journal of Hydrology* **273**, 139-154.

Weiss TH, Mills AL, Hornberger GM, Herman JS (1995) Effect of bacterial cell shape on transport of bacteria in porous media. *Environmental Science & Technology* **29**, 1737-1740.

White I, Sully MJ (1987) Macroscopic and microscopic capillary length and time scales from field infiltration. *Water Resources Research* **23**, 1514-1522.

White RE (1985) The influence of macropores on the transport of dissolved and suspended matter through soil. *Advanced Soil Science* **3**, 95-121.

Xue X, Zhang R, Gui S (2004) An improved disc infiltrometer method for calculating soil hydraulic properties. *Canadian Journal of Soil Science* **84**, 265-273.

Yasuda H, Berndtsson R, Persson H, Bahri A, Takuma K (2001) Characterizing preferential transport during flood irrigation of a heavy clay soil using the dye Vitasyn Blau. *Geoderma* **100**, 49-66.

Yates MV, Yates SR (1991) Modeling microbial transport in the subsurface: a mathematical discussion. In 'Modeling the environmental fate of microorganisms'. (Ed. CJ Hurst) pp. 48-75. (American Society for Microbiology: Washington, D.C.).

Appendices

Appendix I. BTCs of FC and Br^- during Trial 1 (scaled to see the bacterial concentration in leachate of 4^{th}-6^{th} water applications)

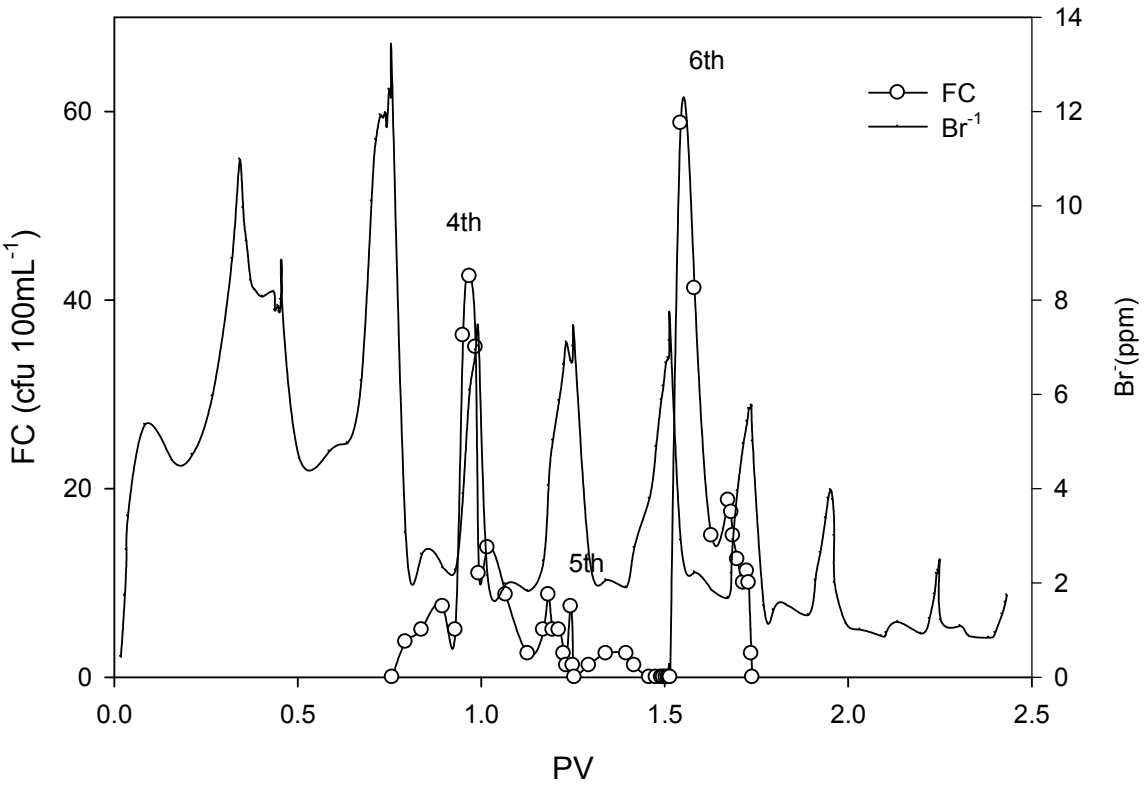

Appendix II FC die-off rates in a liquid phase over a range of temperature: a) 6°C; b) 12°C and c) 18°C

The die-off rate ranged from 0.33 d^{-1} to 0.56 d^{-1}.